Urban Ecohydrology and the Watershed Microbial Continuum

A Dissertation Presented for the
Doctor of Philosophy
Degree
The University of Tennessee, Knoxville

Victoria Christine Rexhausen
May 2024

DEDICATION

I dedicate this work to my family, who's generations of efforts have yielded an opportunity of greater education that I have the privilege to enjoy. I hope to make you proud. I dedicate this work to 1,000 generations of caretakers, healers, and ecowarriors.

ACKNOWLEDGEMENTS

This work would not be possible without financial support from the National Science Foundation (CAREER Award #1553475) and the United States Geological Survey 104b Program, and the University of Tennessee.

I would like to thank my dissertation committee, Dr. Jon Hathaway, Dr. Anja Szynkiewicz, Dr. Sara McMillan, and Dr. Terry Hazen, for their support and feedback. I would like to especially thank my primary investigator, Dr. Jon Hathaway for believing in me and supporting me through all the struggles of the doctoral process. Thank you for giving me the freedom to create this project from start to finish and tailor it to my interests and passions. Thank you to Dr. Anja Szynkiewicz for your special guidance in the laboratory and meticulous review of my work. Thank you, Dr. Terry Hazen, for guidance in applied microbiology research and your sharing of research ideas. Thank you, Dr. Sara McMillan, for your professional guidance and ecological perspective on my work. Thank you to my undergraduate research advisor, Dr. Phil McCreanor, and my undergraduate academic advisor, Dr. Andre Butler, for your encouragement to follow my curiosity to a graduate degree and pursue my love for learning. Laboratory analysis for this body of work was performed in Science and Engineering Research Facility (SERF) 702, the EPS Stable Isotope Laboratory, and the Hazen lab in UTK SERF 728/723.A special thank you is owed to lab managers Dr. Anthony Faiia, Dominique Joyner, Dan Williams, Dr. Sharon Hale, and Dr. Adrian Gonzales. A special thank you is owed to Dr. Clifford Swanson for his immense guidance through the entire 16S rRNA pipeline: from DNA extraction to gene sequencing, and through a statistical analysis of the community. Thank you to (now graduated) undergraduate researchers Jack Elliot, Claudia Bible, and Nicholas Ross for your assistance with data collection and sample processing. I am

immensely grateful to have landed in Knoxville, TN among the members of Hathaway Research Group for my graduate program, all of whom have provided nothing but support and positivity through my journey.

I would also like to thank my family for their unwavering support and encouragement. Mom, Dad, Cassi, Joe, Grandmommy, Granddad, Amanda, Carolyn, Eva, Charlie, Atalaya, Uncle Louis, Uncle Jim, Aunt Becky. You may not have always known what the heck I was talking about, but your love and belief in me inspired my discipline during the most challenging moments. Thank you to all my friends I have kept and made along the way. Thank you for always being willing to offer a source of encouragement and love and for checking on me throughout the process. I am lucky to be surrounded by outstanding peers who bring out the best in everyone around them – thanks for inspiring me and showing me how capable I am.

ABSTRACT

A rapidly urbanizing world is adding unprecedented stress to water resources. Urbanization results in high rates of stream impairment, including but not limited to ecological stress, pollution, and flooding. A fully integrated and holistic perspective is necessary for effective remediation strategies for these wicked problems. This monitoring study from a heterogeneous urban watershed investigated the geospatial and seasonal interactions between urban hydrology and biological processes using stable isotope compositions, anions, and microbial.

This research found that nitrate concentrations in an urban watershed were ecologically driven. NO_3^- concentrations ranged from 0.4 to 12.7 mg/L throughout the watershed. Nitrate concentrations were responsive to seasonal, land use, and wet weather drivers. Average dissolved NO_3^- concentrations in the baseflow water column were the highest in the fall/winter (8.46 and 9.41 mg/L, respectively) and the lowest in the spring/summer (4.844 and 5 mg/L, respectively). Geospatially, the urbanized, downstream region of the watershed had the highest NO_3^- concentrations in the fall/winter seasons, while the forested uplands dominated NO_3^- concentrations in the spring/summer. The stable isotope compositions of $\delta^{15}N$ and $\delta^{18}O$ in the dissolved NO_3^- support for the hypothesis that these variations in NO_3^- concentrations across the watershed are driven by tree canopy cover, decomposition of particulate organic matter, and soil nitrification/denitrification processes.

The microbial community diversity and assembly processes were significantly correlated with changes in land use, though the effect of changes in land use was small. Assembly processes and diversity were more strongly responsive to seasonal and precipitation events. For this reason, it seemed plausible to test a microbial source tracking technique

to partition between different landscapes, such as roadways, grasses, and forest. The study found that MST has potential for accurate portioning of the hydrograph and giving keen insights into the complex landscape response to rainfall intensity, but more sampling efforts are needed.

Overall, this body of work investigated the poorly understood interactions between ecohydrology, the microbiome, and the urban landscape. The complexity of watershed hydrological and ecological response to urbanization must be considered for effective pollutant mitigation and regulation. It also highlighted the need for more studies on the urban microbiome. The literature is lacking consensus among scientists on indicator species or assemblies for implications of urbanization of stream health.

TABLE OF CONTENTS

LIST OF TABLES

LIST OF FIGURES

CHAPTER 1
INTRODUCTION: THE ROLE OF URBAN ECOHYDROLOGY INW ATER RESOURCES ENGINEERING

A rapidly urbanizing world is adding unprecedented stress to water resources. Increasing rates of urbanization are contributing to an unpredictable and growing new ecosystem environment known as the urban landscape, where the ecosystems of urban areas in different regions of the world seem to function more similarly to each other than to their comparable undeveloped environments (Groffman et al., 2014). Urbanization contributes to degradation of water supply through anthropogenic nonpoint source pollution and altered watershed hydrology. Changes in hydrologic function in urban streams are compounded by climate uncertainty, resulting in an increased frequency of flooding and higher peak flows. At the same time, the related increased nutrient loading coupled with decreased opportunity for biological treatment contributes to adverse effects on downstream ecosystems such as eutrophication. Urban groundwater quality suffers as it receives pollutants delivered by urban stormwater, and aquifer recharge is intercepted by impervious connectivity (Vystavna et al., 2019). With over 55% of the human population already living in urban centers (World Urbanization Prospects: The 2018 Revision, n.d.) coinciding with climate change and increasing incidence of water scarcity (WMO), the need to intercept the damage being perpetrated on the freshwater supply is mounting in urgency.

In these homogenized landscapes, the biological intelligence of nature is limited by the hydrologic repercussions of paved surfaces. Earth's biogeochemical phenomena, such as the water cycle and nutrient cycles, are built-in tools programmed for remediating environmental catastrophes and maintaining balance. Fungal species and microbiota are hard at work in our soils and streams converting organic waste into useable building blocks for the next phase of metabolic life; however, the urban landscape's impervious land cover and water conveyance systems interrupt natural treatment processes compared to pristine landscapes (discussed in more detail in the Urban Hydrology introduction section).

In addition, geographical places with primarily human-centered land use types (such as urban centers or agriculture) suffer from increased pollutant loading. Agricultural environments utilizing pesticides and fertilizers contribute nitrate and phosphates to receiving waters, resulting in eutrophication, and deoxygenated dead zones downstream (Paerl, 2009). Human activities in urban environments contribute a variety of pollutants from transportation, commercial, residential, and industrial industries; cars contribute heavy metals and petroleum pollutants to roadways (Bernhardt et al., 2007). The impervious surfaces, especially those directly connected to receiving stream bodies via stormwater conveyance structures, exacerbate pollution in watersheds with impervious land use types (Shuster et al., 2005)

Nature Based Solutions

There is a growing emphasis in the scientific community on the potential of utilizing ecological intelligence for the remediation of anthropogenic impacts on the environment. Engineered "nature-based solutions" focus on restoring, protecting, modifying, and sustainably managing naturally occurring and built ecosystems for the purpose of leveraging natural processes and ecosystems for improved water quality and to the benefit of public health (Osaka et al., 2020; Sowińska-Świerkosz & García, 2022). Examples may include wetland restoration for improved hydrologic connectivity and biological treatment, forest conservation and management to increase ecosystem services derived from tree canopy cover or regulating urban surface runoff through the implementation of urban green infrastructure (GI) designs such as green roofs, rain gardens, or bioswales (Thorslund et al., 2017; Zolch et al., 2017).

Nature-based solutions with a hydrological focus aim to attenuate stormwater surges, enhancing opportunities for infiltration to improve water quality and reduce the risk of flooding (Orta-Ortiz & Geneletti, 2022). Green infrastructure includes regenerative stormwater conveyance (RSC) systems, permeable pavements, rain gardens, and bioswales. Nature-based solutions may also be landscape-scale conservation projects, ranging from wetland restoration for wildlife habitat and water treatment to establishing urban greenways for increased biodiversity and tree canopy cover. Investing in developing nature-based solutions, and scientific research to support effective

solutions, is beneficial not only to ecological health but to human health and wellbeing. Nature provides benefits to human beings through climate regulation, infectious disease modulation, improvements in water and air quality, relieving stress and boosting mental health. (Coutts and Hahn, 2015).

To enhance the efficacy of nature-based solutions, it is imperative for scientists to refine their toolkits for deciphering nature's language, indicating disruptions and guiding ecological best practices. Advancing our capacity to predict the intricate patterns in urban hydrology will enhance comprehension of nutrient transport processes and the representation of challenging non-point source pollutants in watersheds. Despite these objectives, numerous unknowns must be addressed to achieve success. Many existing models and regulatory frameworks designed for watershed management and remediation overly simplify the complex issues specific to the unique needs of individual watersheds. Refinement in biotechnologies, including source tracking techniques and monitoring of a watershed through the memory of its unseen drivers (nutrients and microbial communities), hold promise for a more sophisticated future in Ecologically engineered systems.

Urban Hydrology, Ecohydrology, Urban Ecohydrology

This section will go into greater detail about the essential components of Urban Hydrology, Ecohydrology, and the vision for the unification of the two. This study lens highlights the effectiveness of green infrastructure (GI) and nature-based solutions (NBS) as water management strategies that integrate both hydrology and ecosystem science. GI practices were developed mainly to manage water quality and hydrologic issues of urban stormwater (Fletcher et al., 2015), while NBS emphasizes using ecosystem processes to manage aquatic health (Jarosiewicz et al., 2021).

Urban Hydrology

The urban landscape, composed of its concrete roads and rooftops, sees a hydrologic response to precipitation drastically different from hydrology observed in pristine reference environments.

Urban hydrology is a method or applied science within hydrology that accounts for the impacts of urbanization on receiving water bodies (Fletcher et al., 2012). The application of urban hydrology has revealed increasingly complex interactions between compounding factors, including patchwork land use types, unpredictable subsurface flow patterns, and the introduction of anthropogenic pollutants. The impact of urbanization on the hydrologic cycle can even be observed in microclimates – the urban heat island effect contributes to urban-induced rainfall and impedes accurate predictions of evapotranspiration coefficients (O'Driscoll et al., 2010).

The major difference between the urban watershed and reference environments, and the common denominator for perpetuating stormwater pollution, is impervious area. Landscape developed for residential, commercial, or transportation use replaces permeable landscape with impervious surfaces like roads, buildings, and sidewalks. Imperviousness drives urban hydrology by impacting stormwater volume, velocity, and storage. The increased impervious surface in developed areas decreases the total effective storage of the watershed and contributes to increased peak flow rates (Burns et al., 2011; Walsh et al., 2015). Precipitation is intercepted from infiltration, resulting in an increasing volume of runoff. This increased runoff volume contributes to higher peak flows in receiving water bodies, affecting geomorphology by increased erosion and sediment transport.

Stormwater runoff also leads to increased pollutant delivery (USEPA, 2016). Airborne pollutants in the form of particles and gases–including nitrogen compounds, sulfur compounds, base cations, or heavy metals—settle on surfaces during dry weather (dry deposition) or are brought to the earth through adsorption to water droplets which then fall as precipitation (wet deposition) and are washed into streams. These pollutants may originate from motor vehicles, factory exhausts, or fires (Lear, 1990). Stormwater and urban streams may harbor waterborne diseases and pathogens (McLellan et al., 2015). Introducing these contaminants to receiving water bodies presents an increased risk to public health downstream (Makepeace et al., 1995).

Urban hydrology compounds increased exposure to anthropogenic pollutants by swiftly draining stormwater directly to receiving water bodies. Pollutants accumulated in stormwater that do not

encounter pervious surfaces such as grass, green space, or forests do not have an opportunity for pre-treatment via infiltration processes (Driscoll et al., 2010). These impacts contribute to Urban Stream Syndrome, a term ascribed to streams with poor ecological health resulting from receiving runoff from urban landscapes (Fletcher et al., 2012). Because stormwater quality can have significant impacts to both the aquatic life and public health downstream, understanding the pollutants of concern and the range of severity is important for proper water resource management. Stormwater control measures, including nature-based solutions and GI practices, attempting to slow the rate of discharge from stormwater runoff and allow for pretreatment of contaminants in stormwater via bioinfiltration have shown promise to improve water quality in receiving waters (Trowsdale & Simrock, 2011; Jefferson et al., 2017).

Ecohydrology

Ecohydrology is an interdisciplinary subdiscipline of hydrology concerned with the interactions between hydrologic processes and biological processes in natural and human-impacted systems (UNESCO; Moore et al., 2015). Bridging insights from hydrology, ecology, geography, and geology, ecohydrology serves as a comprehensive lens to unravel the profound impacts of hydrological processes on downstream ecosystems' distribution, structure, and function. This is especially relevant in urban hydrology, where urbanization magnifies downstream impacts on water quality and quantity (Fletcher et al., 2012).

Traditional water resources management focuses predominantly on hydrologic science, especially calculations of volume and flow (Nuttle, 2002). While this focus is undoubtedly important and effective for flood risk control and reducing pollutant transport, a more holistic approach to the role water plays in ecosystem health, and reactively public health, is especially relevant to solving the increasingly complex challenges of the perpetuation of nutrient pollution and attenuation in urban catchments. Ecohydrology emerges as a pivotal field by offering a nuanced understanding of the interdependence and responses of ecosystem patterns and processes to the presence and timing of water (Nuttle, 2002.)

Soil moisture is at the core of the interaction between hydrologic regimes and biological processes (Moore et al., 2015). Soil moisture and vegetation are two of the central parameters in ecohydrology (Porporato and Rodriguez-Iturbe, 2002). Both soil moisture and vegetation are intricately linked to geology and climate (Thorp et al., 2006). Climate variables, such as solar intensity, frequency and intensity of precipitation, and temperature, drive soil moisture content by impacting water volume and freeze-thaw dynamics. These same climate variables are fundamental to vegetation's primary production by providing access to solar energy and water necessary for photosynthesis. Geology acts as an additional driver of soil moisture and vegetation; the parent material of a geological zone and weathering patterns informed by local climate influence the properties of the soil formed and, subsequently, the hydraulic conductivity and mineral ratios available to primary producers (Hunt, 2021).

Ultimately, the environment consists of the lithosphere, the atmosphere, the hydrosphere, and the biosphere; ecohydrology encompasses the interaction between these four spheres and the systems within them. Building on the foundational understanding of ecohydrology, this section delves into the significant roles played by geology and climate as major drivers influencing soil moisture and vegetation. The intricate interplay of these factors shapes the dynamics of ecosystems, making them inseparable components to understanding catchment area's water quality and behavior.

Soil Moisture

Soil moisture serves as the variable regulating the interactions between climate, soil, and vegetation in maintaining water balance (Porporato & Rodrigues-Iturbe, 2002). Soil moisture modulates runoff rates during storm events. Soil porosity is the ratio of non-soild volume to the total volume of the soil. As precipitation infiltrates the soil and fills the storage available in the space between soil grains, runoff will be generated. Precipitation rates, hillslope, precedent soil moisture conditions due to recent weather history and vegetation, and soil characteristics such as depth, porosity, and density, can influence the rate of runoff generated and subsequent biogeochemical response (Singh et al., 2021). Soil moisture mediates the microbial communities

responsible for certain biogeochemical processes including assimilation and mineralization of nutrients and soil redox reactions (Stark, 2000). Taxa responsible for the decomposition of organic matter such as leaf litter, including microbial communities and terrestrial invertebrates such as earthworms, depends on soil moisture content to provide an optimal amount of oxygen and water (Cortex, 1998).

The implications of urbanization on land development and soil compaction (Pitt et al., 2008) add to the relevance of soil moisture content in urban areas. Plant community structure will impact soil storage capacity via evapotranspiration rates and soil aeration compared to the compacted soils of urban developments (Yang & Zhang, 2015). Soil storage capacity impacts availability of oxygen, a biogeochemical parameter essential to microbially-driven nutrient processes. Drying and rewetting patterns have been shown to result in complex microbial response and increased nutrient export (Merbt et al., 2016) and flashy hydrology in urban streams disrupts benthic microbial communities responsible for nutrient processing (O'Driscoll et al., 2010).

Climatology

Climate significantly influences ecohydrological processes, encompassing precipitation patterns, evapotranspiration, canopy ecophysiology, solar intensity, and albedo. These interconnected elements collectively impact soil moisture, driving plant-hydro interactions and connectivity. The atmosphere, biosphere, geosphere, and hydrosphere synergistically contribute to maintaining a crucial role in the water balance.

Climate variables influence the water balance through plant physiology. The stomata are the small pores on the surface of plant leaves that regulate gas exchange. Stomatal conductance of CO_2 and water vapor are influenced by various environmental and climatic factors, including CO_2 concentration in the atmosphere, access to light, temperature, humidity, and soil moisture. Photosynthesis rates increase with increased solar intensity and increased CO_2 concentrations in the atmosphere, meaning increased stomatal conductance and resulting in increased transpiration rates (Vico et al., 2013). Evapotranspiration processes from vegetation have a cooling effect on the ambient air temperature. The water molecules absorb heat energy from the surrounding air in

order to change phase from liquid to gas; this is called the latent heat. Canopy ecophysiology also has an impact on ambient surface temperature by increasing shaded area. For this reason, vegetation coverage is an important element to consider for water-climate-organics interactions. Deforestation, reforestation, and afforestation has an impact on the water balance and on climate through the process of transpiration.

Albedo is a concept from physics that refers to the reflectivity of a surface; albedo is necessary for communicating about Earth's energy balance and the proportion of solar radiation that is reflected:absorbed. For example, snow covered surfaces have a high albedo of 0.80-0.95, meaning it reflects 80-95% of incoming sunlight. Generally speaking, urban areas have a high concentration of dark surfaces such as asphalt and concrete resulting in lower albedo values. Urban areas can have an average albedo of 0.05-0.35%, meaning the majority of the solar radiation is absorbed into the surfaces (Oke, 1987). This high concentration of heat-absorbing surfaces, paired with increased heat-producing behaviors and reactions such as engine combustion and steam production, and decreased cooling effects from low vegetation density, results in increased temperatures in urban areas known as the urban heat island effect (Oke, 1982).

Age of Climate Change

In the current of climate change, when rapid global urbanization is both intensifying anthropogenic influence on the environment and magnifying the felt effects of climate on civilization, ecohydrology has become a more crucial field of study than ever. With unprecedented challenges to our ecosystems and water resources, it is critical not only to understand how our systems are changing but to evaluate how these changes will impact water availability and quality in the future. Changes to precipitation patterns now only exacerbate the effects of climate change on water resources but can also exacerbate already existing water quality issues such as nutrient and other pollutant loading and transport. Anticipated increases in low-frequency high-volume hydrology events can lead to increased likelihood of DOM pulse-shunt in watersheds, increased evapotranspiration rates, and increased watershed connectivity

and uncertainty in flow rates (Raymond et al., 2016). This presents unprecedented challenges in water resource management for flood regulation and maintaining a dependable water supply.

Climate change exerts intricate impacts on ecohydrological processes, creating a web of interconnected implications. Elevated temperatures and carbon coupled with increased uncertainty in precipitation lead contribute to a dual scenario where wet ecosystems getting wetter, experiencing increased water loss, while dry ecosystems getting drier face augmented drought stress on vegetation. increased temperatures result in increased frequency of Iprecipitation events (McGrane, 2015). The anticipated rise in low-frequency, high-volume hydrology events introduces heightened unpredictability in intermittent drying and re-wetting cycles, impact plant physiology, microbial community assembly, and biogeochemical cycles. Increased rainfall frequency may trigger flood-pulse-initiated nutrient export (Raymond et al., 2016). Increased input of anthropogenic aerosols from combustion processes additionally can lead to precipitation events by acting as cloud condensation nuclei (Bonan, 2016). Warmer air temperatures can impact soil moisture levels by increasing evaporation from top layers of soil. Vegetation density and type can also have an impact on soil moisture through transpiration processes.

Aqueous Geochemistry and Soil Properties

Water-rock interactions play an integral role in the chemical properties of water, and thus in water quality and reactivity. Aqueous geochemistry refers to the large number of equilibrium processes of minerals moving between their dissolved and precipitated states where water and rock are in contact. Water-rock interactions take place once precipitation makes contact with the ground through infiltration, overland flow in bare rock landscapes (lacking soil), and in subsurface flow. Depending on the geology of the landscape, the water will meet rocks with different mineral compositions and solubility. These interactions impact many water quality parameters. Water can dissolve minerals from rocks leading to an increase in dissolved solids, impacting water hardness, salinity, conductivity and pH. In some cases, harmful contaminants

including heavy metals such as lead, arsenic, and mercury or trace elements may leach from rocks into soil and water.

One example of water-rock interactions integral to East Tennessee water resources is the interaction between carbon dioxide (CO_2), water (H_2O), and calcium carbonate ($CaCo_3$), known as carbonation, plays a crucial role in the geochemical cycling of carbon in the earth's crust. The dissolution of carbon dioxide from the atmosphere into water forms carbonic acid (H_2CO_3), and the carbonic acid then reacts with solid calcium carbonate found in minerals such as limestone. This reaction accelerates the weathering of carbonate minerals. This interaction between the hydrosphere, atmosphere, and geosphere results has implications for water quality, including especially in areas with carbonate-rich geology. These impacts include increasing water hardness by releasing calcium ions to the dissolution of calcium carbonate and the contribution to the formation of caves, sinkholes, and underground drainage.

Besides water quality, the geology of a landscape also impacts vegetation and soil moisture through soil texture and mineral content. Soils are formed over long periods of time and influenced by the geologic parent material. The solubility of the parent material determines how quickly the minerals composing the parent material will break down, which can impact soil characteristics. Soil properties, especially chemical composition and nutrients available for vegetation, are highly influenced by the parent geology of the site. In the Ridge and Valley region of East Tennessee, for example, the parent materials consist of primarily of shale, limestones and sandstones. The dolomitic limestone characteristic of the low rolling hills consists primarily of calcite ($CaCO_3$) and dolomite ($CaMg(CO_3)_2$ contributing calcium oxide/lime (CaO) to the soils (Bailey et al., 1994; USDA, 1981; Sharma & Sharma, 2021). The shale valleys, however, contribute primarily quarts (SiO_2) and other silica-containing minerals as well as feldspars.

As these parent materials breakdown and become soil, the size and shape of the composite soil particles contribute to the composite texture. Soil textures can be categorized as clays, silts, or sands (Figure 1.1). Particle size and shape is a result not only of the minerals present in the

material, but also the weathering processes. Soil texture can change with depth. Soil texture is an important component in determining soil porosity and subsequently infiltration rate, susceptibility to compaction, and volume of water storage available for plants. Soil texture also influences nutrient losses, where sandy soil types result in higher recorded N losses but lower P losses due to increased filtering of particulates (P is more likely to transport via suspended sediments than N) (Djodjic et al., 2021). Mineral content in soil can also impact sorption capacity, impacting primarily P transport (Djodjic et al., 2021).

Stable Isotope Geochemistry

Stable isotope geochemistry is a field of study which investigates isotopic compositions of elemental compounds for insights on behavior and source (USGS; Ehleringer et al., 2000). Isotope fractionations are caused by naturally occurring chemical and metabolic processes, providing information about the source and behavior of the object. Fractionation events associated with biological and physical processes can create variations in isotopic abundance, thus leaving a signature of recent activity and acting as spatial and temporal tracers.

Results of stable isotope analyses are reported by comparing the ratio of heavy isotopes to light isotopes for a particular element within a sample to a standard using the delta notation (δ) where:

$$\delta = \left(\frac{R_{sample}}{R_{standard}} - 1\right) * 1000\ ‰ \quad \text{(Eq. 1)}$$

Equilibrium isotope fractionations are temperature dependent exchange reactions. These reactions are helpful for developing isotope thermometers, used for estimating temperatures in geological history. Kinetic isotope fractionations are associated with rapid, irreversible, unidirectional processes and biological reactions. Examples of kinetic fractionation reactions include evaporation, dissociation, and biological metabolic processes. Kinetic fractionations are more difficult to quantify than equilibrium fractionations.

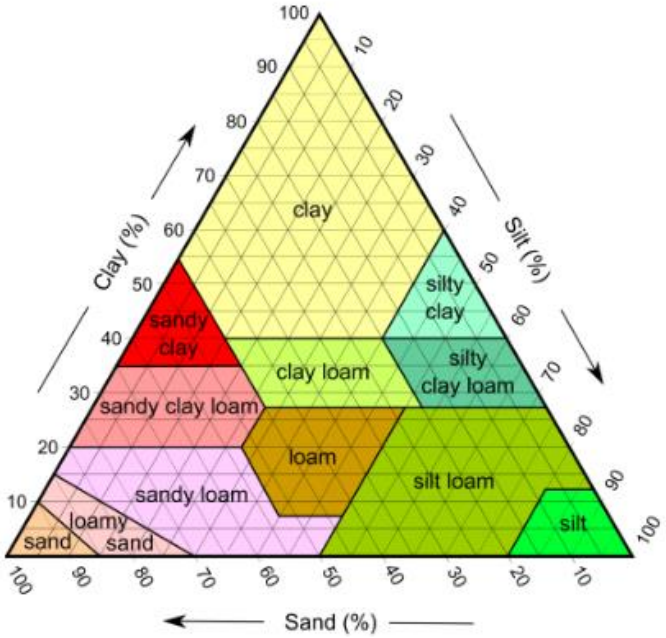

Figure 1.1 Soil texture diagram providing soil texture descriptions based on soil components from the US Department of Agriculture.

Stable isotope signatures can reveal relevant information to the interactions of the hydrosphere on geochemical processes. Water-rock interactions, such as chemical weathering, result in isotope fractionations. Chemical weathering is the process of the dissolution of rocks in response to contact with water, or the reaction of water with minerals contained in rock. Chemical weathering is intensified with acidic conditions. Acid rain due to combustion pollution can increase the occurrence/rate of chemical weathering. Acidic conditions can also be resultant of biological activity such as microbial metabolic reactions, especially in soils. Physical conditions can also impact the rate of dissolution due to chemical weathering, including geology of rock formations in the environment and climate. If the geology of the environment is made up of rocks/minerals with high solubility, such as the limestone common to East Tennessee, the rocks will dissolve at a higher rate. High temperatures and rainfall intensity can also increase the rate of chemical weathering. Most rocks increase solubility with increasing temperature. Increased rainfall intensity results in greater frequency of rock-water interactions

Chemical weathering will impact sulfide minerals found in soils. Exposure to dissolved oxygen in water will oxidize sulfide minerals producing sulfuric acid (H_2SO_4), contributing to increased acidity and chemical weathering of other minerals. The sulfate from dissolved sulfuric acid can combine with other cations, such as Ca^{+} and Fe^{2+}, upon the dissolution of sulfuric acid, or it will further oxidize into dissolved sulfur. Sulfur chemical weathering can also result from bacterial metabolic processes. Microorganisms can reduce sulfate into sulfide through both assimilation and dissimilation processes. All of these reactions are highly dependent on the geochemical environment.

Sedimentary rock deposits resulting from chemical weathering processes are called “evaporites”. Bedrock evaporite minerals containing sulfate will have similar isotope composition as sulfate dissolved in the adjacent groundwater. Bacterial sulfate reduction, in contrast, results in significant enrichment of sulfate in heavier sulfur isotopes. Due to these variations, the ratio of sulfur isotopes in Baker Creek can give hints to the depth of the subsurface flow which primarily contributes to baseflow in the surface stream. Lighter sulfate isotopes will indicate greater influence from bedrock evaporites and less influence from microbial assimilatory processes,

indicating that the water has spent less time out of the groundwater aquifer and in the vadose zone. Lighter sulfur isotope compositions can indicate higher instances of metabolic reactions, indicating more shallow flows. Therefore, lighter sulfur isotope compositions in stream water baseflow indicate deeper flows, versus heavier isotopes which indicate more shallow flows.

Stable isotopes of dissolved sulfate are especially useful for identifying geochemical history of water sources, where the chief processes affecting fractionations are evaporation, water-rock interaction, and mixing (Seal, Alpers & Rye, 2016). Insights that can be derived from sulfate isotopes that are related to water resources include the relative depth of the water source (it being primarily surface water or deeper groundwater) or implications of anthropogenic sulfate on water salinity (Horst et al., 2011; Szynkiewicz et al., 2015).

Metabolic processes, including nutrient transformations, also result in various isotope fractionations. These fractionations, when utilized as tracers, can lend insight into potential sources of a constituent of concern. For example, stable isotope composition of nitrogen and oxygen in nitrate has been used to approximate nitrogen pollutant source contributions (Kaushal et al., 2011; Baral et al., 2018).

Nitrogen Pathways In Urban Systems

Of water chemistry parameters, nitrogen (N) is a nutrient of particular interest in water resources due to its association with human-altered environments, complex reactions, and pervasiveness as a pollutant (Bosch et al., 2018). It is of particular interest in urban streams to slow the export of N, which may accumulate in downstream reaches causing ecological harm or eutrophication of coastal waters (Cadenasso et al., 2008). Many methodologies to reducing N export have been employed, from regulation to treatment (Melosi 2000).

Nitrate, a form of N, is a critical pollutant, the most common groundwater pollutant in the United States (USEPA, 1990). Because nitrate is a fundamental element to life cycles and a limiting nutrient in ecosystems, its presence is somewhat ubiquitous (Cadenasso et al., 2008). In addition, human activities now exorbitantly escalate nitrate pollution by increasing inputs from fertilizers

and waste products. Runoff carrying fertilizers and leaky sanitary sewers contribute nitrate pollution to surface and groundwaters (Bernhardt et al., 2008). As such, the source of nitrate pollution is often defined as nonpoint source, meaning it results from many diffuse sources. This makes nitrate particularly difficult to model, prevent, and regulate.

The functional alterations of urban land use on hydrology and ecosystems impact nitrogen cycle beyond anthropogenic inputs. The implications of urban hydrology on stream function have decreased ecological efficiency of riparian zones in urban systems (Groffman et al., 2004). Understanding the potential zones in an urban landscape where N uptake can take place is crucial for developing effective mitigation strategies. Patches of greenspace in the urban landscape can serve as sinks or sources of nitrate (Cadenasso et al., 2008). A "sink" is a component of the ecosystem that effectively removes reactive nitrate / reduced concentration through biogeochemical transformation. A "source" will contribute nitrate. A depiction of some urban nitrate sources and sinks and respective biogeochemical processes can be seen in Figure 1.2.

A properly functioning sink will require proper environmental conditions for denitrification, fixation, or assimilation. Denitrification and fixation are microbially driven processes that convert reactive nitrogen into nitrogen gas (N_2), and both will require an environment that can properly host the appropriate bacteria. Denitrification typically occurs in waterlogged soils under anaerobic conditions and requires the availability of other organic compounds and electron donors (Firestone, 1982). Biological N_2 fixation requires solar energy to convert N_2 gas into ammonia (NH_3), a form of N usable by plants (Burris & Roberts, 1993). Assimilation is process in which plants uptake ammonium (NH_4^+) or nitrate (NO_3^-) from soil and incorporate the N into the plant's biomass (Xu et al., 2012).

From this point, N products become a source. Once assimilated into organic matter, N awaits its fate to be reintroduced into the ecosystem through the processes of ammonification. Ammonification modulates reintroduction of N into the soil via biological agents such as bacteria, aquatic plants, and biofilms (Strock, 2008). Nitrification is the two-step oxidation of

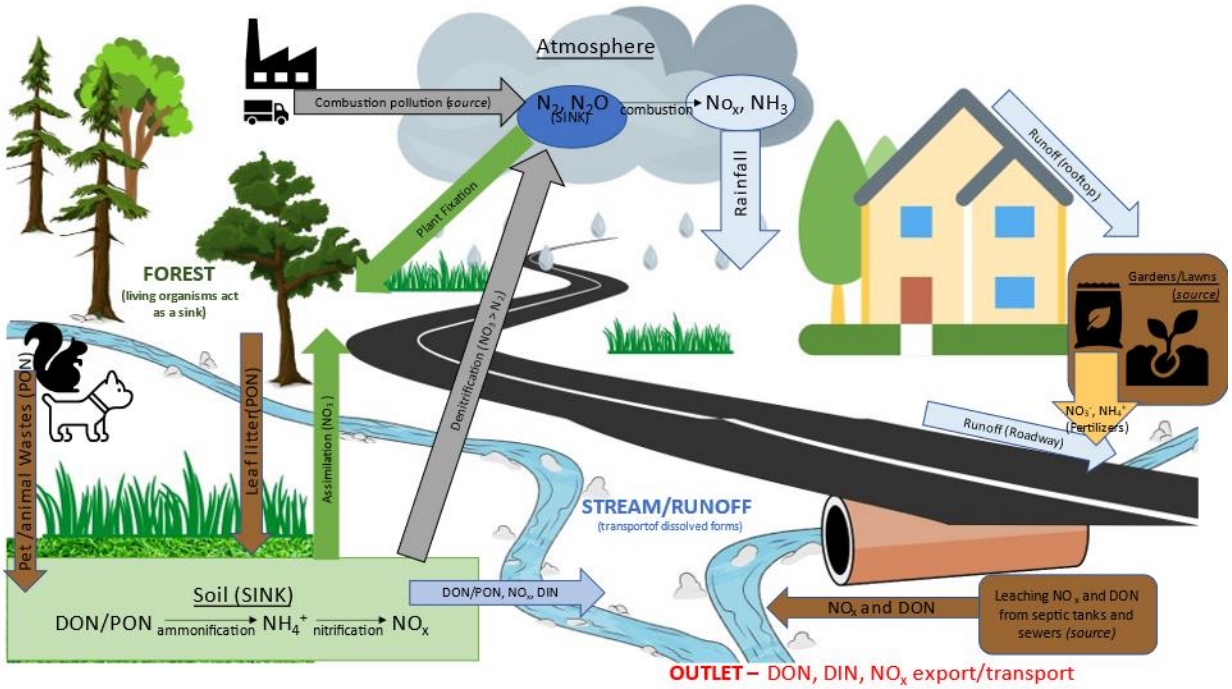

Figure 1.2 Nitrogen sources and sinks in an urban watershed.

ammonium (NH4+) to nitrite (NO_2^-) and then nitrate (NO_3^-), and is affected by soil temperature, pH, moisture content, and aeration (Sahrawat, 2006).

Proper function of the N cycle requires a balance of each of these reactions; this becomes incredibly difficult with excess anthropogenic inputs. An excess of decaying matter without appropriate biological storage, plant assimilation/uptake demand, or conditions for denitrifying bacteria can act as a source. Understanding the contexts that impact the rates and efficiency of these mechanisms is important to understanding the complex picture of nutrient cycling as well as the ecological function of different urban ecosystem contexts.

The fate of nitrogen species in the watershed refers to both the ultimate transport destination/receiving water body and the microbially driven reactions and transformations, or mechanisms, resulting in the nitrogen cycle. Physical attributes such as geomorphology, soil characteristics, and vegetation type and density can impact hydrology in urban ecological conditions, creating variations in temperature and retention times and subsequently impacting reaction rates (Tank et al., 2007; Reisinger et al., 2016). Biological activity can be increased by increased access to sunlight, increased mixing/contact with sediment, increased retention time, increased temperatures, (Peterson et al., 2001; Roberts et al., 2007; Reisinger et al., 2019; Tank et al., 2007). For these reasons, shallow headwater streams with lower flow rates tend to have increased rates of N uptake (Alexander et al., 2001). Availability of other limiting nutrients, such as phosphorus, can also impact the uptake potential of the biota; for this reason, nutrient ratios such as N:P ratio can support or impede uptake rates (Bernet and Dodds, 2005).

Microbiome in Ecohydrology

The microbiome is the unseen operator of our natural world, making a vast portion of biosphere and driving nutrient processes and transformations (Lovely, 2003). Microbial communities are intricately connected to ecohydrology concepts, influencing and being influenced by the interplay of water and ecological processes. These microorganisms play pivotal roles in nutrient cycling, organic matter decomposition, and biogeochemical transformations within aquatic

ecosystems. Their activities contribute to the regulation of water quality, including nutrient levels and pollutant degradation (McLellan et al., 2015).

Natural selection of communities based on resilience to change in environmental parameters, as well as available nutrients and organics, present different potential patterns of microbial assemblage (Lovley, 2003). In turn, ecohydrological factors such as precipitation patterns, soil moisture, and temperature impact microbial community composition, diversity, and function. These factors are increasingly impacted by urbanization. Therefore, understanding this dynamic interaction is essential for unraveling the complexities of ecohydrological processes and developing sustainable water resource management strategies. Overall understanding of the urban microbiome is underdeveloped within the fields of microbial ecology and environmental engineering. More research in this field is needed in order to harness our understanding of the impacts of urbanization on ecohydrological processes through the interactions of the microbial community.

Hydrological and Biological Connectivity and the Lineage of Lotic Ecosystem Theory

Connectivity is the uniting concept of hydrology. Connectivity controls the flow of resources – water, pollutants, sediments, and nutrients – through a watershed. Water resource engineering most commonly refer to impervious connectivity when designing stormwater conveyance infrastructure, however connectivity can also be considered a "dimension of ecosystem complexity", as was eloquently phrased by Cadensasso et al. (2006). Ecosystem services provided by connectivity between resources and organisms are very sensitive to fluctuations, and ecosystem health is often dependent on stable patterns of hydrologic connectivity. Connectivity sees variation in mode, magnitude, timing, and duration; for example, antecedent moisture levels will determine the timing and mode of hydrologic connectivity; as precipitation fills soil cavities, overland flow dominates infiltration resulting in episodic surface connectivity. Drier periods, by contrast, will result in dominance of slower groundwater connectivity. These fluctuations in connectivity in turn impact the connection of resources and organisms, creating a feedback between the rise and fall of water in the floodplain and the "morphological, anatomical,

physiological, phenological, and/or ethological adaptations of the biota utilizing the floodplain habitats" (Junk *et al*., 1989).

This impact of hydrologic connectivity on ecosystem function has been discussed in the literature with several different conceptual models. With increased access to data over time, these conceptual models build off of each other forming a philosophical foundation for lotic ecosystems. In one of the most influential papers in stream science of the twentieth century, the River Continuum Concept (RCC) portrays stream ecosystems as longitudinal unidirectional networks where headwater conditions impact downstream water quality and ecosystem adaptations (Vannote et al., 1980). This built off of the energy equilibrium theory employed by fluvial geomorphologists, predicting that downstream food webs derived organic matter from upstream sources washing downstream. The RCC additionally states that the functional characteristics of stream ecosystems adapt to the "mean state of the physical system". The idea of rivers and lotic systems behaving longitudinally, where upstream nutrient sources influence downstream communities in a linear continuum, has been criticized as overlooking the lateral and vertical dimensions of floodplain connectivity (Junk et al., 1989).

The Flood Pulse Concept (FPC), or pulse-shunt concept, describes how the diffuse infiltration of precipitation, and subsequent drainage through the landscape, results in the transport of dissolved organic matter (DOM) from within the floodplains to receiving streams and rivers. These "hydrologically activated pulses" of nutrient transport are driven by large precipitation or snowmelt events. Larger and higher intensity events are responsible for a greater push or "shunt" of DOM into downstream, higher order rivers due to increases in velocity and decreases in hydrologic residence time. In fact, studies have found the majority of DOC export to occur during hydrologic events, with as much as 60% of export resulting from higher intensity storms/melts making up less than 20 of a 365 day calendar year (Raymond and Saiers, 2010), meaning a disproportionately low amount of DOM transports during baseflow.

The lateral and vertical connectivity of a floodplain to its stream, as well as the longitudinal nature of the gravitational pull of water from higher to lower potential, demonstrates well that

rivers are not simply the conduits of flowing water represented by blue lines drawn on a map. The rise and fall of water in the floodplain, the timing and duration of its presents impacts the biological communities of these ecosystems. Hydrologic connectivity, and the subsequent movement of nutrients in the form of DOM as well as anthropogenic nutrients like dissolved fertilizers, also allows for species and resource transfer. As the DOM and other dissolved nutrient species fuel the biochemical functions, the presence of particular ratios of nutrient sources will result in the assemblage of varying microbial community structures (Lovley, 2003). Thus, hydrologic connectivity forms a distribution network for food and microbial communities between segments of a watershed, playing a vital role in community composition and biodiversity (Cohen et al., 2016).

Riverine Ecosystem Synthesis (RES), a framework for conceptualizing the dimensional complexities of river networks and ecological systems across geospatial and temporal spans, integrates the longitudinal methods of the RCC and the lateral/vertical perspective of the FPC with modern perspectives from fluvial geomorphologists and ecologists (Thorp et al., 2006) Through the RES approach, river networks can be understood as a compilation of 'hydrogeomorphic patches', where the chemio-physical conditions distinguished by geomorphology and climate create variations in the mode, duration and magnitude of hydraulic connectivity. The feedback between these geospatial patches with varying connectivity, flow regimes, and flow histories and the subsequent biota result in ecological 'functional process zones'.

Examples of these zones/patches include constrained headwaters, constrained lowlands, meandering reaches, floodplains, upland forests (Thorp et al., 2006). The distinct variations in temporal responses to hydrologic events creates different ecoregions with altering biotic responses. For example, headwater regions are often understood to be higher elevation with steeper slopes resulting in faster drainage. The higher election may also indicate a deeper water table and increased storage capacity. The vegetation of the zone may also make a difference in its broader ecological function; a forested headwaters region will likely contribute a greater volume of DOM during rain events compared to a craggy, bedrock exposed headwaters region.

These zones, which are initialized by abiotic criteria, are further distinguished by the activities of heterotrophic and autotrophic communities. A community of beavers, for example, may increase channel complexity through the formation of dams, impacting both the fluvial mechanics of the water column by slowing or diverting flow and the input of POM through the addition of woody debris. A floodplain with high duration and frequency of inundation may give rise to clusters of species such as freshwater mussels, as the increased connectivity allows for the dispersal or mussel larvae and the build up of substrate for their habitat and nutrients. Autotrophic communities also create and respond to hydrogeomorphic conditions such as water flow and stability, availability of sunlight, and nutrient composition. It is more likely for sunlight to penetrate in more streams of more shallow depth, allowing benthic vegetation. Fast moving, deeper waters are conversely less suitable for primary production. Vegetated stream beds may slow water flows, increasing stability. A stream corridor lined with trees may also limit access to sunlight and inhibit growth of single cell primary producers like algae, cyanobacteria, and diatoms.

The RES framework can be used to communicate about zones of a stream or river network with more information than arbitrarily breaking the stream into linear reaches. It also gives scientists the opportunity to forecast downstream ecosystem functional responses to upstream climatic stimuli. More research is needed in order to accurately model the hierarchy of ecological function for different spatio-temporal patches (Thorp et al., 2006), but RES is useful for conceptually understanding the complexity of bio-interactions central to ecohydrology and appropriately scaling potential impacts of water resources engineering efforts on environmental processes.

In the twenty-first century, the struggle to accurately model anthropogenic nutrient pollution transport phenomenon for remediation efforts has led to the Hot Spot Hot Moment or Ecosystem Control Point (ECP) theory (McClain et al., 2003; Bernhardt et al., 2016). The observation from the FPC that nutrient diffusion is a highly temporally regulated process with precipitation events driving disproportionately large ecosystem nutrient “flushes”, paired with the understanding of geospatial and temporal variability in nutrient transport due to intricacies of geomorphology and

connectivity from RES, gives a framework for why ephemeral points in time-space (or Ecosystem Control Points) are observationally shown in literature to drive the flow of elements through an ecosystem. The impact of connectivity on the timing of the delivery of resources within a watershed can be seen by examining the timing of increased concentrations of pollutant loads. This is exemplified by the first-flush effect, where pollutants built up on impervious surfaces are removed by precipitation during a storm and quickly delivered to receiving water bodies via impervious drainage conveyance. A study by Flint and Davis (2007) revealed nitrogen species frequently exhibited first flush behavior.

While impervious connectivity perpetuates increased concentrations of nitrogen pollution, increasing connectivity between a stream and its floodplain or riparian corridor increases opportunity for nitrogen removal (Wolf et al., 2013). McMillan and Noe (2017) showed that increased hydrologic connectivity via inundation of the floodplain resulted in a gradient increase of nutrient transformations. This is due to increased residence time and surface area for biological treatment. Progressive urban stormwater management practices attempt to model floodplain connectivity through green infrastructure. Green infrastructure (GI) is a method to slow stormwater surges in urban landscapes by providing opportunity for infiltration during storm events, effectively disrupting impervious connectivity. In a review of the impact of best management practices on water quality, bioretention systems showed a median total nitrogen reduction of 49% (Liu et al., 2017). GI practices also serve the role of increasing storage capacity in urban areas. This is important for decreasing runoff depth during high volume storm events and mitigating risk of flooding.

Urban Ecohydrology: Synthesis

Urban systems tend to disrupt connectivity between ecosystem resources and services with the development of impervious surface. The connectivity of impervious surface, which has been quantified as effective impervious area, contributes to the perpetuation of pollution and of altered hydrologic response to storm events. This, in the face of climate change, results in increased risk of flooding. Connectivity of urban streams to their (now paved over) floodplains can be

mimicked by the installation of green infrastructure practices, as well as through the restoration of riparian zones. These management practices increase storage to decrease runoff volume, slow storm surges, and increase opportunity for pollutant removal such as nitrogen.

Water resource management in urban systems have traditionally been designed to efficiently move water out of streets and away from homes and businesses, effectively removing connectivity between the floodplain and the receiving water body. Due to these most immediate needs, urban centers show high connectivity of impervious stormwater infrastructure. For this reason, urban hydrologists tend to focus on connectivity of impervious land types. While this perspective is helpful in quantifying and remediating negative impacts of urbanization on stream health, hydrologists must consider the positive implications of floodplain connectivity in order to obtain a holistic understanding of a watershed function. Hydrologic connectivity leads to increased storage capacity and reliability of storage during rain events, resulting in decreased flood risk, decreased peak flows, and increased consistency of hydrologic regimes for aquatic biota. Increased retention times resulting from increased storage lead to increased potential for biological removal or uptake of pollutants and nutrients.

Understanding the framework of biological and hydrologic connectivity in tandem with ecohydrology, we begin to tease apart a framework for understanding catchment response to anthropogenic shifts in environmental conditions. Water is on a continuous journey, and on every segment of that journey – condensing until freefall through the atmosphere, traversing gray stormwater conveyance infrastructure, infiltrating into a heavy metal contaminated urban lawn, or falling through a forest canopy and transpiring back to the atmosphere before ever touching the ground – the molecule encounters microbial and chemical evidence of the place it has encountered. In this way, the watershed holds a memory. Insights about the recent history of a molecule can be obtained from analyzing the signature of these chemical and microbial interactions.

Urbanization impacts the hydrosphere through adjustments to hydrologic response, through implications of urban areas on local climate, and through adjustments to vegetative density and

tree canopy cover. Through these mechanisms, the urban landscape introduces particular implications on hydrologic function and interactions between the hydrosphere with biological life. As such, water in an urban environment encounters additional ecosystem 'functional process zones'. Examples include: (1) road side drainage ditches that remain dry until surging with runoff during storm events, (2) residential lawns with highly impacted soils and short rooting zones, (3) novel green infrastructure installations such as step pools and rain gardens, and (4) urban recreational forested areas which provides rainfall interception heat island mitigation, and other canopy cover benefits—all of which play a role in the nutrient transformations and pathways taken by organic and anthropogenic nutrient inputs on their journey downstream. As water interacts with these different micro-ecosystems, it meets different geochemical constituents and organisms, carrying with it a signature of what it has encountered through the isotope composition of the geochemical constituents it carries and through the functional diversity of the microbial community.

Knowledge Gaps & Contributions

This dissertation will explore one urban watershed containing each of the example functional zones described above through the lens of stable isotope geochemistry and microbial community assembly. The dissertation contains three chapters focusing, in short, on (1) identifying ecological trends in the sources and concentrations of nitrate, (2) the response of the microbial community and drivers of assembly along the gradient from urban forest to high developed zones, and (3) applications of microbial source tracking to distinguish between runoff generated from these unique functional zones. The field of the urban microbiome is underdeveloped, and researchers are still investigating the environmental drivers of microbial community assembly in the urban landscape, as well as the specific responses of the communities. We hypothesize that community assembly in the water column is more responsive to landscape changes, but this has yet to be validated (Hosen et al., 2017). The quantification of stochastic assembly processes in water column microbial communities remains unexplored in both urban and pristine streams. Likewise, there is a lack of thorough investigation into the impact of stormwater on microbial community assembly. Understanding how these ecological assembly processes respond to the

environment and impact variability in nutrient pollution is paramount to advancing watershed remediation strategies.

These three chapters will address existing knowledge gaps by investigating the following research questions:

1. How does nitrate source indicated by stable isotope analysis change by land use, season, and the onset of wet weather?
2. How does microbial community assembly respond to urbanization of forested headwater streams? Are communities in urban reaches more or less impacted by deterministic assembly, and what environmental parameters play major roles?
3. Can microbial community fingerprints of runoff from different landscapes be effective at partitioning a hydrograph during a storm surge?

REFERENCES

Bailey, R.G., Avers, P.E., King, T., and McNab, W.H., eds., 1994, Ecoregions and subregions of the United States (map) (supplementary table of map unit descriptions compiled and edited by McNab, W.H. and Bailey, R.G.): Washington, D.C., U.S. Department of Agriculture - Forest Service, scale 1:7,500,000.

Bernhardt, E. S., & Palmer, M. A. (2007). Restoring streams in an urbanizing world. *Freshwater biology*, *52*(4), 738-751.

Burris, R. H., & Roberts, G. P. (1993). Biological nitrogen fixation. *Annual review of nutrition*, *13*(1), 317-335.

Cadenasso, M. L., Pickett, S. T. A., Groffman, P. M., Band, L. E., Brush, G. S., Galvin, M. F., ... & Troy, A. R. (2008). Exchanges across land-water-scape boundaries in urban systems: Strategies for reducing nitrate pollution. *Annals of the New York Academy of Sciences*, *1134*(1), 213-232.

Cortex, J. (1997). Field Decomposition of Leaf Litters: Relationships Between Decomposition Rates and Soil moisture, Soil Temperature and Earthworm Activity. *Soil Biol. Biochem*. Vol. 30, 6. 783-793. PII: S0038-0717(97)00163-6

Ehleringer, J. R., Roden, J., & Dawson, T. E. (2000). Assessing ecosystem-level water relations through stable isotope ratio analyses. In *Methods in ecosystem science* (pp. 181-198). New York, NY: Springer New York.

Firestone, M. K. (1982). Biological denitrification. *Nitrogen in agricultural soils*, *22*, 289-326.

Förstner, U., Ahlf, W., Calmano, W., & Kersten, M. (1990). Sediment criteria development: contributions from environmental geochemistry to water quality management. In *Sediments*

and environmental geochemistry: selected aspects and case histories (pp. 311-338). Berlin, Heidelberg: Springer Berlin Heidelberg.

Groffman, P.M., N.L. Law, K.T. Belt, et al. 2004. Nitrogen fluxes and retention in urban watershed ecosystems. Ecosystems 7: 393–403.

Harper, H. H. 1994 " Stormwater Loading Rate Parameters for Central and South Florida." Revised.

Hunt, A. G. (Allen G., Egli, M., & Faybishenko, B. (Eds.). (2021). *Hydrogeology, chemical weathering, and soil formation*. John Wiley & Sons, Inc.

Jefferson, A. J., Bhaskar, A. S., Hopkins, K. G., Fanelli, R., Avellaneda, P. M., & McMillan, S. K. (2017). Stormwater management network effectiveness and implications for urban watershed function: A critical review. *Hydrological Processes, 31*(23), 4056-4080.

Lear. (1990) *Inside Rain: A Look at the National Atmospheric Deposition Program* [Brochure]. Citizen Printing, Fort Collins, Colorado. https://nadp.slh.wisc.edu/wp-content/uploads/2021/05/insideRain.pdf

Makepeace, D. K., Smith, D. W., & Stanley, S. J. (1995). Urban stormwater quality: summary of contaminant data. *Critical Reviews in Environmental Science and Technology*, *25*(2), 93-139.

McLellan, S. L., Fisher, J. C., & Newton, R. J. (2015). The microbiome of urban waters. *International microbiology: The official journal of the Spanish Society for Microbiology*, *18*(3), 141.

Melosi, M.V. 2000. The Sanitary City: Urban Infrastructure in America from Colonial Times to the Present. Johns Hopkins University Press. Baltimore , MD .

Paerl, H. W. (2009). Controlling eutrophication along the freshwater–marine continuum: dual nutrient (N and P) reductions are essential. *Estuaries and Coasts*, *32*, 593-601.

Randall, C.W.; Ellis, K.; Grizzard, T.J.; and Knocke, W.R. 1982. "Urban Runoff Pollutant Removal by Sedimentation. " Proceedings of the Conference on Stormwater Detention Facilities, ASCE.

Sahrawat, K. L. (2008) Factors Affecting Nitrification in Soils, Communications in Soil Science and Plant Analysis, 39:9-10, 1436-1446, DOI: 10.1080/00103620802004235

Shuster, W. D., Bonta, J., Thurston, H., Warnemuende, E., & Smith, D. R. (2005). Impacts of impervious surface on watershed hydrology: A review. *Urban Water Journal*, *2*(4), 263-275.

Stark, J.M. (2000). Nutrient Transformations. In: Sala, O.E., Jackson, R.B., Mooney, H.A., Howarth, R.W. (eds) Methods in Ecosystem Science. Springer, New York, NY. https://doi.org/10.1007/978-1-4612-1224-9_15

Strock, J. S. (2008). Ammonification. In *Encyclopedia of ecology, five-volume set* (pp. 162-165). Elsevier Inc..

Thilagavathi, R., Chidambaram, S., Prasanna, M. V., Thivya, C., & Singaraja, C. (2012). A study on groundwater geochemistry and water quality in layered aquifers system of Pondicherry region, southeast India. *Applied water science*, *2*, 253-269.

Trowsdale, S. A., & Simcock, R. (2011). Urban stormwater treatment using bioretention. *Journal of Hydrology*, *397*(3-4), 167-174.

U.S. Department of Agriculture - Soil Conservation Service, 1981, Land resource regions and major land resource areas of the United States: Agriculture Handbook 296, 156 p

USEPA (US Environmental Protection Agency). 1990. National pesticide survey: nitrate. Office of Water, Office of Pesticides and Toxic Substances. Washington , DC .

Vico, G., Manzoni, S., Palmroth, S., Weih, M., & Katul, G. (2013). A perspective on optimal leaf stomatal conductance under CO2 and light co-limitations. Agricultural and forest meteorology, 182, 191-199.

Vitousek, P.M., J.D. Aber, R.W. Howarth, et al. 1997. Human alteration of the global nitrogen cycle: sources and consequences. Ecol. Appl. 7: 737–750.

Wanty, R. B., Goldhaber, M. B., Morrison, J. M., & Lee, L. (2009). Regional variations in water quality and relationships to soil and bedrock weathering in the southern Sacramento Valley, California, USA. *Applied Geochemistry*, *24*(8), 1512-1523.

Xu, G., Fan, X., & Miller, A. J. (2012). Plant nitrogen assimilation and use efficiency. *Annual review of plant biology*, *63*, 153-182.

CHAPTER 2

URBAN FOREST UPLANDS DRIVE NITROGEN DYNAMICS IN HETEROGENEOUS URBAN WATERSHEDV—STABLE ISOTOPE STUDY

This article was written primarily by Victoria Rexhausen with revisions from Jon Hathaway and Anna Szynkievics.

2.0. ABSTRACT

Understanding complex biogeochemical processing and transport phenomena is one of the crucial problems facing the field of water resources today. Nitrogen cycling is an incredibly complex process which gains further complexity in the context of urban stream ecohydrology. Until recent years, specific ways that urban development impacts stream biogeochemistry remained in the dark. Studies investigating N retention and flux in urban watersheds have revealed that urban landscapes tend to function as net exporters of nutrients. (Baker et al., 2001; Groffman et al., 2004; Pellerin et al., 2012) High frequency monitoring studies of nutrient and hydrologic flux have revealed sophisticated seasonal, diurnal, and event-based patterns of in-stream nitrate concentrations and nutrient processes that may have been dismissed as "environmental and sampling noise" in studies with intermittent sampling methods. (Jordan et al., 2005; Duncan et al., 2017; Pellerin et al., 2012; Vaughan et. al 2017). Even with this increased information, inconsistencies in the speculated reasoning behind the observed trends speaks to gaps in knowledge about the complex nature of whole-catchment biogeochemical dynamics.

This case study on a small urban watershed seeks to understand catchment-scale patterns in sources of dissolved NO_3^- in a heterogeneous urban watershed. Three hydrologic monitoring sites and 21 baseflow sampling sites were established throughout a 1,664 acre urban catchment with headwaters in a recreational forest preserve. Baseflow and storm flow samples were collected from four seasons and analyzed for NO_3^- concentration as well as $NO_3^-$and SO_4^{2-} stable isotope composition. The study findings reiterated literature in that the biggest driver of high N flux is high flow rates in highly imperviously connected urban streams but determined that stormwater was an insignificant source of dissolved NO_3^- in Baker Creek. Results show that seasonal trends drive excess NO_3^-, and that the primary sources are soil building denitrification and remineralization processes. These findings challenge prevailing assumptions regarding the

relationship between increased nitrate concentrations and nonpoint source pollution in urban ecosystems, highlighting the need to improve regulatory considerations for first order urban streams.

2.1. INTRODUCTION

Nitrogen plays a vital role in aquatic ecosystems. In the last several decades, humans have doubled nitrogen inputs to the biosphere (Mulhammod, 2009). The ecological consequences of heightened reactive nitrogen introduced to watersheds by agricultural and urban runoff have prompted a surge in nitrogen-focused studies and the implementation of government-sanctioned programs to address these issues. Operating under the Clean Water Act (CWA), the US Environmental Protection Agency (EPA) manages the 303(d) list to identify compromised streams and the Total Maximum Daily Load (TMDL) protocol to tackle impaired waters. These programs are often based on a limited number of samples from a conservative number of sample points within the watershed. The efficacy of TMDL plans is a matter of contention; these plans are costly, ranging $4,000 to $1 million (Birkeland, 2001), and are based on limited information with no guarantee of positive impacts. This is particularly the case for TMDL plans designed for nutrient pollutants-- substances that undergo a complex web of interactions that, in some cases, are unpredictable and highly sensitive to environmental parameters.

The intricate interplay between geomorphologies, land use, and land cover create spatial and temporal variations in nutrient and organic matter supply to streams and rivers (Rode et al., 2016; Carey et al., 2014). Streams located in urban areas are at increased risk for nitrogen pollution due to anthropogenic inputs, including nitrogen fertilizers applied to lawns, pet waste, or leaky septic systems. Urban streams have decreased assimilatory and dissimilatory uptake potential due to flashy flow regimes, eliminated riparian zones, and reduced infiltration (Rode et al., 2016). Moreover, the increased prevalence of impervious surfaces in urban watersheds reduces water retention by interrupting stormwater infiltration, thereby amplifying the volume and rate of surface runoff delivered to streams (Epps, 2018). The diminished ecologically functioning area and shallower rooting zone depths in lawns, in comparison to undisturbed forests and meadows, contribute to a reduction in the pretreatment of surface runoff (Wollheim, 2005; Leopold, 1968).

Scientific advancements have significantly enhanced our capacity to investigate temporal patterns in nitrate (NO_3^-) uptake and flux in urban spaces, as well as identify sources of in-stream dissolved nitrate. For instance, high frequency monitoring has unveiled patterns in nutrient fluxes that may be linked to seasonal drivers, which may have been dismissed as environmental noise in studies relying on intermittent sampling methods (Jordan et al., 2005). Stable isotope composition of dissolved nitrate has been used in water resources engineering to approximate nitrogen pollutant source contributions (Kaushal et al., 2011; Baral et al., 2018). However, these sophisticated techniques are seldom available for the initial EPA 303(d) assessment due to their extensive requirements. This limitation implies that instances of elevated of nitrate loads recorded in a 303(d) report may have ecological explanations, and there is no way to verify that dissolved nitrate loads are indeed from anthropogenic sources prior to developing a TMDL plan.

This study takes a detailed approach to understanding the distribution of nitrate concentrations and sources throughout a heterogeneous watershed with a forest-to-urban gradient listed on the 303(d) list for nitrate pollution in the state of Tennessee. The investigation utilizes stable isotope analysis of $\delta^{15}N$ and $\delta^{18}O$ of NO_3^- and $\delta^{18}O$ and $\delta^{34}S$ of dissolved SO42- over a broad distribution of sampling sites to determine (a) the primary source of NO_3^- to different reaches of the watershed, (b) potential seasonal and geospatial variability in NO_3^- sources and concentrations related to land use.

Few studies have endeavored to identify both spatial and temporal variations in nutrient concentrations and sources in mixed land-use watersheds, creating a literature gap in the exploration of inner-catchment interactions between subcatchments of such areas. Most studies investigating inner-catchment NO_3^- behavior use a linear sampling pattern, providing information solely about the changes in NO_3^- flux along a specific reach of the stream. In contrast, this study observes geospatial dependencies in NO_3^- concentrations and sources. There is a lack of studies investigating seasonal inner-catchment trends in nitrate cycling in the Southeastern region of the United States where rainfall dominates hydrologic processes (Stoddard 1994). The majority of studies cite snowmelt as a major driver of seasonal nitrogen input, which is not relevant to watersheds of this region. Moreover, many studies employing

stable isotope analysis of dissolved NO_3^- did not investigate seasonal differences in NO_3^- sources, or compare results to NO_3^- dissolved in different types of runoff endmembers for a thorough analysis of source.

2.2. METHODS

2.2.1. Site Description

This study was conducted in the 6.73 km^2 Baker Creek (BC) catchment within the Tennessee River watershed located in Knoxville, TN, in the valley and ridge geological region at approximately 275 m above sea level. The area is characterized by its hilly terrain with deep, well-draining, clayey and loamy Telico-Alcoa soils and is underlain with calcareous sandstone and sandy limestone (US Soil Conservation Service, 1981). Knoxville receives an average annual rainfall of 1270 mm. The BC catchment encompasses urban terrain with the exception of a forested headwaters region, home to a recreational preserve heavily trafficked by hikers and mountain bikers. The forested area is home to 89% deciduous trees, 6% evergreen trees, and 4% mixed forest types. As the BC stream transitions into urban terrain, it meanders under a four-lane highway and through suburban neighborhoods characterized by low and medium density development, featuring grassy land covers in the form of residential lawns and several small parks.

2.2.2. Sample Collection

Baseflow sampling sites (#1 – 21 in Figure 2.1) and three hydrologic and stormflow quality monitoring sites (#4, 9, and 21) were strategically placed across the BC watershed. These hydrologic monitoring stations were positioned at key locations: the main discharge point of the forest preserve (FOR), at the outlet of an urban drainage point (URB) with a comparably sized drainage area to that of FOR, and further downstream where the drainage areas of FOR, URB, and a highly developed four-lane highway, converge (COM).

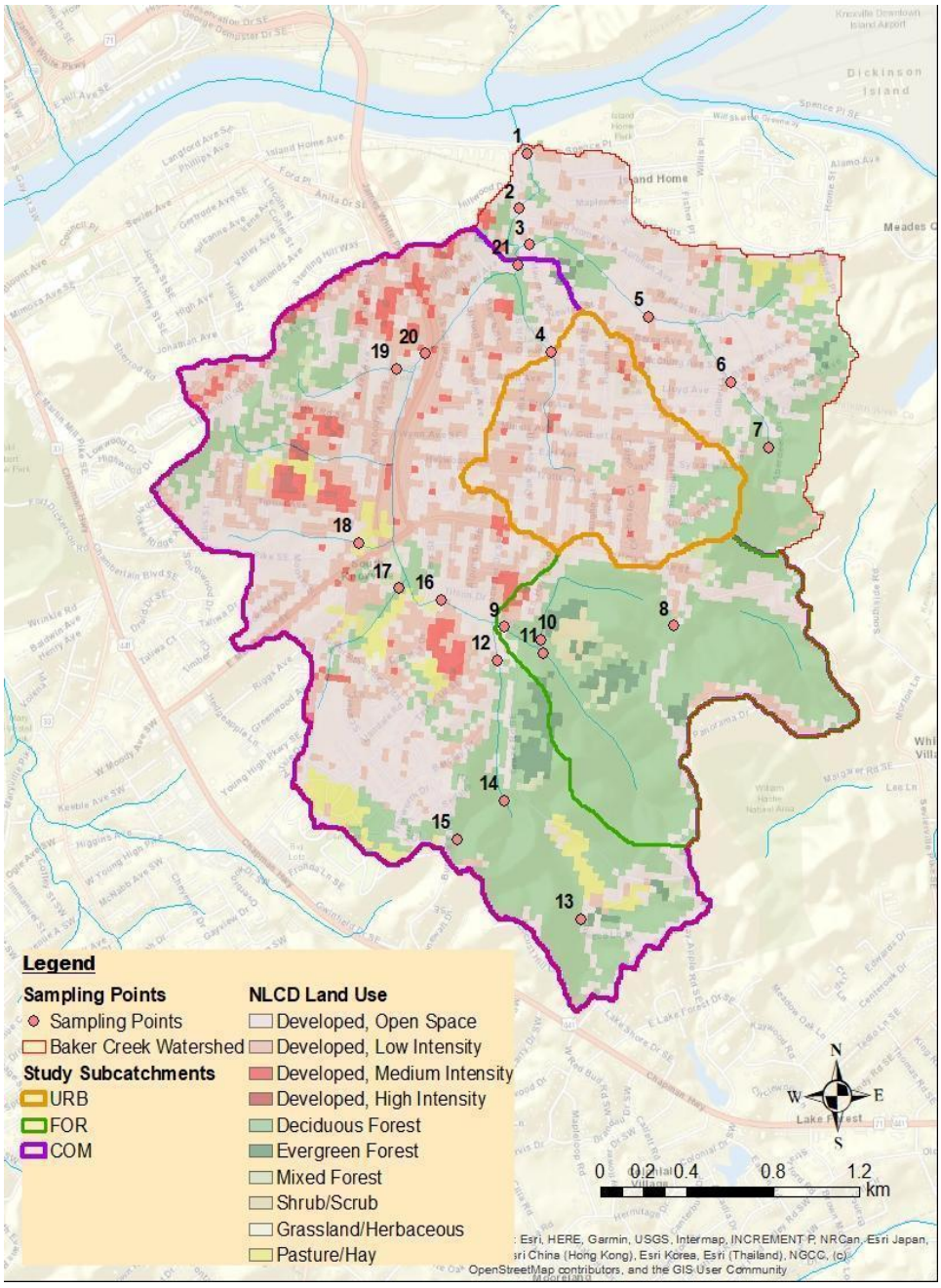

Figure 2.1 Map of the study site labeled with sampling points and monitoring sites and a land use layer adopted from the US Geological Survey national land cover database (NLCD) (source: https://www.usgs.gov/centers/eros/science/national-land-cover-database).

Velocity measurements from a Teledyne ISCO 2150 Area Velocity Doppler flow meter were used to create a stage discharge relationship for each monitoring site. A 730 bubbler flow module was then used to record stage discharge data at a 1-minute interval which was converted to flow using this relationship. Each monitoring site has a manual and an automated tipping bucket rain gauge which recorded rainfall intensity at 5-minute intervals. Average temperature data was taken from the McGhee Tyson weather monitoring station located 19 km away. Drainage area for each sampling site was determined using the watershed delineation tool in ArcGIS 10.6.1 using a 1 m resolution digital elevation model (DEM) layer of Knox County. Land use statistics were obtained by clipping the USGS 2016 NLCD land use layer to the delineated subcatchments. Table 2.1 describes the characteristics of each studied subcatchment.

Monitoring sites were established within concrete drainage infrastructure so that cross sections would remain constant for area-velocity calculations (Figure 2.2). The URB's monitoring equipment was attached to a spring ring inside a 1.2 m diameter culvert which directly routed runoff from drainage infrastructure primarily located along residential streets. Sheet flow runoff from houses and lawn contributes directly into these drains that empty into Baker Creek at the URB site. Because this monitoring station was at the very beginning of the stream reach, the flow was often undetectable in this culvert when not raining, especially in the summer months when tall vegetation blocked any potential flow. The FOR's monitoring equipment was mounted to a concrete paving stone and lodged into the stream bed of a double barrel elliptical roadway underpass with a height of 1.2 m and a width of 2.4 m. A bubbler flow module was used in each elliptical conduit to verify the level was equal between the two, and thus the stage discharge relationship was assumed to be equal. The COM's monitoring equipment was also mounted to a concrete paving stone which was placed inside an elliptical roadway underpass that was 2.4 m tall and 4.9 m wide. The concrete paving stones were 5 cm in height, and were accounted for in the calibration of the bubbler and doppler velocity flow modules.

Baseflow discharge rates were calculated for each site by using a rolling average baseflow separation method similar to that discussed by Smakhtin (2004). Composite curve number was

Table 2.1 Land use characteristics and baseflow of sampling sites. Curve numbers for each subcatchment were calculated using the TR-55 cover descriptions based on the NRCS land cover ratios in each drainage basin.

Monitoring Site	Catchment Size (km^2)	% Developed	% Forested	Curve Number	Total EIA (%)	Average Baseflow (m^3/s)
URBAN (URB)	0.8	90.0	8.9	70	5.9	0.10
FOREST (FOR)	1.3	18.7	79.4	58	1.5	0.02
COMBINED (COM)	6.0	61.2	34.9	65		0.29

Figure 2.2 (a-c) Images 2a, 2b, and 2c show the drainage culverts used to install sites URBAN (URB), FOREST (FOR), and COMBINED (COM), respectively.

calculated for each subcatchment using the land use types provided by the NLCD land cover shown in Figure 2.1. calculated for each subcatchment using the land use types provided by the NLCD land cover shown in Figure 2.1. Effective impervious area (EIA) quantity was estimated for each monitoring subcatchment by analyzing the trends of observed storm event rainfall-runoff depth data while accounting for pervious attenuation using the method described in Epps and Hathaway (2018).

2.2.2.1. Baseflow Sample Collection

Baseflow samples were taken at all 21 sites on 12 separate occasions across all four seasons between July 2017, and January 2021. Samples were collected in 900 mL polypropylene bottles. Prior to field sampling, the bottles were thoroughly cleaned using a bottle brush and then triple rinsed with DI water. In the field, the bottles and lids were rinsed twice with stream water before sample collection. Water samples were taken from a minimum of 12 sites during each sampling campaign. Some sites were dry during baseflow conditions during some sampling campaigns negating the ability to sample. In total, 137 baseflow samples were collected across four different seasons: spring, summer, fall and winter. Details of these sampling efforts are detailed in Table 2.2.

2.2.2.2. Stormflow Sample Collection

Stormflow samples were collected at sites #4, 9, and 21 (MJP, FOR, and COM, respectively) using a 6712 Teledyne Isco Autosampler. Stream water was pumped from the creek into clean 900 mL polypropylene bottles during each event. Before taking each sample, the autosampler double rinsed the tubing line with stream water. The samples were flow paced to allow representative sampling from each stage of the storm, defined herein as: start of the storm, rising limb, peak flow, falling limb, and end of the storm. The flow pacing was modified before each storm to ensure good coverage. Adjustments were based on the anticipated size of the storm, flow responses from previous storms, and a limitation of 24 bottles in the autosampler. If pacing was too small, leading to numerous

Table 2.2 Weather conditions during baseflow sampling events.

Season	Sample Date	Antece-dent Dry Days	Average Daily Tempera-tur (°F)	Daily High (°F)	Daily Low (°F)	Average Weekly Tempera-ture (°F)	Weekly High (°F)	Weekly Low (°F)
Spring	4/15/2020	2	48.6	60.0	41.0	53.0	70.0	35.0
	5/28/2020	5	70.9	79.0	65.0	71.6	86.0	60.0
	6/19/2018	8	83.2	92.0	72.0	80.0	93.9	64.9
Summer	7/7/2020	1	78.8	86.0	72.0	79.0	91.9	68.0
	7/22/2017	7	84.8	96.0	74.0	81.7	96.1	66.9
	9/1/2018	1	73.8	87.0	67.0	77.5	91.0	66.0
Fall	9/22/2020	5	59.2	71.0	49.0	65.5	81.0	46.9
	9/23/2019	26	74.0	85.0	62.0	76.3	91.9	62.1
	11/27/2018	3	31.8	35.0	28.0	42.1	57.9	28.0
Winter	1/20/21	5	42.0	48.0	33.0	39.0	52.0	21.9
	1/27/2020	0	44.8	50.0	38.0	38.1	52.0	18.0
	3/4/2020	1	53.5	63.0	44.0	45.9	69.1	25.0

sample bottles representing a single stage of the storm, several samples were combined to create one sample to best represent that portion of the event. This ensured a representative water sample was collected for each portion of the hydrograph.

In total, 101 total stormflow samples from 14 different storm events over three seasons (Table 1.3) were analyzed for anion concentrations and stable isotope analysis of NO_3^- ($\delta^{15}N$ and $\delta^{18}O$) and SO_4^{2-} ($\delta^{34}S$ and $\delta^{18}O$). Nine of the 14 storm events (Table 2.3), one per season per monitoring site, were represented by 4-5 discrete water samples over the entire storm hydrograph (storm start, rising limb, peak flow, falling limb, and storm end). The rest of the storm events were not prioritized for analysis due to poor sample pacing and/or limited resources for analysis. In summary, the stormflow data from three seasons were compared in this study: spring/early summer (April 1, 2020 to May 22, 2020), late summer/autumn (August 30, 2020 to October 10, 2020), and winter (January 20, 2021 to February 22, 2021).

Table 2.3 Storm event characteristics for the prioritized storms (when full hydrograph was analyzed). Average rainfall intensity was calculated by dividing the storm volume over the duration. The peak stormwater runoff rate (Q) was calculated using the rational equation. Greater storm volume, duration, peak intensity, and average intensity, and antecedent dry day periods are shaded darker than lesser valued characteristics.

Storm Date	Season	Site	Storm Volume (in)	Storm Duration (hr)	Average Rainfall Intensity (in/hr)	Cum. Runoff Depth (in)	% Runoff Captured	Antecedent Dry Period (days)	[NO_3-N] Range (mg/L)
4/20/2020	Spring/early summer	FOR	1	0.73	0.14	0.03	96.9%	2	0.62-0.89
4/20/2020	Spring/early summer	URB	1	0.73	0.14	0.35	64.7%	2	0.44-0.83
4/29/2020	Spring/early summer	COM	0.42	7	0.06	0.13	67.8%	4	0.26-0.83
9/13/2020	Late summer/fall	COM	0.41	6.5	0.06	0.05	88.4%	2	0.49-1.53
9/28/2020	Late summer/fall	COM	0.86	8	0.11	0..03	97.1%	9	1.13-2.49
10/10/2020	Late summer/fall	FOR	1.9	20	0.1	0.32	82.9%	7	0.37-2.15
01/25/2021	Winter	URB	0.94	9	0.1	0.13	86.2%	3	0.79-1.25
2/11/2020	Winter	FOR	0.95	20	0.05	0.04	95.4%	14	1.67-2.69
2/11/2020	Winter	COM	0.95	20	0.05	0.11	88.8%	14	0.68-1.69

2.2.2.3. Endmember Sample Collection

Representative samples of stormwater runoff from 4 different land cover types--Rooftop, Roadway, Grass, and Soil--were taken during 7 storm events from throughout the watershed. Samples were collected from different time points within the storm during each event. Bottles and caps were first rinsed with sampled water from the source before filling and taking to the lab for analysis. The runoff from rooftops was taken from storm gutter discharge from both private residences and public storefronts with owner permission. The roadway samples were taken from the streets where stormwater entered drainage infrastructure. The soil and grass samples were taken from a ponded area within a slight gradient or a grassy swale that was not immediately fed by roadway drainage; soil and grass samples were obtained by laying the bottle horizontally on the ground and slowly filling it with water. In some cases, water was encouraged into the bottle with a sweeping motion.

2.2.3. Laboratory and Data Analysis

Samples were stored in a cooler while being transported to the Science and Engineering Research Facility (SERF) at the University of Tennessee, Knoxville, where they were prepared for analysis. Upon arrival to the laboratory, approximately 45 mL of water sample was immediately filtered with a 0.45 micron luer-loc syringe filter and stored in a -20˚C freezer until analysis in the Stable Isotope Laboratory located in the Department of Earth and Planetary Sciences at the University of Tennessee. Samples were prepared for analysis of anion concentration, stable isotope analysis of of NO_3^- ($\delta^{15}N$ and $\delta^{18}O$), and stable isotope analysis of of SO_4^{2-} ($\delta^{34}S$ and $\delta^{18}O$). Major anion concentrations, including NO_3^-, were determined using a Dionex Ion Chromatograph (ICS-2000).

2.2.3.1. Stable Isotope Analysis

Isotope composition of a sample (δ) is calculated by comparing the ratios of heavy to light isotopes in the sample to an international reference standard and expressed in units of per mil ‰ as follows:

$$\delta(‰) = \left(\frac{R_{sample} - R_{standard}}{R_{standard}}\right) \times 100 \quad (1)$$

where *R* indicates the ratio of heavy to light isotopes. Specifically, R would be ^{15}N:^{14}N and ^{18}O:^{16}O for nitrate or ^{34}S:^{32}S and ^{18}O:^{16}O for sulfate. Isotope composition of NO_3^- was determined using the bacterial denitrifier method after Sigman et al. (1998). In this method, the dissolved NO_3^-/NO_2^- is reduced to nitrous oxide (N_2O) by inoculating the sample with lab-cultured denitrifying bacteria. The ratio of water sample to inoculant is based on the measured nitrate concentration in the sample. The $\delta^{15}N$ and $\delta^{18}O$ of nitrous oxide was analyzed using a Thermo-Scientific Gas Bench II and compared to Air N_2 and VSMOW, respectively.

Samples were combined to volumes between 1 and 4 liters for $\delta^{34}S$ and $\delta^{18}O$ analysis of SO_4^{2-}. Samples were filtered to remove suspended sediment and then acidified to a pH <2 using 10% HCl. Afterward, 10 mL of 10% $BaCl_2$ was added to precipitate the dissolved SO_4^{2-} $BaSO_4$, which was then rinsed several times with DI water. In the end, $BaSO_4$ was analyzed in the Stable Isotope Laboratory in the Earth and Planetary Sciences department at University of Tennessee using a Costech elemental analyzer (EA) for $\delta^{34}S$ and a continuous flow system with a high temperature conversion elemental analyzer (TC/EA) for $\delta^{18}O$. The measured isotope values were reported with respect to Vienna Canon Diablo Troilite (VCDT) for $\delta^{34}S$ and VSMOW for $\delta^{18}O$.

2.2.3.3. Data Analysis

The results were parsed and analyzed based on the sample type (storm, baseflow, or endmember), season, and the land use type or primary subcatchment. This study investigated 5 dependent variables: NO_3 concentration, $\delta^{15}N$ and $\delta^{18}O$ of dissolved NO_x, and $\delta^{34}S$ and $\delta^{18}O$ of SO_4^{2-}.

The RStudio version 2022.02.1+461 "Prairie Trillium" was used to analyze the distribution of datasets and sub-datasets to determine normality using the Shapiro-Wilk's test. Approximately half of the distributions analyzed had a p-value less than 0.05, indicating that a normal distribution could not be assumed. The large number of abnormal distributions and the variation in sample sizes led to the use of nonparametric statistical analyses. The Mann Whitney U test

was used to determine if differences between two datasets were statistically significant. The Mann Whitney U test assumes two independent random samples with at least one ordinally scaled variable. The test assigns ranks by ordering the sample data in both independent groups from smallest to largest, and comparing the sum of the ranks for each group. The Kruskal-Wallis test was also applied to compare outcomes among more than two independent groups. This test was used because sample sizes are small and not equal between comparison groups. The Kruskal-Wallis test assumes independent random samples with a continuous, ordinally scaled variable. Plots and charts were created in Microsoft Excel, Grapher Golden software, and R studio 2022.02.1.

2.3. RESULTS

2.3.1. Hydrologic Regime Characteristics

Hydrologic regimes strongly influence nitrogen cycling in urban watersheds, so it is critical to characterize the catchment's drainage and storm flow (Pellerin et al., 2012). Hydrologic monitoring at the three key drainage points within the Baker Creek watershed revealed distinctive hydrologic responses to storm-events of various sizes as well as characterization of drought periods. Sample hydrographs from the monitoring period can be viewed in Figures 2.3 and 2.4. Site FOREST (FOR) represents the forested headwaters for our study. FOR showed the smallest difference in volumetric flow rate between storm flow

and baseflow conditions due to the higher ratio of pervious surfaces in a smaller catchment.

The site URBAN (URB), a small, developed catchment, is the inception point of the middle branch of Baker Creek fed mostly by drainage infrastructure serving the surrounding residential area. Notably, runoff depths from this site are still comparably small to densely developed land uses, likely due to the low amount of connected imperviousness in the form of roadways. The majority of rooftops were disconnected from the drainage network, instead flowing onto the surrounding landscape. The site COMBINED (COM) exists just downstream of the confluence of left and middle branches of Baker Creek, and contain the FOR and URB subcatchments, respectively. COM, having the largest drainage area, showed the highest baseflow and the

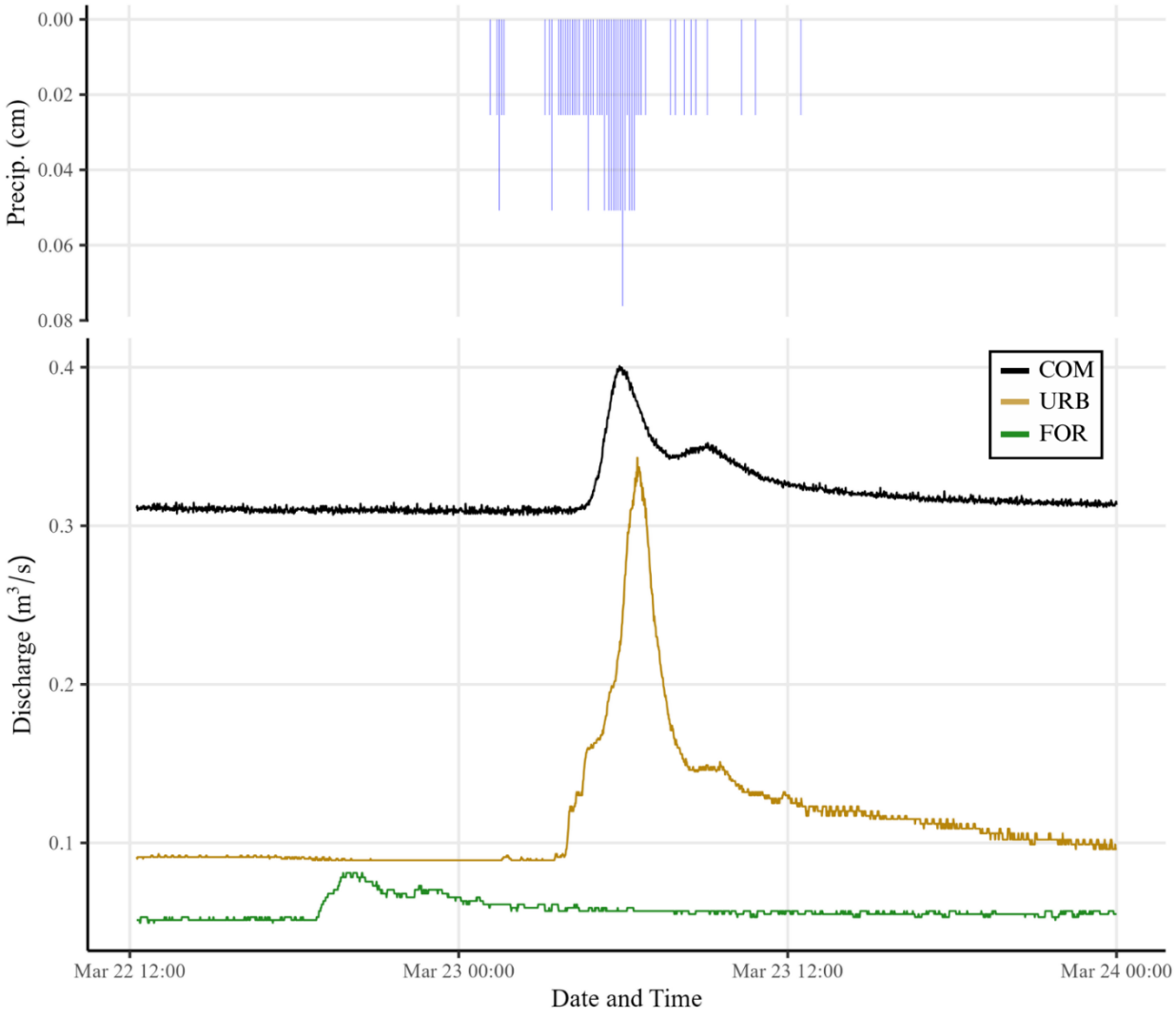

Figure 2.3 Hydrograph and hyetograph for a selection of monitoring data for the 3 hydrologic monitoring stations in BC watershed showing stream response to the storm event on March 23, 2020.

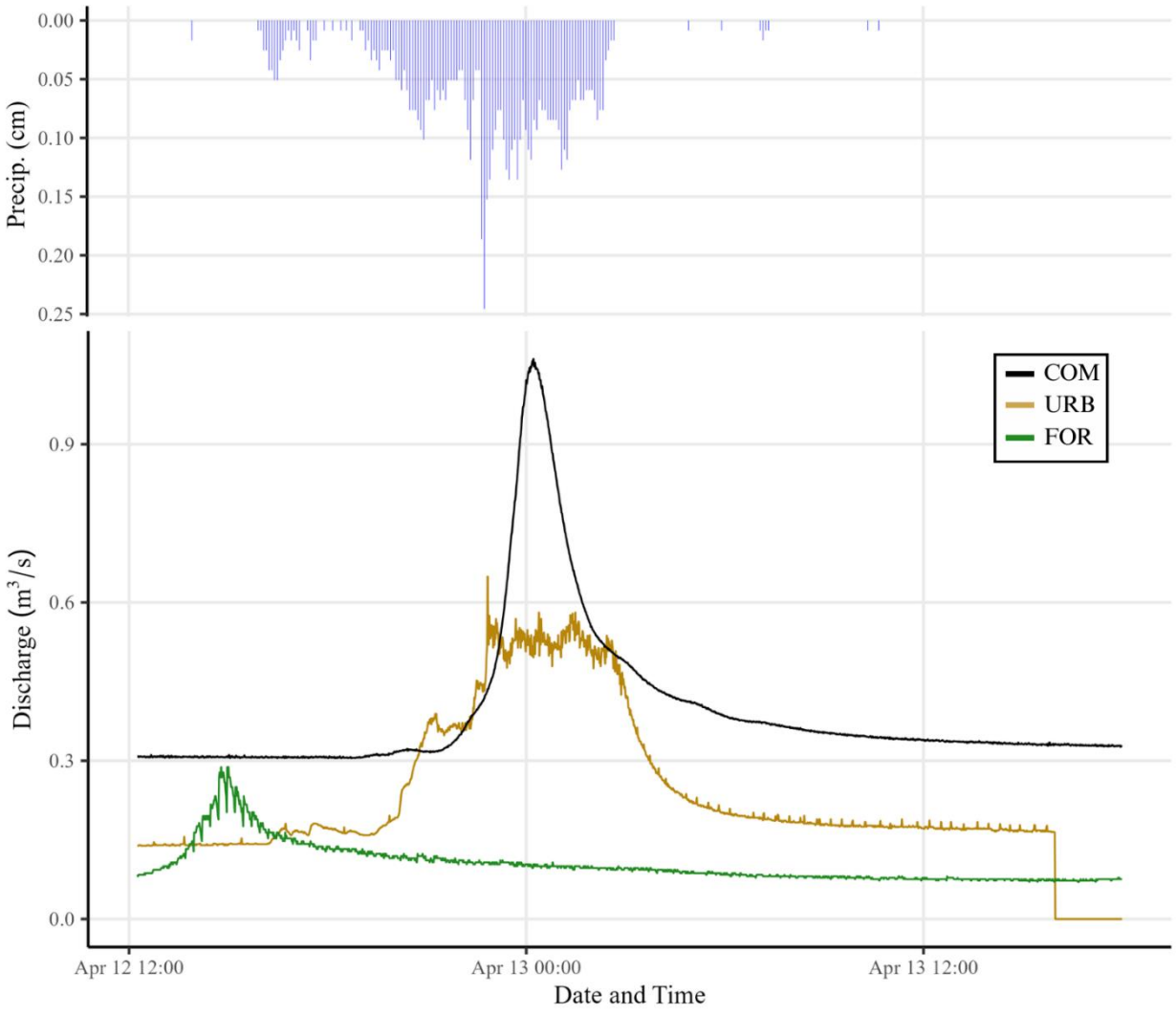

Figure 2.4 Hydrograph and hyetograph for a selection of monitoring data for the 3 hydrologic monitoring stations in BC watershed showing stream response to the storm event on April 12-13, 2020.

longest hydrograph representing a longer time of concentration, or time required for runoff to drain from the furthest point in the subcatchment.

Unlike FOR and COM, URB showed inconsistencies in the stage-discharge relationship at storm flow. Seasonal changes in vegetation resulted in slower discharge rates through the station culvert during summer months, sometimes slowing to a rate that could not be reliably detected by the area velocity sensor. Seasonal changes in water availability also impacted the standing level of water during baseflow. The average baseflow and peak flow rates, NO_3 concentrations, as well as notes on flow during dry periods, are reported in Table 2.4, and seasonal average baseflows are detailed in Table 2.5. Winter months generally show a greater baseflow rate than other seasons, except for site URB. Greater baseflow during winter months is to be expected as evapotranspiration rates slow in the winter and the water table rises. This trend is disrupted at URB by high in-stream vegetation in the summer, slowing water flow to almost mimic a wetland.

2.3.2. Distribution of NO_3^- Concentrations

2.3.2.1. Baseflow Conditions

Seasonal differences in NO_3^- concentrations

In Baker Creek, very small differences in average base flow nitrate concentrations (concentrations from each site in Figure 1.1 averaged) between seasons at the catchment level can be seen in the violin plots in Figure 2.5a. In both baseflow and stormflow datasets, the range of NO_3^- concentrations have a more uniform distribution during the fall and winter months than during the spring and summer months. This is likely due to individual hydrologic leaching events dominating NO_3^- transport occurring during the warmer months, where spring storms flush NO_3^- fixed in soils, as opposed to more consistent input of N from particulate organic matter (POM) from leaf-off in the fall and early winter. Leaching refers to the export of NO_3^- from soil in saturated conditions. The distributions of the seasonal average NO_3^- concentrations (Figure 2.5b) show slight increases from spring to winter in base flow, and more prominently in storm flow.

Table 2.4 Hydrologic regime (average baseflow and peak flow) and nitrate concentrations associated with flow stages at each monitoring site.

Monitoring Site (ID)	Catchment Size (km^2)	Average Baseflow (m^3/s)	Average Peak Flow (m^3/s)	Baseflow Average NO_3-N (mg/L)	Peak Flow Average NO_3-N (mg/L)	Average NO_3 Flux Rising Limb (mg/s)	Average NO_3 Flux at Peak Flow (mg/s)	Average NO_3 Flux Falling Limb (mg/s)
URBAN (4)	0.85	0.10	0.22	1.79	1.10	0.56	0.63	0.59
FOREST (9)	1.29	0.01	0.04	1.50	1.24	0.13	0.14	0.15
COMBINED (21)	5.96	0.29	0.48	1.19	0.74	0.88	1.42	1.06

Table 2.5 Seasonal averages for baseflow conditions in m^3/s at three monitoring subcatchments. Higher flow rates are shaded darker.

Site	Annual Average (m^3/s)	Spring (m^3/s)	Summer (m^3/s)	Fall (m^3/s)	Winter (m^3/s)
FOREST	0.01	0.01	0.01	0.01	0.03
URBAN	0.10	0.13	0.11	0.34	0.08
COMBINED	0.29	0.26	0.25	0.31	0.32

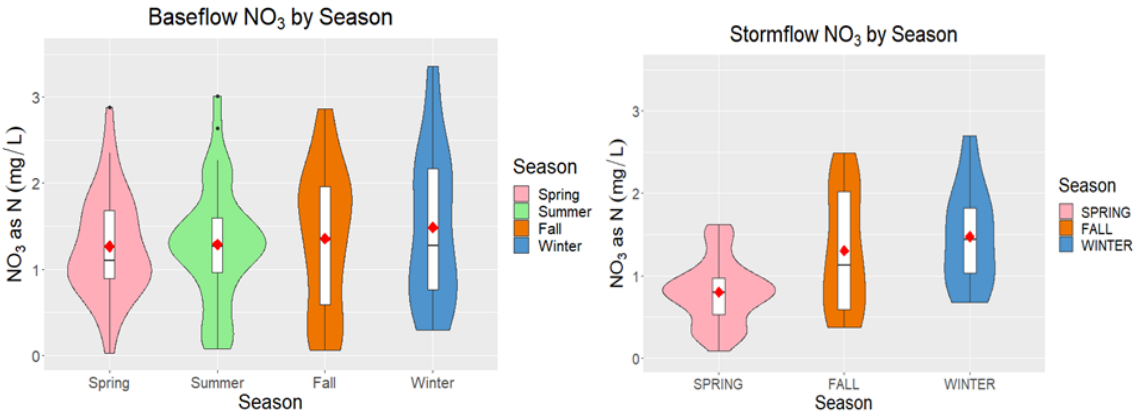

Figure 2.5 (a-b) Violin plot (color-coded) and boxplot (white) comparing seasonal average NO_3 concentrations for baseflow (a) and stormflow (b) conditions. The width of violin plots represents the number of occurrences of NO_3^- concentration, showing the distribution of values. The mean of the sample is indicated by a red diamond.

The range of NO_3^- concentrations is the lowest during the summer for both stormflow and baseflow datasets (5.76 and 6.5, respectively). The range of NO_3^- concentrations is comparable for fall, winter, and spring baseflow samples (11.2, 11.3, and 10.3, respectively) and for late summer/fall and winter storm flow samples (9.4 and 9.1, respectively). The difference in the range of NO_3 concentrations between baseflow and stormflow was greater in the spring season than in the cooler seasons.

Water samples have a higher NO_3^- concentration on average during cold seasons compared to warm seasons; a Mann Whitney U test determined that the difference in NO_3 concentration in base flow between the cold and warm seasons is statistically significant for all land use types (Table 2.6). A Kruskal-Wallis test determined that watershed baseflow NO_3 concentrations between the 4 seasons were statistically different with a chi-squared value of 20.1 and a p-value of 0.0005. Results from the statistical analysis show that NO_3 concentrations in storm flow also differ significantly between warm and cold seasons for all three land use types. Seasonal difference in average NO_3 concentrations between spring and fall/winter seasons is more visually apparent in stormflow than baseflow, however a Kruskall-Wallis test determined the difference in NO_3 concentrations between the three stormflow sampling seasons to only be statistically significant at site FOR when parsed by subcatchment (chi-squared and p-value of 11.10 and 0.004, 0 and 1, 4.42 and 0.11, and 11.86 and 0.003 for all storm data, URB, COM, and FOR respectively).

Inner-catchment geospatial distribution

Additional insights can be made when baseflow data are parsed by season and plotted geospatially. A heat map created with the inverse distance weighting (IDW) tool in ArcMap 10.6.1 illustrates the geospatial distribution of NO_3^- concentration throughout the watershed over the course of four seasons (Figure 2.6). The overall average NO_3^- concentration for the entire catchment at baseflow has little variation between seasons, but the location of instances of elevated NO_3^- is seasonally relevant. NO_3^- concentrations in the forested subcatchments are lowest in the fall and highest during warm weather. Suburban reaches of Baker creek show the lowest NO_3^- concentrations in the summer. During baseflow, several first order reaches of the

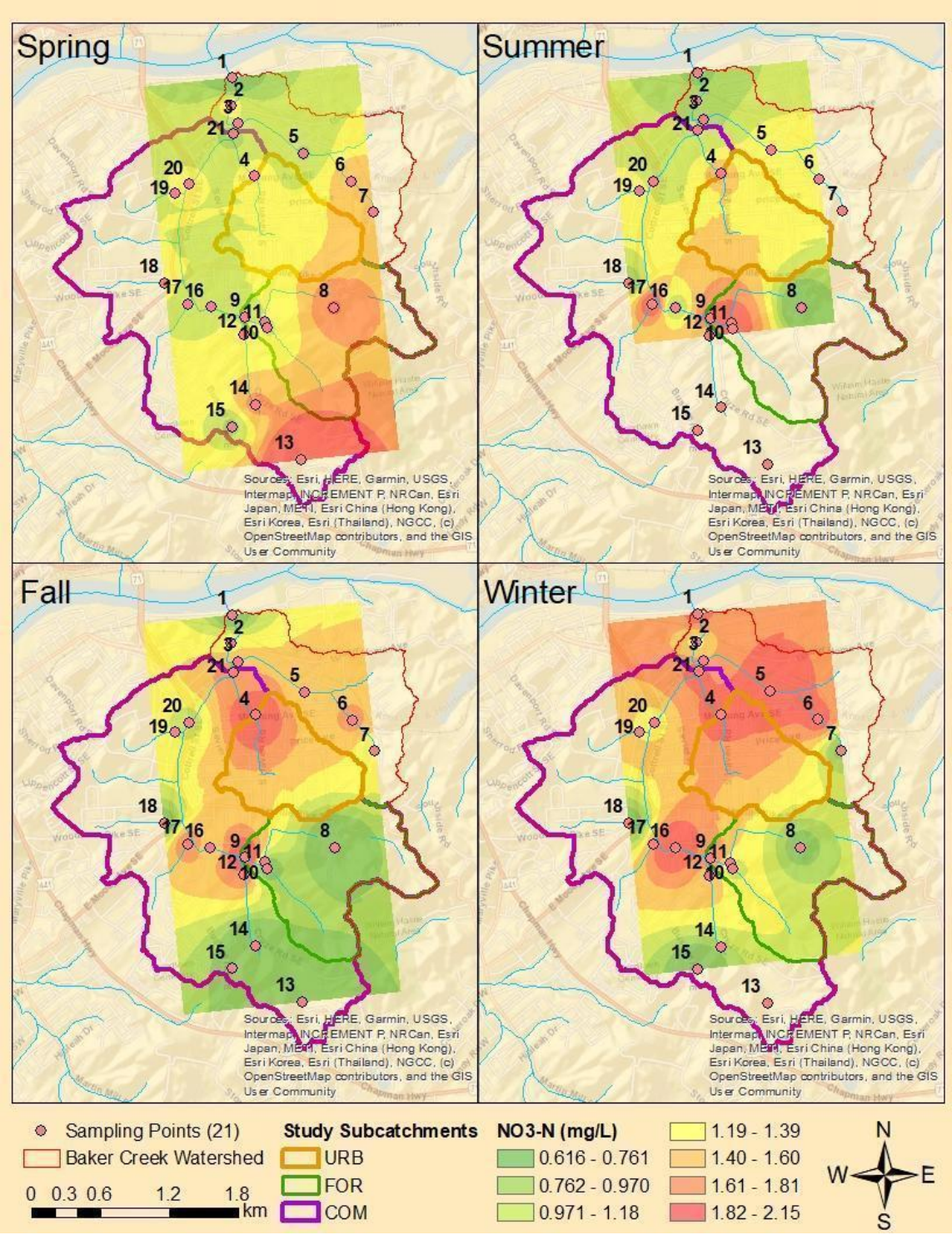

Figure 2.6 Seasonal geo-spatial distribution of nitrate concentrations shows a flooding of nitrate from the forested headwaters during the spring.

stream either approached zero flow or were entirely dry during periods of low precipitation or high vegetation. As such, upstream monitoring sites #7, 13, 14, and 15 were commonly found dry during the warmer months.

Ecologically driven trends and phenology

Seasonal fluctuations in hydrologic conditions such as evapotranspiration rates, groundwater table levels, and weather patterns can contribute to microbial-driven variations in rates of biogeochemical processes, such as nutrient source and transport. In pristine ecosystems in literature, baseflow nitrate concentrations are elevated during the Spring season throughout the watershed. This is normal ecosystem behavior, as seasonal leaching is common during spring hydrologic events in a healthy, undisturbed watershed (Stoddard 1994). Case studies of urban and developing streams, however, have found alternative seasonal responses to this norm where nitrate concentrations decreased during the spring and increased in the summer, possibly due to lack of particulate organic matter input into the streams because of lower vegetation density (Duncan et al., 2017; Carey et al., 2014). Baker Creek, with its forested headwaters region, showed a seasonal pattern in geographical distribution of NO_3^- concentrations (Figure 2.6) that may mirror pristine-ecosystem processes. This could be explained by increased particulate organic matter in the form of leaf litter and decaying plant matter contributing seasonally to nutrient concentrations in the fall and winter, with less sunlight contributing to plant growth and microbial activity.

Studies investigating stream metabolism and assimilatory NO_3^- uptake have found that net uptake rates show distinct seasonal patterns in forested streams, with the highest uptake rates existing in the spring during the open canopy period (Rode et al., 2016). Decline of stream assimilatory NO_3^- uptake is associated with increased canopy cover, decreased temp, and increased discharge; all of which are seasonally dependent, with canopy cover and discharge being additionally modulated by land use. In BC watershed, NO_3^- concentrations are higher in the forested headwaters than the developed downstream reaches during the spring and summer, but higher in the downstream reaches in the fall/winter. Tree canopy cover in recreational forests can slow nutrient uptake during the summer months compared to open urban stretches of stream,

as well as disproportionately contribute nutrient inputs that wash downstream during fall leaf fall-out. NO_3^- flux at URB and COM show higher variation within seasons than at site FOR, indicating that seasonality in nitrate concentrations becomes more random and less ecologically relevant as we move further downstream.

Highly urbanized watersheds often demonstrate trends in nitrate concentrations that are not explainable by broadly established ecological principles, and instead trends are more explainable by stream discharge rates and surface water contamination. For example, Duncan et al. 2017 found that in their experimental watershed in Baltimore, MD, concentrations decreased during the spring and then rebounded during the summer. Nitrate concentration was highest in the winter season, and then decreased in the fall. The nitrate flux in this watershed paralleled changes in stream discharge, and lower discharge was attributed to increased evapotranspiration. Similarly, Carey et al. (2014) found that the nitrate flux rate was the highest during the summer months in a rural-to-urban transitionary watershed with a highly forested ratio. In most studies, wetter years lead to increased in-stream nitrate concentrations (Wollheim et al., 2005; Duncan et al. 2017), perhaps because increased discharge results in decreased in-stream NO_3^- assimilatory processes.

2.3.2.2. Stormflow Conditions

Storm event-based trends in in-stream nitrate concentrations are often hydrologically, land-use, and source driven. Varying degrees of impervious connectivity in the three study subcatchments result in different nitrate concentration responses to stormflow. Figure 2.7 compares the distribution of NO_3 concentration in mg/L between the three study subcatchments in baseflow and stormflow samples. The results show that NO_3 concentrations are typically diluted during storm events. A Mann Whitney U test confirmed that the sum of ranks differs between the stormflow and baseflow datasets (with $U= 1412$ and $p= 0.046$). The difference between baseflow and stormflow NO_3 concentrations is statistically significant for the URBAN subcatchment ($U=161$, $p=0.016$), but not for the FOREST or COMBINED subcatchments ($U=141.5$, $p=0.857$ and $U=162.5$, $p=0.619$, respectively).

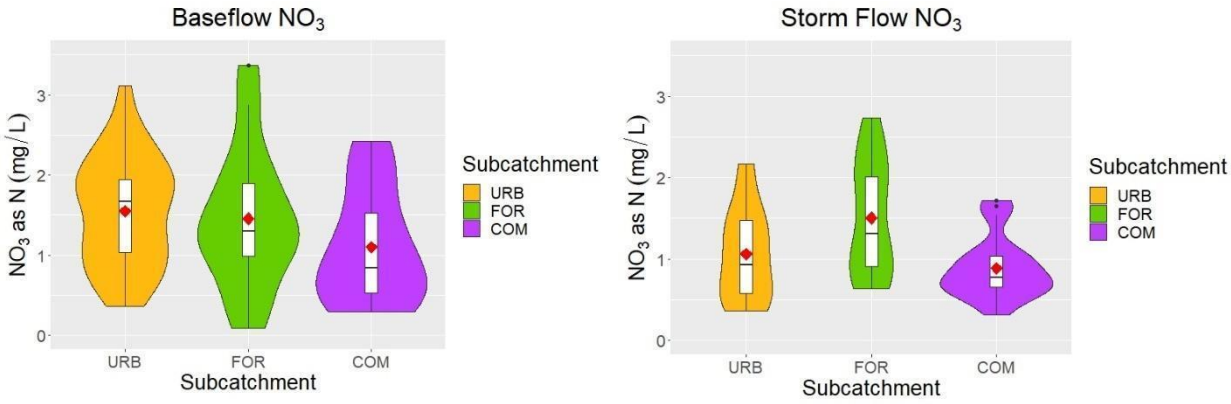

Figure 2.7 Box and whisker plots comparing nitrate concentration in baseflow to that in stormflow, broken down by subcatchment.

Hysteresis analysis reveals hydrology-driven temporal trends

In-stream NO_3^- concentrations and sources are responsive to land-use driven changes in hydrology during storm events. Larger, urbanized or developed watersheds with "patchwork" land use create a more dynamic response; greater variation in drainage times from potential NO_3^- sources results in increased temporal variation of in-stream NO_3^- concentrations over the course of the storm event (Carey et al., 2014). In addition, as previously discussed, increased discharge rate results in decreased NO_3^- removal rates. Intra-storm NO_3^- responses can be analyzed by plotting NO_3^- concentration by stream discharge. If nitrate concentrations are higher on the rising limb than the falling limb, or vise-versa, this can result in a loop on the plot known as a *hysteresis.* These cyclical relationships between concentration and discharge may indicate the distance of dominant flow paths from influential sources (Carey et al., 2014; Evans & Davies, 1998).

The results of the hysteresis analysis for the study in BC are displayed in Table 2.7 for the 9 storm events monitored in the study (1 per subcatchment per season). A clockwise hysteresis pattern indicates higher concentrations on the rising limb, while an anti-clockwise pattern indicates the falling limb provided the majority of nutrients from the storm event (Frazar et al., 2019). A clockwise pattern may indicate a closer distance to the source or depletion of supply, while an anti-clockwise pattern may indicate a further distance from source, or that a transport limited source needed increased connectivity from a large runoff volume filling soil cavities (Epps et al., 2021).

Urban forest mirrors pristine conditions

The forested upstream subcatchment showed no indication of hysteresis for 2 out of 3 events, and an overall dilution in nitrate concentration during precipitation (as compared to baseflow). Seasonal variation in NO_3^- response to storm events is minimal. This indicates that the supply of nitrate for the forested headwaters is not regulated by transport and is relatively consistent. Supply limitation occurs when solutes mobilized during storms are limited by the mass contributed by specific sources. Transport limitation occurs when discharge variability

Table 2.6 Hysteresis results for 9 analyzed storm events. Each storm is assessed to determine if it showed a clockwise (c) or anticlockwise (a) hysteresis pattern or no clear hysteresis (n), if it was an overall contribution (+) or dilution (--) in nitrate concentration (compared to baseflow), and if there was a pulse on the rising (r) or falling (f) limb (classifications adapted from Frazar et al., 2019, Evans & Davies, 1998, and Carey et al., 2014).

Subcatchment	Storm Date	Storm Volume (in)	Antecedent Dry Days	Hysteresis Dynamics	Notes
URBAN (4)	4/20/2020	1.00	2	c, +, f	starting baseflow [NO_3] was lower than usual
	10/10/2020	1.90	7	a, –	truly diluted from baseflow
	1/26/2021	0.94	3	c, –	
FOREST (9)	4/20/2020	1.00	2	n, –	zig zag pattern, baseflow [NO3] not restored
	9/28/2020	0.863	9	n, –	zig zag pattern, baseflow [NO3] not restored
	2/11/2021	0.95	14	c, –	
COMBINED (21)	4/29/2020	0.42	4	c/a, +, f	pattern inverts, there is a anti-clockwise loop within a counter-clockwise loop due to pulse in falling limb
	9/13/2020	0.41	2	c, +, f	
	2/11/2021	0.95	14	c, –	

determines when readily available solutes are mobilized. Carey et al. (2014) proposed that supply limitation is more common in small, forested catchments, where hydrologic response and nutrient inputs more similarly mirror pristine conditions; transport limitation is more likely in small urban catchments, where supply of nutrients commonly outweighs the uptake potential.

2.1.2.3 Developed catchments show variable NO_3^- response

The small, urbanized catchment fed mostly from stormflow, URB, usually showed the highest nitrate concentrations at the beginning of storm flow. This pattern flips, however, during the rain event on October 10, 2020 (Figure 2.8) which was 83% larger than the average observed rainfall depth. It is worth noting that the URB subcatchment is disconnected from other drainage areas, being the starting point of an independent tributary to Baker Creek. URB NO_3^- concentrations are usually diluted by storm flow, however the April 20, 2020 storm (Figure 2.9) shows a contribution in NO_3^-. This is likely due to a previous storm event diluting in-stream NO_3^- concentration, resulting in lower than average baseflow concentrations at the start of the rain event. The urban downstream convergence point, COM, showed contributions to nitrate concentrations for two out of the three storm events, with pulses in nitrate concentrations common on the falling limb of the hydrograph. Because this is a downstream monitoring site with a larger drainage area consisting of both forested and developed land use, COM will have a longer time of concentration than the smaller urbanized subcatchment and have the potential for multiple stages of nitrate washout. Pulses on the falling limb indicate nitrate flushing from reaches further upstream in the watershed.

A pulse in nitrate concentration can be defined as a point in either the rising or falling limb of the hydrograph where there is a sudden increase in concentration, but not necessarily a permanent increase in concentration over the remainder of the event. A pulse can indicate distance from source that is contributing to nutrient loading. (Carey et al., 2014) A pulse on the rising limb of a hydrograph followed by dilution can indicate a first flush dynamic, which is the initial wash-off of pollutants in a developed watershed. First flush dynamics for nitrate concentrations have been recorded in many urban stream water quality studies (Hathaway et al., 2012; Carey et al .,2014), but other studies have cited first flush of nitrate as a rare occurrence (Duncan et al., 2017). Pulses

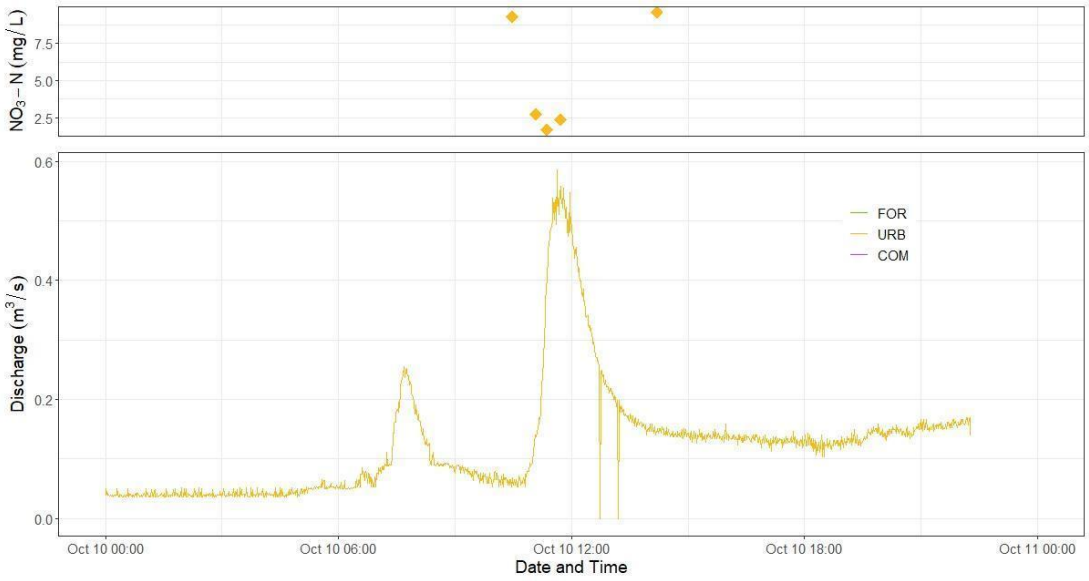

Figure 2.8 Discharge and NO_3^- concentrations at site URB during the October 10, 2020 storm event.

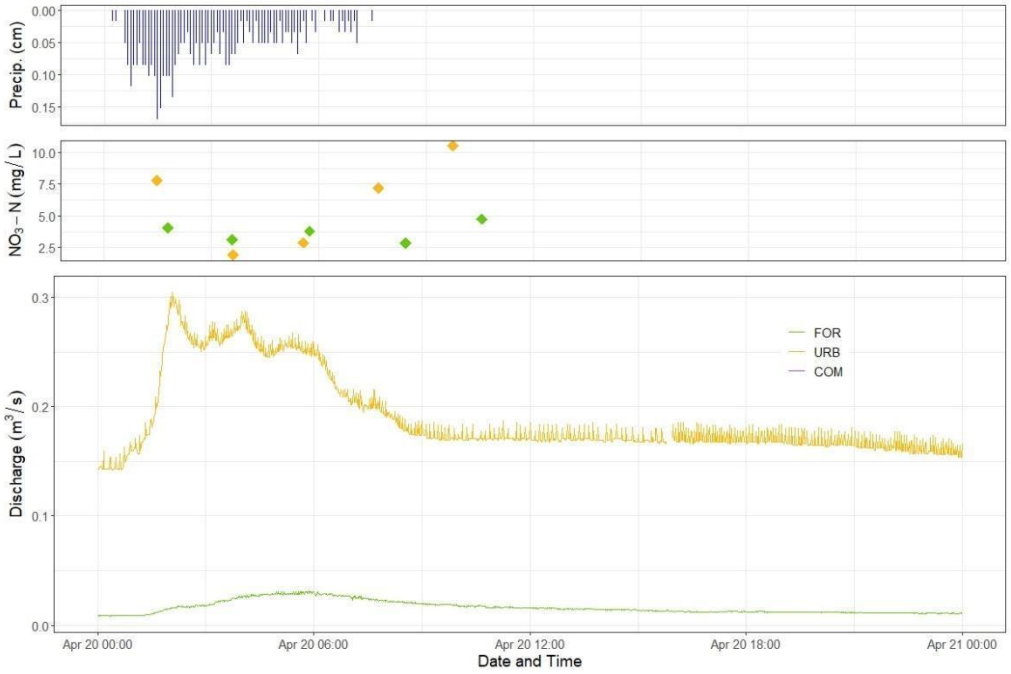

Figure 2.9 Discharge, rainfall, and NO_3^- concentrations at sites URB and FOR during the April 20, 2020 storm event.

of NO_3^- concentrations may also be indicative of soil N dynamics, where accumulated NO_3^- is flushed from soils (Carey et al., 2014). Intermittent drying of streams may also contribute to first-flush nitrate export, as the change in environment creates a hotspot for microbial ammonia oxidation (Merbt et al., 2016). Several studies cite a "first flush" phenomenon in urban streams, where there is a pulse in nitrate concentrations on the rising limb of a storm hydrograph (Carey et al., 2014; Hathaway, 2012; Duncan et al., 2017). In highly urbanized or developed watersheds, first-flush phenomenon becomes less common in smaller storm events, where there is more likely to be a positive correlation between nitrate concentration and stream discharge (Duncan et al., 2017). Studies employing hysteresis analysis of in-stream nitrate response to hydrologic events show that the timing of storm pulses can reveal information about varying distances and connectivity between nonpoint sources in different upstream subcatchments (Carey et al., 2014).

Some seasonal variability is evident in the hydrologic response of NO_3^- in the developed catchments that is not present in the forested catchment. In general, winter storms appeared to dilute NO_3^- concentrations while spring storms resulted in flushes. Fall storms showed more variability. The Carey et al. study also showed that alterations in between dilution and flushing during storm events appeared to have some seasonal relevance. Discrepancies between conductivity and $NO_{3,}^-$ concentrations suggested that fall storms likely sourced NO_3^- concentrations from soil (increased conductivity and $NO_{3,}^-$ concentrations), while spring and summer storms were more surface driven, supply-limited sources (diluted conductivity and quick $NO_{3\cdot}$ pulses) hypothesized to be atmospheric deposition and fertilizers. The difference between diluting events and flushing events in BC, however, appeared to have more to do with storm volume and increased connectivity between sources and sampling points than a difference in the source itself (hypothesis strengthened by isotope analysis in section 2 of this discussion). The falling limb pulse in nitrate concentration at site COM is present in the spring and fall storms, but not the winter storm. The spring and fall storms also happen to be smaller storm events, with a lower discharge rate, and indicating less subterranean connectivity with the flood plain and more influence from surface-level wash out.

2.3.3. Nitrate Stable Isotope Analysis

Examination of $\delta^{15}N$ and $\delta^{18}O$ values of dissolved NO_3^- concentration in samples provided valuable insights into the primary sources influencing NO_3^- concentrations in Baker Creek. Our analysis involved a comparative assessment of isotope compositions in our samples key endmembers identified in the literature, including atmospheric deposition (AD), manure & septic waste (MS), soil nitrogen (SN), and nitrogen resulting from NO_3 or NH_3 in fertilizers (FN). All stable isotope results were plotted using Grapher Golden software and Microsoft Excel. Average, min, max, and standard deviation were calculated for samples from different monitoring sites (both overall and by cold/warm weather condition), runoff types, and by season and land use type at the baseflow condition.

2.3.3.1. Isotope Analysis of NO_3^-

The measured variations of $\delta^{15}N$ and $\delta^{18}O$ were large for each sample type (Figure 2.10 & Table 2.8). URB showed the greatest variation with a standard deviation of 4.7 and 2.3‰ for $\delta^{18}O$ and $\delta^{15}N$, respectively. Comparatively, standard deviations of samples from site FOR were 2.5 and 0.8‰ for $\delta^{18}O$ and $\delta^{15}N$, respectively, and 2.8 and 2.8‰ for COM samples. In general, $\delta^{18}O$ varied in a larger range compared to $\delta^{15}N$, suggesting greater variation in the contribution of AD to NO_3^- concentrations compared to other endmember sources.

In-stream sub-datasets from the three stormflow monitoring locations and from baseflow at all sampling locations have more similar $\delta^{15}N$ and $\delta^{18}O$ values to each other than to endmember samples. Isotope compositions of NO_3 differ significantly between storm and endmembers samples (Mann Whitney U test results for $\delta^{15}N$: U=237 and $p=8.9x10^{-09}$; for $\delta^{18}O$: U=1348.5, $p=2.3x10^{-4}$) as well as between baseflow and endmember samples ($\delta^{15}N$: U=170 and $p=3.5\ x10^{-10}$, $\delta^{18}O$: U=1600, $p=1.59\ x10^{-09}$). The Wilcoxon ranked sum test indicated there is a difference between the $\delta^{18}O$ of NO_3 of stormflow and baseflow pooled across all sites, but not of $\delta^{15}N$. When storm samples are broken down by URB,

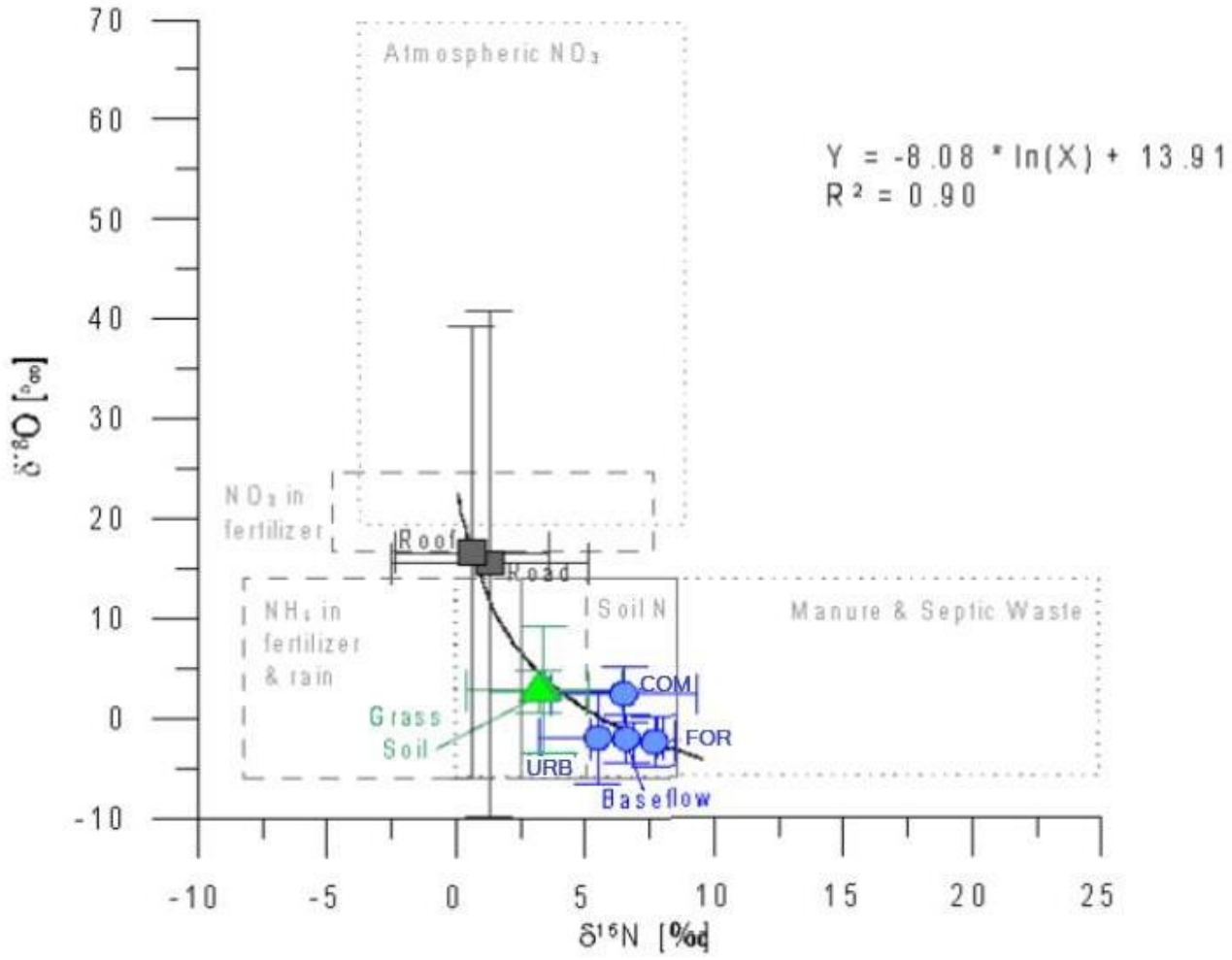

Figure 2.10 Average $\delta^{15}N$ and $\delta^{18}O$ for dissolved NO_3^- in the storm flow, baseflow, and runoff datasets. The stream samples are indicated by blue circles. Stormflow is separated into subdatasets based on subcatchment- URBAN, FOREST, and COMBINED. The runoff samples from rooftops and roadways are indicated by gray squares; and from grass and soil are indicated by green triangles. Typical endmember ranges are indicated with gray boxes after Baral, 2017.

Table 2.7 Average, minimum and maximum $\delta^{15}N$ and $\delta^{18}O$ of dissolved NO_3 in each of the analyzed sub-datasets.

	$\delta^{18}O$			$\delta^{15}N$		
	Average	**Min**	**Max**	**Average**	**Min**	**Max**
URBAN	-2.0	-13.6	7.1	5.5	-1.8	7.7
FOREST	-2.4	-6.2	-1.8	7.7	6.0	8.5
COMBINED	2.4	-1.7	10.2	6.5	0.0	12.3
Baseflow	-2.1	-11.4	2.2	6.6	2.6	9.7
Roof	16.6	0.6	59.9	0.6	-7.0	3.2
Road	15.5	-19.6	52.6	1.3	-2.4	11.4
Soil	2.6	1.1	4.0	3.2	1.8	4.6
Grass	2.8	-5.3	13.0	3.4	-1.0	7.6

FOR, and COM sub-datasets, and storm flow and base flow are compared, the difference in $\delta^{18}O$ is only significant at the COM site. This indicates that a significantly larger proportion of the dissolved NO_3^- concentrations at baseflow conditions is sourced from atmospheric deposition when compared to samples taken during storm events.

Rooftop and road samples have the most distinctive isotope composition of NO_3^-, with high $\delta^{18}O$ values and low $\delta^{15}N$ values relative to the NO_3^- isotope composition of stream samples. Using the Mann Whitney U test, we determined that there is a statistically significant difference between the $\delta^{18}O$ of dissolved NO_3 in grass/soil runoff types and road/roof runoff types ($U=157.5$, p-value=0.02794), but the difference between the $\delta^{15}N$ values of the same sample types is not statistically significant ($U=84$, $p=0.3858$). This indicates greater influence of atmospheric deposition on dissolved NO_3^- in runoff from impermeable surfaces (rooftops and roadways) compared to soils and grasses, as is exemplified in previous literature (Baral et al., 2017). Investigation into changes of NO_3^- source during storm events by comparing $\delta^{15}N$ and $\delta^{18}O$ values for samples taken over a storm's hydrograph showed too much variability for conclusive results; if anything, there seemed to be an inconsistent first flush of lighter $\delta^{15}N$ values in some storm events, which could be indicative of a small amount of fertilizer runoff.

There appears to be a greater influence of AD on dissolved NO_3^- concentrations in baseflow conditions compared to stormflow, however AD is considered a consistent source of NO_3^- in stormwater (Baral et al., 2017). The Mann Whitney U test showed that average NO_3^- concentrations in roof and road runoff samples (0.4 mg/L and 0.9 mg/L, respectively) were significantly lower than those in the grass and soil runoff samples (5.1 mg/L and 4.4 mg/L, respectively) with $U=45.5$ and $p=0.0019$. This evidence suggests that while Baker Creek may contain a large proportion of runoff during stormflow conditions, runoff from impervious surfaces such as roadways and rooftops is not a major contributing source to dissolved $NO_{3,}^-$ concentrations.

Compared to existing literature that has applied similar stable isotope source tracking methods to dissolved NO_3^- in urban streams, our study found a smaller influence of AD and MS for similar ranges of in-stream NO_3^- concentration. For example, Drivers et al., 2014 found AD to be

responsible for approximately 34% of nitrate loads in stream water during storm events. $\delta^{18}O$ values during storm events ranged from -13.6 to +10.2 ‰, depending on the site and the storm size. In comparison, Drivers observed $\delta^{18}O$ values ranging from ~0-30 ‰ for most storm events, but ~25-33 ‰ for the smallest storm event. NO_3^- concentrations during storm events ranged from 0.26-2.69 in our study, comparable to a range of 0.3-2.3 mg/L NO_3^-N in Drivers et al., 2014. This is explainable by regional differences in atmospheric deposition. According to the National Atmospheric Deposition Program (NADP) database, Pittsburgh, PA (the study site of Drivers et al.) approximately 10-12 kg/ha of NO_3^- ion wet deposition in 2012 and 2013, compared to the 6 kg/ha in the East Tennessee / Knoxville region in 2019 and 2020. According to NADP reports, wet deposition of NO_3^- ion has generally decreased across the nation since Drivers et al.'s study in 2014, and Knoxville has lower rates of atmospheric deposition of NO_3^-.

Besides relative contribution from AD, our study found similar trends of NO_3^- isotopes to other studies. One notable common trend was an inverse relationship between $\delta^{15}N$ and $\delta^{18}O$ (~ -1:1 slope) present in stormflow samples, suggesting micing of MS and AD sources. A positive relationship between $\delta^{15}N$ and $\delta^{18}O$ (~ +1:2.3 slope), most prevalent in our study among baseflow samples, indicates denitrification processes. In both our study and Kuashall et al., 2011, the highest $\delta^{18}O$ values accompanied the samples with lowest NO_3^- concentrations; in our study, this category contained the runoff endmember samples (see Fig. 2.9 b & d). Both our study and Drivers et al., 2014 found that high flow rate resulted in higher δ18O values and lower δ15N values than during low flows, indicating increased atmospheric deposition during more intense precipitation. Other studies showed increased influence of AD depending on antecedent weather and storm conditions. For example, Baral et al. (2017) found a stronger correlation between atmospheric NO_3^- and dissolved NO_3^- concentration for smaller storm events. Our study saw statistically significant correlations between storm conditions and $\delta^{18}O$ values, indicating atmospheric deposition, only at site FOR.

Duncan et al. (2017) found that storm size had a significant impact on the dominant source of in-stream NO_3^- concentrations, with large events contributing a greater proportion of "new water", or surface runoff and rainwater, compared to smaller events where the stream flow remains primarily groundwater. An increase in storm volume can dilute NO_3^- concentrations and increase

nutrient concentrations from other sources including pervious cover such as soil. We investigated correlations between $\delta^{15}N$ and $\delta^{18}O$ values of dissolved nitrate and (a) NO_3^- concentration (Figure 2.11) and (b) stream discharge rate (Figures 2.12-2.13). We found no significant correlation between NO_3^- concentration and either $\delta^{15}N$ or $\delta^{18}O$ for either of the three datasets- stormflow, baseflow, or runoff endmembers- with R^2 values less than or equal to 0.25. There is a notable negative correlation between NO_3^- concentration and $\delta^{18}O$ at the forested subcatchment FOR, with an R^2 value of 0.77. There is no significant correlation between NO_3^- concentration and the $\delta^{18}O$ ratio at the other two subcatchments, COM and URB, with R^2 values of 0.14 and 0.007 respectively. Similarly, there is no significant correlation between NO_3^- concentration and the $\delta^{15}N$ of any of the datasets, with R^2 values less than or equal to 0.25. There is a slight positive correlation with an R^2 value of 0.38 at FOR, however the more urbanized sites show no significant correlation between NO_3^- concentration and the δ15N ratio. This indicates that NO_3^- concentration has little correlation with NO_3^- source, except for in the stream flow from the forested subcatchment. In FOR, increased NO_3^- concentration appears to correlate with decreased influence from atmospheric deposition. This further supports that the driving source of NO_3^- concentrations in the watershed is organic matter from Baker Creek Preserve.

<u>NO_3^- isotope compositions by cumulative runoff</u>

In Figures 2.12 and 2.13, it was noted that a larger storm event showed instances of enrichment in lighter $\delta^{15}N$ isotopes at site COM on one occasion. Site FOR showed little variation in $\delta^{15}N$ or $\delta^{18}O$ over the duration of storm events, while sites COM and URB showed large variations with no clearly discernible patterns. The r^2 values for the linear regression models suggested that $\delta^{15}N$ is most correlated with discharge rate for the spring storm at site FOR (r^2=0.55), followed by fall storms at site URB (r^2=0.55) and winter storms at site FOR (r^2=0.31). All other r^2 values in Figure 2.12 are less than or equal to 0.18. For Figure 2.13, $\delta^{18}O$ values were most correlated with discharge during fall storm events at site COM (r^2=0.67), winter sites at site URB (r^2=0.62), and winter storms at site FOR (r^2=0.56). All other linear regressions in Figure 2.13 had an r^2 value less than or equal to 0.16. It was interesting that $\delta^{18}O$ values seemed to have a positive linear relationship with discharge rate at for sites and seasons except for spring storms at site COM,

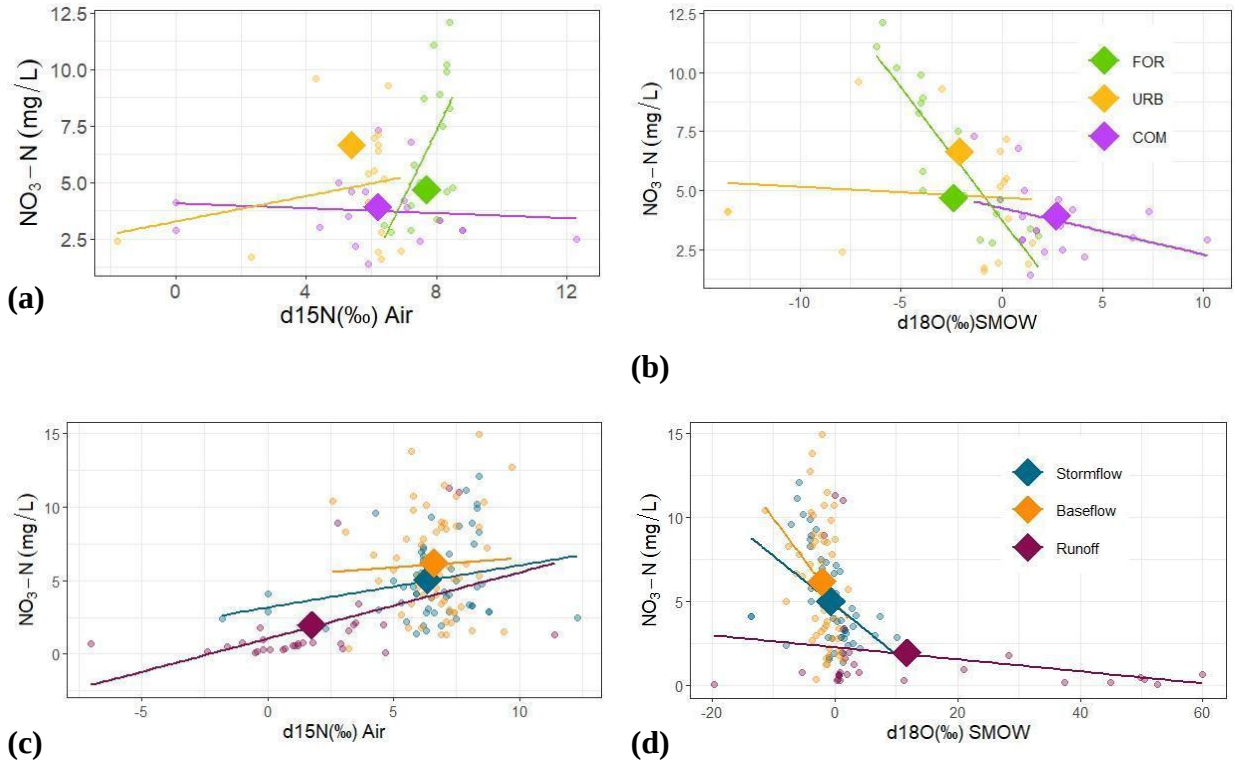

Figure 2.11 (a-d) Average NO_3^- concentration compared to average $\delta^{15}N$ (a and c) and $\delta^{18}O$ (b and d) and for stormflow samples (a and b) categorized by the three subcatchments (URB, FOR, or COM) and for all samples (c and d) categorized by sample type (Baseflow, Stormflow, or Runoff samples).

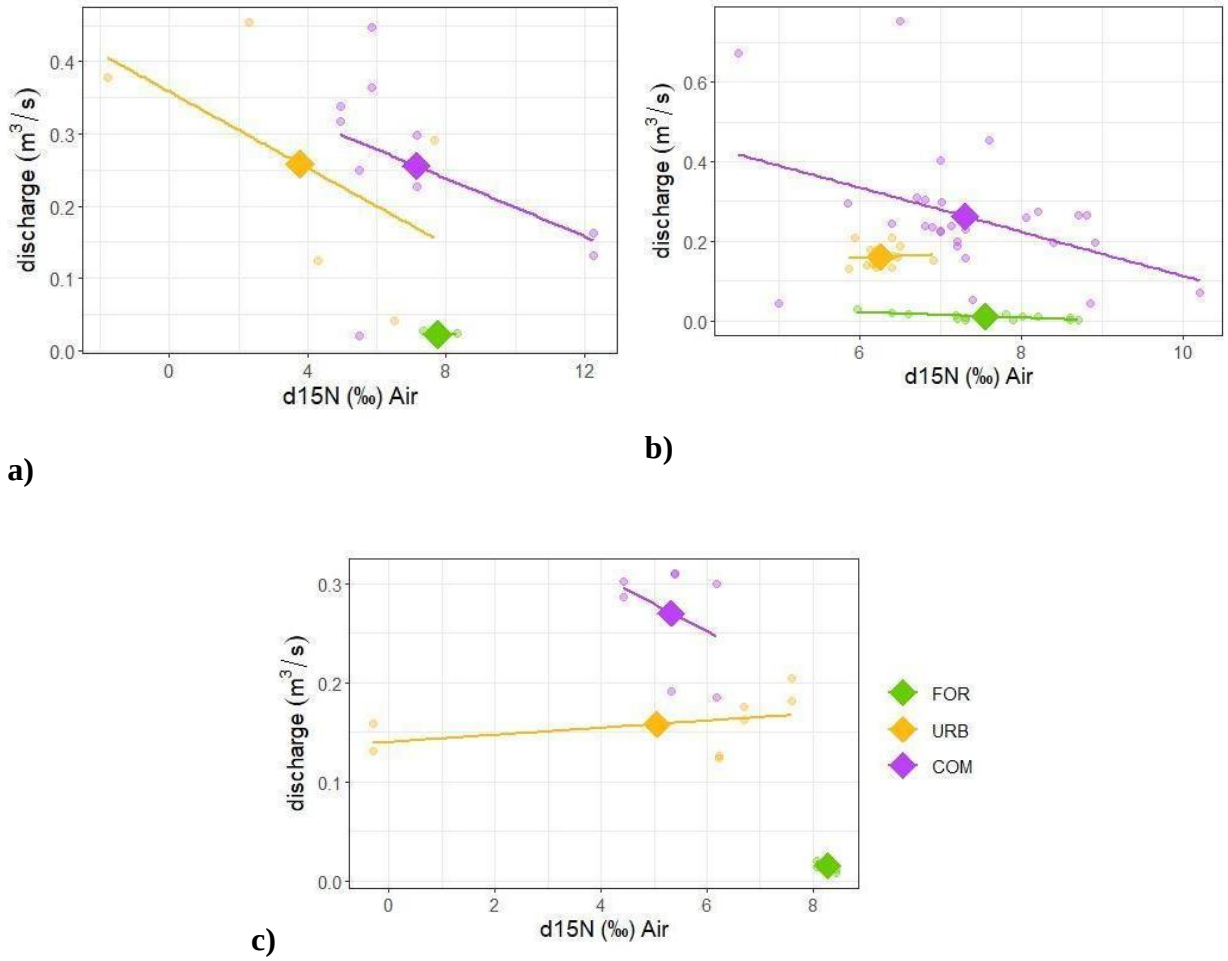

Figure 2.12 (a-c) Discharge in m^3/s plotted by $\delta^{15}N$ of dissolved nitrate for storm events collected at each monitoring site during the (a) spring, (b) fall, and (c) winter season. A best fit linear regression was fitted to each sample group.

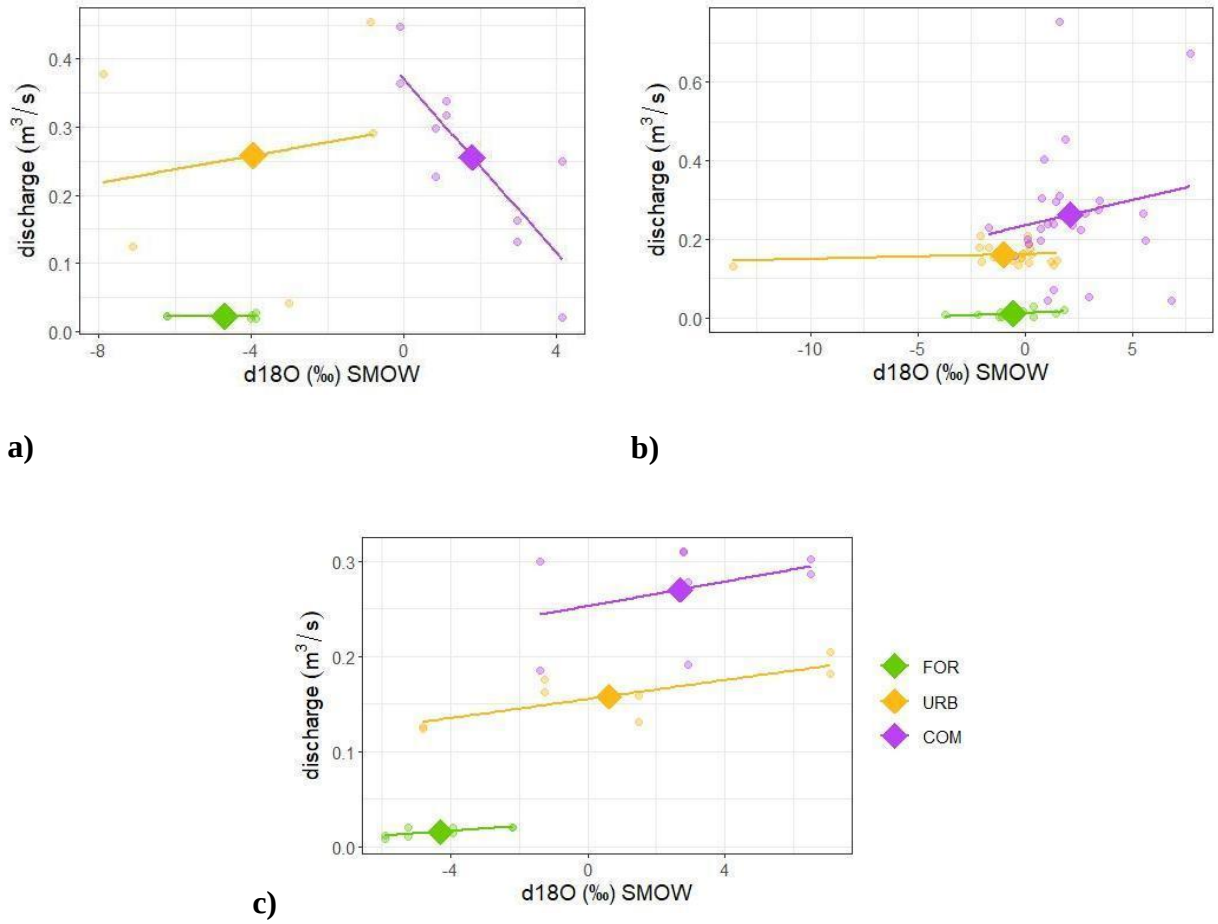

Figure 2.13 (a-c) Discharge in m^3/s plotted by $\delta^{18}O$ of dissolved nitrate for storm events collected at each monitoring site during the (a) spring, (b) fall, and (c) winter season. A best fit linear regression was fitted to each sample group.

which had a negative linear relationship. This may suggest that there was an increased occurrence of atmospheric deposition influence nitrate source in smaller storm events at downstream site COM compared to other sites. This could be related to an increased ratio of rooftop/roadway surface runoff and rainwater compared to groundwater and water infiltrating through riparian zones for smaller storm events. This relationship, however, had an r^2 value of only 0.03.

Stable Isotope Analysis by Runoff Type

Average NO_3^- isotope composition of the samples showed separation between road/rooftop runoff endmember samples, soil/grass runoff endmember samples, and streamflow samples (Figure 1.10). Road and rooftop runoff types showed atmospheric deposition (AD) as the primary contributor of nitrate, while soil and grass runoff types showed a mixture of nitrogen fertilizers (NF) and soil nitrification processes (SN) as the primary contributors of nitrate. The standard deviation of NO_3^- isotope compositions for each runoff type are noted in Table 2.9 below. There was high variability in $\delta^{15}N$ and especially in $\delta^{18}O$ of nitrate in each runoff sample, suggesting that the runoff types would not be good “endmembers" for a mixing model, Bayesian or otherwise, to determine relative contribution of runoff types in a sample based on results from stable isotope analysis.

Figure 2.14a-b displays the plot $\delta^{15}N$ (a) and $\delta^{18}O$ (b) of dissolved NO_3 vs NO_3 concentration for the runoff endmember samples. Runoff endmembers by source type (roof, road, grass, or soil) do not show trends indicating a relationship between NO_3 concentrations and enrichment of heavier or lighter N or O isotopes. There is a slight enrichment of heavier nitrogen isotopes with the increase of nitrate concentration when you remove the bias of runoff type. This indicates that within runoff types, there does not seem to be an indication of nitrate source changing with concentration. However, there may be a general trend that increased nitrate concentration in runoff (of any type) is indicative of soil processes or septic/manure waste nitrate sources.

Table 2.8 Standard deviation of $\delta^{15}N$ and $\delta^{18}O$ for each of the 4 sampled runoff endmember types.

	Rooftop	Roadway	Grass	Soil
$\delta^{15}N$	3.0 ‰	3.8 ‰	1.9 ‰	3.0 ‰
$\delta^{18}O$	22.7 ‰	25.3 ‰	2.21 ‰	6.3 ‰

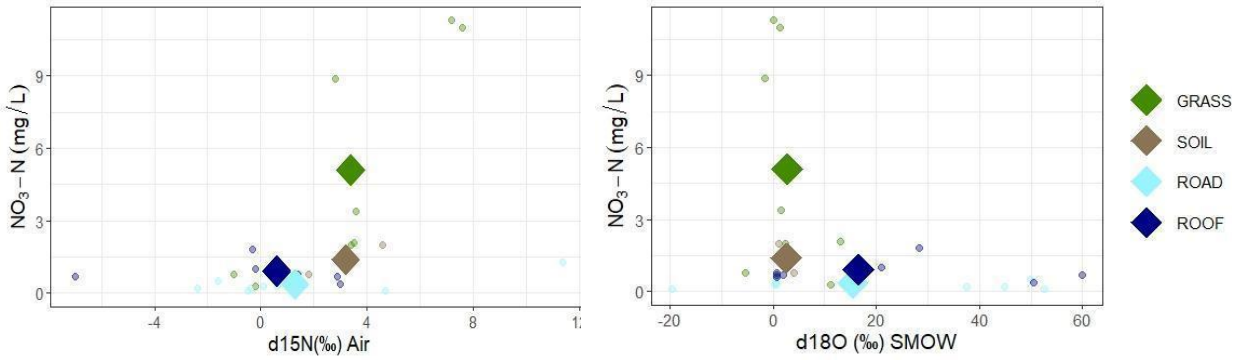

Figure 2.14 (a-b) The dissolved NO_3^- concentration in mg/L compared to $\delta^{15}N$ value (a) and $\delta^{18}O$ value (b) for the runoff endmembers.

Seasonal variation in NO_3^- isotope compositions

Figure 2.15 plots average $\delta^{18}O$ vs $\delta^{15}N$ by season. A Mann Whitney U test revealed no significant difference between the ranks of $\delta^{15}N$ and $\delta^{18}O$ of NO_3 between cool and warm weather baseflow samples for all three land use types, indicating no seasonal change in nitrate source. Seasonal variation is limited to distribution and magnitude of NO_3^- concentration, with no observable change in source. It is worth noting that, while statistically insignificant, there does seem to be a greater difference between cool and warm weather NO_3^- sources in the forested watershed during storm events. This may be caused by the buildup of particulate organic matter (POM) and forest canopy throughfall.

2.3.3.2. Sulfate Stable Isotope Analysis

Figure 2.16 plots average $\delta^{34}S$ by average $\delta^{18}O$ of dissolved SO_4^{2-} in baseflow and stormflow samples. Stormflow samples are distinguished by the 3 study subcatchments: URBAN, FOREST, and COMBINED. The trimmed mean concentration of dissolved sulfate in land cover runoff endmember samples, excluding the top and bottom 5% of the distribution, is 2.74 mg/L. Lower concentrations of SO_4^{2-} often did not precipitate enough barium sulfate for successful stable isotope analysis; at least 0.39 mg of $BaSO_4$ is necessary for a reliable reading. For this reason, land cover runoff samples (rooftop, grass, etc.) were not included in sulfate isotope analysis.

The results of the sulfate stable isotope analysis show low $\delta^{34}S$ and $\delta^{18}O$ values in storm samples when compared to baseflow samples (Figure 2.15), with an average $\delta^{34}S$ value of 7.7‰ and $\delta^{18}O$ value of 12.6‰ in baseflow water samples versus 3.4‰ and 6.3‰ (respectively) across all stormflow water samples. Statistical analysis revealed that there is a significant difference between both $\delta^{34}S$ and $\delta^{18}O$ isotopes in sulfate dissolved in baseflow compared to that of stormflow (Mann Whitney U test results: U=1443.5, p=7.20E-10 for $\delta^{34}S$; U=147, p=1.59E-3 for $\delta^{18}O$). The $\delta^{34}S$ and $\delta^{18}O$ values of the three stormflow subcatchments (FOR, COM, and URB) are significantly lower from those of baseflow water samples in every case besides one; the difference of $\delta^{18}O$ values of stormflow samples at site URB and baseflow samples are not

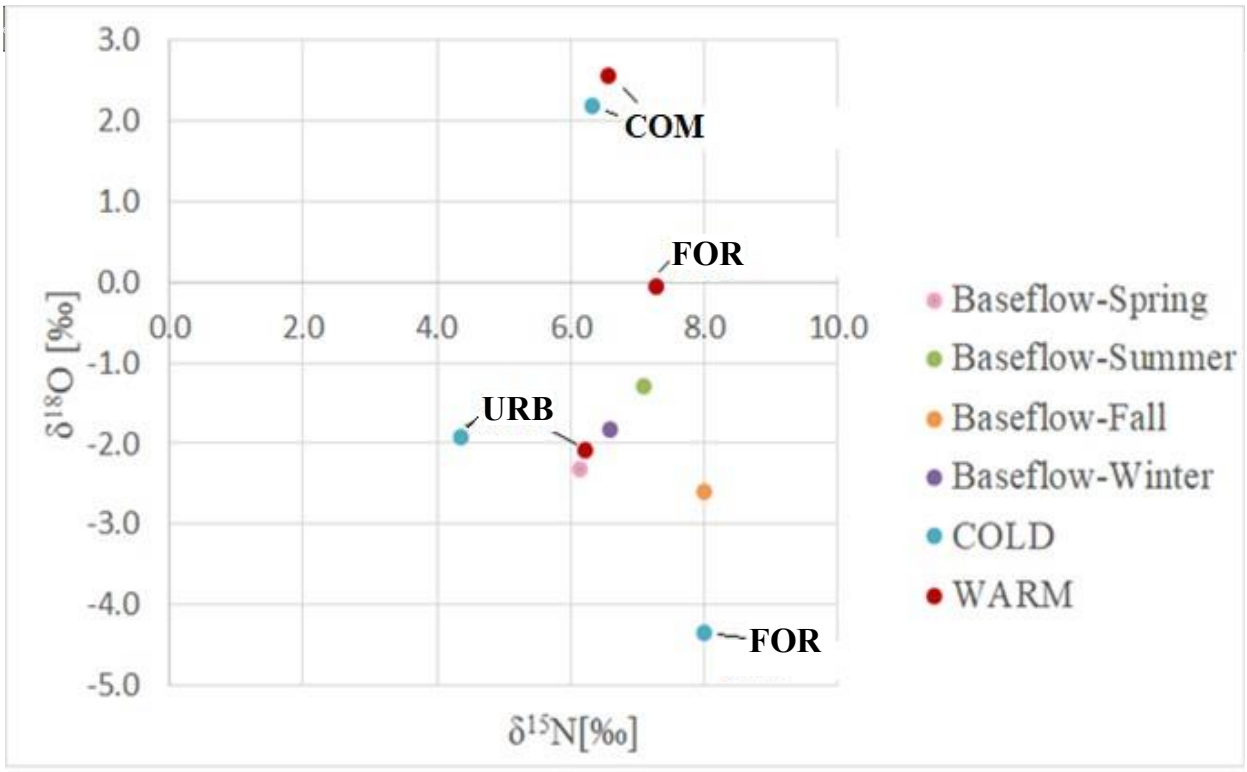

Figure 2.15 Seasonal variation in baseflow and stormflow average stable isotope of dissolved NO_3^-.

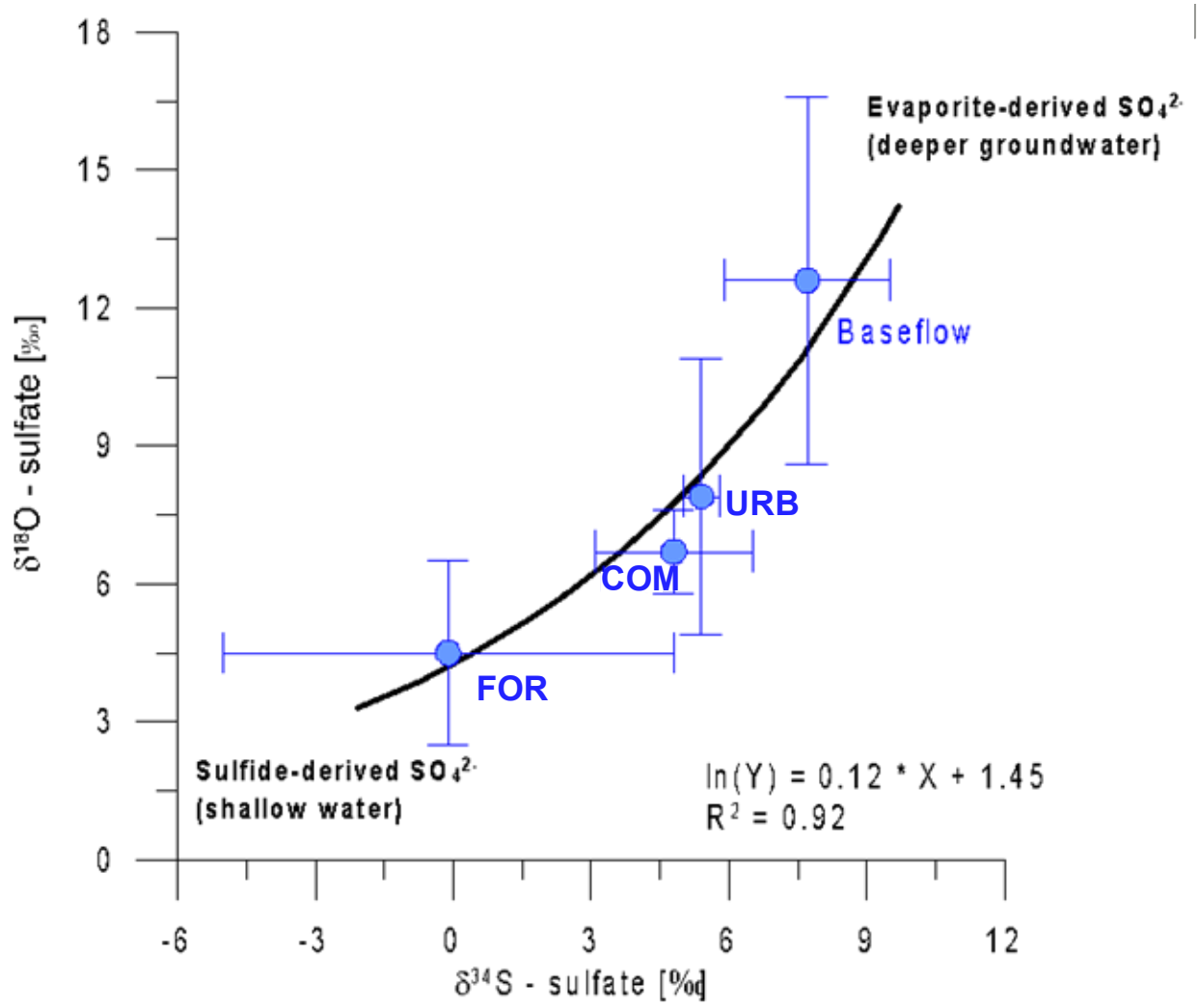

Figure 2.16 Average $\delta^{34}S$ and $\delta^{18}O$ of dissolved sulfate in baseflow versus the three sampling sites

statistically significant. Sulfate isotope composition in stormflow samples taken from subcatchment FOR show significantly lower $\delta^{34}S$ and $\delta^{18}O$ values compared to subcatchments URB and COM, average $\delta^{34}S$ values of -.01‰, 5.4‰, and 4.8‰ and $\delta^{18}O$ values of 4.5‰, 7.9‰, and 6.7‰, respectively. There is no significant difference between the dissolved sulfate isotope composition in stormflow samples at sites URB and COM. Seasonal variation in average $\delta^{34}S$ was apparent in the forested subcatchment, but not any other sample group. Fall storm samples from site FOR had an average $\delta^{34}S$ of -4.2‰, compared to an average of 3.6‰ for all other seasons. There was no correlation between storm size and sulfate isotope composition.

Insignificant differences between baseflow and stormflow NO_3^- concentrations, high $\delta^{34}S$ and $\delta^{18}O$ values of dissolved SO_4^{2-}, and little change in $\delta^{15}N$ and $\delta^{18}O$ values of dissolved NO_3^- between baseflow and stormflow datasets are all evidence that groundwater serves as the primary NO_3^- source for subcatchment FOREST. Comparing average $\delta^{34}S$ and $\delta^{18}O$ values of dissolved SO_4^{2-} between stormflow samples from sites FOR, URB, and COM and baseflow samples from the 21 sampling sites suggests that baseflow has a greater influence from groundwater derived NO_3^- than stormflow does. We also see in Figure 2.15 that sites URB and COM have greater influence of deeper groundwater compared to samples taken from site FOR. This may be explained by a more easily saturated vadose zone due to higher elevation and deeper bedrock level paired with increased permeable land cover. These conditions would decrease potential for water-bedrock evaporite interactions. A seasonal difference in SO_4^{2-} isotope composition at site FOR mirrors seasonal climate patterns; it is expected that the wetter season would result in a greater contribution of more shallow water. The observed $\delta^{18}O$ values of SO_4^{2-} from baseflow samples and storm flow samples from sites COM and URB are within the range of geologic and anthropogenic sources. These results strengthen the indication that the groundwater is a strong driver of the water quality in the entire watershed.

2.4 COMBINED DISCUSSION

Results from stable isotope analysis of nitrate and sulfate suggest that water-rock and water-soil interactions are the largest sources of NO_3^- in BC watershed, indicating natural processes (such as nitrification in soil) and minimal pollution from upland nonpoint sources or manure/septic.

Microbial nitrification processes fix NO_3^- in the soil, which is dissolved into infiltrating rainwater. Over time, groundwater NO_3^- isotope compositions have come to reflect the signature of soil nitrogen endmembers. Atmospheric deposition influenced NO_3^- sources in stormflow at the most downstream monitoring site, COMBINED, however this was still not the main contributing source. This indicates that anthropogenic sources transported to the stream from impervious surfaces in runoff are not a large contributor of NO_3^- in BC watershed. Greater NO_3^- concentrations during baseflow in comparison to stormflow at both the larger downstream catchment, site COM, and the small urban catchment, site URB, further supports that nutrient loading from nonpoint sources during storm events is not a large contributor to nitrate concentrations.

Land cover runoff endmember samples indicated a higher influence of NO_3^- sourced from atmospheric deposition than stream flow samples. Dissolved NO_3^-- in road and rooftop runoff samples indicated a higher influence of atmospheric deposition than grass and soil samples, however there was too high of variance (standard deviations of 22.7‰ and 25.3‰ for $\delta^{18}O$ of rooftop and roadway samples, respectively) to be used reliably for source partitioning using runoff as endmembers. The low contribution of atmospheric deposition to in-stream NO_3^- sources, especially when compared to runoff endmembers in this study and to similar urban streams in other studies, may be explained by the relatively high influence from terrestrial loading resulting from subsurface nitrification and denitrification processes. A study employing stable isotope analysis to compare NO_3^- sources in forested, low residential, agricultural, urban, and suburban land use types in the Baltimore Long-Term Ecological Research site found urban streams to have a negative correlation between $\delta^{15}N$ and $\delta^{18}O$, indicating mixing between atmospheric deposition and wastewater (Kaushal et al., 2011). Nitrate isotope composition ranges for Baker Creek samples were more compatible to low-residential land use in the Kaushal study, with a similar positive correlation between $\delta^{15}N$ and $\delta^{18}O$ indicating denitrification in spring datasets. These results are representative of the low to medium intensity development present in Baker Creek.

2.4 CONCLUSION

In conclusion, our investigation challenges conventional notions regarding the relationship between increased nitrate concentrations and nonpoint source pollution in urban ecosystems. Contrary to the common understanding that human-induced alterations to nitrogen inputs contribute to elevated nitrogen concentrations, our case study of Baker Creek suggests a more nuanced picture. While the general global trend of rising reactive nitrogen may be observable in this watershed, the specific effects are not extraordinary or unique, challenging the perception of this catchment as a distinct hotspot for potential pollution.

The nitrate isotope signatures collected from Baker Creek during this study period indicate that dissolved NO_3^- concentrations appear to be sourced primarily from soil microbial processes, not pollution. While some anthropogenic sources may have initially influenced the watershed, microbial processes have altered their isotope signatures over time. Despite the lack of strong isotopic evidence for nonpoint source pollution, the stream's average NO_3^- concentrations still indicate poor water quality, justifying its inclusion on the 303(d) depleted streams list. However, stormwater contributes insignificantly to NO_3^- concentrations in the watershed, challenging assumptions made for streams targeted for nutrient pollution mitigation. This is critical, as plans to remove streams from the EPA 303(d) list include the development of a Total Maximum Daily Load (TMDL). Based on this study, surface runoff retrofits would likely have little to no impact on observed in-stream NO_3 concentrations. Understanding what is contributing to nitrate concentrations in a watershed before implementing a restoration is imperative to avoid costly and ultimately unnecessary interventions.

While stormwater is unlikely to contribute nitrate pollution to the stream in this catchment, it does increase nitrate transport out of the watershed as highlighted by Reisinger et al., 2016. Interventions may elect a more nuanced approach to TMDL plans, considering seasonal variability in nitrate to identify potential focus windows for preventing excess nitrogen export downstream. It is essential to delineate specific goals specific to the targeted watershed; developing a TMDL plan for Baker Creek would most likely benefit receiving water bodies

downstream. If the goal is to improve ecological health of first order streams, we need to critically consider if excess nitrate concentrations are harmful to ecosystem function. As of 2007, Tennessee Department of Environment and Conservation (TDEC, 2007) does not have specific nutrient criteria for streams to qualify for the state's 303(d) nutrient-impaired streams list (TDEC, 2007). General water quality criteria outlined in chapter 0400-40-03 state that "waters shall not constrain nutrients in concentrations that stimulate aquatic plant and/or algae growth" to an extent that impacts recreation or causes downstream detriment. The EPA recommends rivers and streams within the central and eastern forested uplands ecoregion maintain a total nitrogen concentration less than 0.31 mg/L (TDEC, 2007). In the future, state environmental agencies may take seasonal and vegetation-derived bias into account when determining a stream's impairment status.

In summary, our research underscores the complexity of nitrogen dynamics in urban ecosystems and challenges the conventional wisdom surrounding the relationship between increased nitrate concentrations and nonpoint source pollution. The study highlights the need for caution in labeling nutrient concentrations as "pollution," emphasizing the natural occurrence of nitrate in ecological cycles and suggests more comprehensive analysis before moving forward with regulatory remediation plans. Factors such as the watershed's drainage area, hydrological response, microbiome, vegetated land cover, and temporal patterns in biological demand should be taken into account. As we strive to develop effective management strategies, a more nuanced understanding of the factors influencing nitrogen transport and uptake is crucial to guide targeted and impactful interventions for improving water quality and ecological health in urban first order streams.

REFERENCES

Alpers, C. N. (2016). Stable Isotope Systematics of Sulfate Minerals Mars geochemistry, mineralogy, and biosignatures, and Earth analogs *Arsenic Geochemistry, Mineralogy, and Bioavailability in Mine Waste.* https://doi.org/10.2138/rmg.2000.40.12

Arfken, A. M., Song, B., & Mallin, M. A. (2015). Assessing hog lagoon waste contamination in the Cape Fear Watershed using Bacteroidetes 16S rRNA gene pyrosequencing. *Applied Microbiology and Biotechnology*, *99*(17), 7283–7293. https://doi.org/10.1007/S00253-015-6784-X/TABLES/3

Badgley, B., & Hagedorn, C. (2015). *Microbial Source Tracking: Advances in Research and a Guide to Application*. https://doi.org/10.1007/978-3-319-14212-8_10

Bai, Y., Ochuodho, T. O., & Yang, J. (2019). Impact of land use and climate change on water-related ecosystem services in Kentucky, USA. *Ecological Indicators*, *102*, 51–64. https://doi.org/10.1016/j.ecolind.2019.01.079

Baral, D., Asce, S. M., Fisher, J. R., Asce, M., Michael, ;, Iii, J. F., Bruce, ;, Dvorak, I., Snow, D. D., Admiraal, D. M., & Asce, A. M. (2017). *Atmospheric Contributions of Nitrate to Stormwater Runoff from Two Urban Watersheds*. https://doi.org/10.1061/(ASCE)EE.1943-7870.0001323

Baral, D., Speicher, A., Dvorak, B., Admiraal, D., & Li, X. (2018). Quantifying the relative contributions of environmental sources to the microbial community in an urban stream under dry and wet weather conditions. *Applied and Environmental Microbiology*, *84*(15). https://doi.org/10.1128/AEM.00896-18

Bell, C. D., McMillan, S. K., Clinton, S. M., & Jefferson, A. J. (2017). Characterizing the Effects of Stormwater Mitigation on Nutrient Export and Stream Concentrations. *Environmental Management*, *59*(4), 604–618. https://doi.org/10.1007/s00267-016-0801-4

Bernhardt, E. S., Blaszczak, J. R., Ficken, C. D., Fork, M. L., Kaiser, K. E., & Seybold, E. C. (2017). Control Points in Ecosystems: Moving Beyond the Hot Spot Hot Moment Concept. *Ecosystems*, *20*(4), 665–682. https://doi.org/10.1007/s10021-016-0103-y

Bosch, D. J., Wagena, M. B., Ross, A. C., Collick, A. S., & Easton, Z. M. (2018). Meeting Water Quality Goals under Climate Change in Chesapeake Bay Watershed, USA. *Journal of the American Water Resources Association*, *54*(6), 1239–1257. https://doi.org/10.1111/1752-1688.12684

Bowles, M. W., Nigro, L. M., Teske, A. P., & Joye, S. B. (2012). Denitrification and environmental factors influencing nitrate removal in Guaymas Basin hydrothermally altered sediments. *Frontiers in Microbiology*, *3*(OCT), 377. https://doi.org/10.3389/FMICB.2012.00377/BIBTEX

Bushon, R. N., Brady, A. M. G., Christensen, E. D., & Stelzer, E. A. (2017). Multi-Year Microbial Source Tracking Study Characterizing Fecal Contamination in an Urban Watershed. *Water Environment Research*, *89*(2). https://doi.org/10.2175/106143016X14798353399412

Cadenasso, M. L., & Pickett, S. T. A. (2008). Cities and the Environment (CATE) Cities and the Environment (CATE) Urban Principles for Ecological Landscape Design and Urban Principles for Ecological Landscape Design and Maintenance: Scientific Fundamentals Maintenance: Scientific Fundamentals Urban Principles for Ecological Landscape Design and Maintenance: Scientific Urban Principles for Ecological Landscape Design and Maintenance: Scientific Fundamentals Fundamentals. *Cities and the Environment (CATE)*, *1*(2).

Carey, R. O., Wollheim, W. M., Mulukutla, G. K., & Mineau, M. M. (2014). Characterizing storm-event nitrate fluxes in a fifth order suburbanizing watershed using in situ sensors. *Environmental Science and Technology*, *48*(14), 7756–7765. https://doi.org/10.1021/ES500252J

Chang, H., & Bonnette, M. R. (2016). Climate change and water-related ecosystem services: impacts of drought in california, usa. *Ecosystem Health and Sustainability*, *2*(12). https://doi.org/10.1002/ehs2.1254

Christian, L., Epps, T., Diab, G., & Hathaway, J. (2020). Pollutant concentration patterns of in-stream urban stormwater runoff. *Water (Switzerland)*, *12*(9). https://doi.org/10.3390/w12092534

Denk, T. R. A., Mohn, J., Decock, C., Lewicka-Szczebak, D., Harris, E., Butterbach-Bahl, K., Kiese, R., & Wolf, B. (2017). The nitrogen cycle: A review of isotope effects and isotope modeling approaches. *Soil Biology and Biochemistry*, *105*, 121–137. https://doi.org/10.1016/J.SOILBIO.2016.11.015

Derek R. Lovley. (2003). Cleaning up with Genomics: Applying molecular biology to bioremediation. *NATURE REVIEWS | MICROBIOLOGY*, *1*, 5. https://doi.org/10.1038/nrmicro731

Divers, M. T., Elliott, E. M., & Bain, D. J. (2014). *Quantification of Nitrate Sources to an Urban Stream Using Dual Nitrate Isotopes*. https://doi.org/10.1021/es404880j

Duncan, J. M., Welty, C., Kemper, J. T., Groffman, P. M., & Band, L. E. (2017). Dynamics of nitrate concentration-discharge patterns in an urban watershed. *Water Resources Research*, *53*(8), 7349–7365. https://doi.org/10.1002/2017WR020500

Dvorak, B. I., Fisher, J. R., Florek, I. M. J., Snow, D. D., & Admiraal, D. M. (2014). Isotopic Analysis for Characterizing Nutrient Sources in a Small Urban Nebraska Watershed. *World Environmental and Water Resources Congress 2014: Water Without Borders - Proceedings of the 2014 World Environmental and Water Resources Congress*, 38–45. https://doi.org/10.1061/9780784413548.006

Epps, T. H., Hathaway, J. M., & Asce, M. (2021). *Inter-Event Water Quality Variability and Intra-Event Pollutant Dynamics in Context of Effective Impervious Area*. https://doi.org/10.1061/JSWBAY.0000953

Evans, C., & Davies, T. D. (1998). Causes of concentration/discharge hysteresis and its potential as a tool for analysis of episode hydrochemistry. *Water Resources Research*, *34*(1), 129–137. https://doi.org/10.1029/97WR01881

Fenn, M. E., & Poth, M. A. (1999). Temporal and Spatial Trends in Streamwater Nitrate Concentrations in the San Bernardino Mountains, Southern California. *Journal of Environmental Quality*, *28*(3), 822–836. https://doi.org/10.2134/JEQ1999.00472425002800030013X

Fletcher, T. D., Andrieu, H., & Hamel, P. (2012). *Understanding, management and modelling of urban hydrology and its consequences for receiving waters: A state of the art*. https://doi.org/10.1016/j.advwatres.2012.09.001

Fletcher, T. D., Shuster, W., Hunt, W. F., Ashley, R., Butler, D., Arthur, S., Trowsdale, S., Barraud, S., Semadeni-Davies, A., Bertrand-Krajewski, J.-L., Steen Mikkelsen, P., Rivard, G., Uhl, M., Dagenais, D., & Viklander, M. (2015). SUDS, LID, BMPs, WSUD and more-The evolution and application of terminology surrounding urban drainage. *Urban Water Journal*, *12*(7), 525–542. https://doi.org/10.1080/1573062X.2014.916314

Fowler, D., Coyle, M., Skiba, U., Sutton, M. A., Cape, J. N., Reis, S., Sheppard, L. J., Jenkins, A., Grizzetti, B., Galloway, J. N., Vitousek, P., Leach, A., Bouwman, A. F., Butterbach-Bahl, K., Dentener, F., Stevenson, D., Amann, M., & Voss, M. (2013). The global nitrogen cycle in the twenty-first century. *Philosophical Transactions of the Royal Society B: Biological Sciences*, *368*(1621). https://doi.org/10.1098/RSTB.2013.0164

Frazar, Á. J., Gold, S. A., Addy Á D Q Kellogg, Á. K., Moatar, F., Birgand, F., Schroth, A. W., & Pradhanang, S. M. (2019). *Contrasting behavior of nitrate and phosphate flux from high*

flow events on small agricultural and urban watersheds. *145*, 141–160. https://doi.org/10.1007/s10533-019-00596-z

Fremaux, B., Gritzfeld, J., Boa, T., & Yost, C. K. (2009). Evaluation of host-specific Bacteroidales 16S rRNA gene markers as a complementary tool for detecting fecal pollution in a prairie watershed. *Water Research*, *43*(19), 4838–4849. https://doi.org/10.1016/J.WATRES.2009.06.045

Groffman, P. M., Butterbach-Bahl, K., Fulweiler, R. W., Gold, A. J., Morse, J. L., Stander, E. K., Tague, C., Tonitto, C., Vidon, P., Grovman, P. M., Butterbach-Bahl, K., Fulweiler, R. W., Gold, A. J., Morse, J. L., Stander, E. K., Tague, C., Bren, D., Tonitto, C., & Vidon, P. (2009). *Challenges to incorporating spatially and temporally explicit phenomena (hotspots and hot moments) in denitriWcation models*. *93*, 49–77. https://doi.org/10.1007/s10533-008-9277-5

Groffman, P. M., Cavender-Bares, J., Bettez, N. D., Grove, J. M., Hall, S. J., Heffernan, J. B., Hobbie, S. E., Larson, K. L., Morse, J. L., Neill, C., Nelson, K., O'Neil-Dunne, J., Ogden, L., Pataki, D. E., Polsky, C., Chowdhury, R. R., & Steele, M. K. (2014). Ecological homogenization of urban USA. *Frontiers in Ecology and the Environment*, *12*(1), 74–81. https://doi.org/10.1890/120374

Groffman, P. M., Law, N. L., Belt, K. T., Band, L. E., & Fisher, G. T. (2004a). *Nitrogen Fluxes and Retention in Urban Watershed Ecosystems*. https://doi.org/10.1007/s10021-003-0039-x

Groffman, P. M., Law, N. L., Belt, K. T., Band, L. E., & Fisher, G. T. (2004b). *Nitrogen Fluxes and Retention in Urban Watershed Ecosystems*. https://doi.org/10.1007/s10021-003-0039-x

Guérineau, H., Dorner, S., Carrière, A., McQuaid, N., Sauvé, S., Aboulfadl, K., Hajj-Mohamad, M., & Prévost, M. (2014). Source tracking of leaky sewers: A novel approach combining fecal indicators in water and sediments. *Water Research, 58*, 50–61. https://doi.org/10.1016/J.WATRES.2014.03.057

Hao, X., Jiang, R., & Chen, T. (2011). Clustering 16S rRNA for OTU prediction: a method of unsupervised Bayesian clustering. *Bioinformatics*, *27*(5), 611–618. https://doi.org/10.1093/BIOINFORMATICS/BTQ725

Hathaway, J. M., Asce, M., Krometis, ; L H, & Hunt, W. F. (2014). Exploring Seasonality in Escherichia coli and Fecal Coliform Ratios in Urban Watersheds . *Journal of Irrigation and Drainage Engineering*, *140*(4), 04014003. https://doi.org/10.1061/(ASCE)IR.1943-4774.0000700

Haygarth, P. M., Condron, L. M., Heathwaite, A. L., Turner, B. L., & Harris, G. P. (n.d.). *The phosphorus transfer continuum: Linking source to impact with an interdisciplinary and multi-scaled approach*. https://doi.org/10.1016/j.scitotenv.2005.02.001

Hong, W. Y., Park, M. J., Park, J. Y., Park, G. A., & Kim, S. J. (2010). The spatial and temporal correlation analysis between MODIS NDVI and SWAT predicted soil moisture during forest NDVI increasing and decreasing periods. *KSCE Journal of Civil Engineering*, *14*(6), 931–939. https://doi.org/10.1007/s12205-010-0851-8

Horst, A., Jü, •, Miguel, M. •, López-Zavala, A., & Mayer, B. (n.d.). *The origin of salinity and sulphate contamination of groundwater in the Colima State, Mexico, constrained by stable isotopes*. https://doi.org/10.1007/s12665-011-1008-x

Husic, A., Fox, J., Adams, E., Pollock, E., Ford, W., Agouridis, C., & Backus, J. (2020). Quantification of nitrate fate in a karst conduit using stable isotopes and numerical modeling. *Water Research*, *170*. https://doi.org/10.1016/J.WATRES.2019.115348

Ishii, S., & Sadowsky, M. J. (2008). Minireview Escherichia coli in the Environment: Implications for Water Quality and Human Health. *Microbes Environ*, *23*(2), 101–108. https://doi.org/10.1264/jsme2.23.101

Jani, J., Yang, Y. Y., Lusk, M. G., & Toor, G. S. (2020). Composition of nitrogen in urban residential stormwater runoff: Concentrations, loads, and source characterization of nitrate and organic nitrogen. *PloS One*, *15*(2), e0229715. https://doi.org/10.1371/journal.pone.0229715

Jarosiewicz, P., Fazi, S., & Zalewski, M. (2021). How to boost Ecohydrological Nature-Based Solutions in water quality management. *Ecohydrology and Hydrobiology*. https://doi.org/10.1016/J.ECOHYD.2021.11.005

Jordan, P., Arnscheidt, J., Mcgrogan, H., & Mccormick, S. (2005). High-resolution phosphorus transfers at the catchment scale: the hidden importance of non-storm transfers. *Hydrology and Earth System Sciences*, *9*(6), 685–691.

Kaushal, S. S., Groffman, P. M., Band, L. E., Elliott, E. M., Shields, C. A., & Kendall, C. (2011). Tracking Nonpoint Source Nitrogen Pollution in Human-Impacted Watersheds. *Environ. Sci. Technol*, *45*, 8225–8232. https://doi.org/10.1021/es200779e

Kildare, B. J., Leutenegger, C. M., McSwain, B. S., Bambic, D. G., Rajal, V. B., & Wuertz, S. (2007). 16S rRNA-based assays for quantitative detection of universal, human-, cow-, and dog-specific fecal Bacteroidales: A Bayesian approach. *Water Research*, *41*(16), 3701–3715. https://doi.org/10.1016/J.WATRES.2007.06.037

Kuypers, M. M. M., Sliekers, A. O., Lavik, G., Schmid, M., Jergensen, B. B., Kuenen, J. gijs, Damste, J. S. S., Strous, M., & Jetten, M. S. M. (3 C.E.). Anaerobic ammonium oxidation by anammox bacteria in the Black Sea. *Nature*, *422*, 608–611. https://www.nature.com/articles/nature01472.pdf

Lamendella, R., Domingo, J. W. S., Oerther, D. B., Vogel, J. R., & Stoeckel, D. M. (2007). Assessment of fecal pollution sources in a small northern-plains watershed using PCR and phylogenetic analyses of Bacteroidetes 16S rRNA gene. *FEMS Microbiology Ecology*, *59*(3), 651–660. https://doi.org/10.1111/J.1574-6941.2006.00211.X

Martin, C., Aquilina, L., Gascuel-Odoux, C., Molénat, J., Faucheux, M., & Ruiz, L. (2004). Seasonal and interannual variations of nitrate and chloride in stream waters related to spatial and temporal patterns of groundwater concentrations in agricultural catchments. *Hydrological Processes*, *18*(7), 1237–1254. https://doi.org/10.1002/HYP.1395

Merbt, S. N., Proia, L., Prosser, J. I., Marti, E., Casamayor, E. O., & von Schiller, D. (2016). Stream drying drives microbial ammonia oxidation and first-flush nitrate export. *Ecology*, *97*(9), 2192–2198. https://doi.org/10.1002/ECY.1486

Moore, G., McGuire, K., Troch, P., & Barron-Gafford, G. (2015). Ecohydrology and the Critical Zone: Processes and Patterns Across Scales. *Developments in Earth Surface Processes*, *19*, 239–266. https://doi.org/10.1016/B978-0-444-63369-9.00008-2

Morrissy, J. G., Currell, M. J., Reichman, S. M., Surapaneni, A., Megharaj, M., Crosbie, N. D., Hirth, D., Aquilina, S., Rajendram, W., & Ball, A. S. (2021). Nitrogen contamination and bioremediation in groundwater and the environment: A review. *Earth-Science Reviews*, *222*, 103816. https://doi.org/10.1016/J.EARSCIREV.2021.103816

National Atmospheric Deposition Program, 2013. National Atmospheric Deposition Program 2012 Annual Summary. NADP Data Report 2013-01. Illinois State Water Survey, University of Illinois at Urbana-Champaign, IL.

National Atmospheric Deposition Program, 2014. National Atmospheric Deposition Program 2013 Annual Summary. NADP Data Report 2014-01. Illinois State Water Survey, University of Illinois at Urbana-Champaign, IL.

National Atmospheric Deposition Program, 2021. National Atmospheric Deposition Program 2020 Annual Summary. NADP Data Report 2021-01. Illinois State Water Survey, University of Illinois at Urbana-Champaign, IL.

Newbold, J. D., O'Neill, R. v., Elwood, J. W., & van Winkle, W. (2015). Nutrient Spiraling in Streams: Implications for Nutrient Limitation and Invertebrate Activity. *Https://Doi.Org/10.1086/284017*, *120*(5), 628–652. https://doi.org/10.1086/284017

Nuttle, W. K. (2002). Is ecohydrology one idea or many? *Hydrological Sciences Journal*, *47*(5), 805–807. https://doi.org/10.1080/02626660209492983

O'Driscoll, M., Clinton, S., Jefferson, A., Manda, A., & McMillan, S. (2010). Urbanization effects on watershed hydrology and in-stream processes in the southern United States. *Water (Switzerland)*, *2*(3), 605–648. https://doi.org/10.3390/W2030605

Pace, N. R., Stahl, D. A., Lane, D. J., & Olsen, G. J. (1986). *The Analysis of Natural Microbial Populations by Ribosomal RNA Sequences*. 1–55. https://doi.org/10.1007/978-1-4757-0611-6_1

Piña-Ochoa, E., & Álvarez-Cobelas, M. (2006). Denitrification in Aquatic Environments: A Cross-system Analysis. *Biogeochemistry 2006 81:1*, *81*(1), 111–130. https://doi.org/10.1007/S10533-006-9033-7

Pitt, R., Chen, S.-E., Clark, S. E., Swenson, J., & Ong, C. K. (2008). Compaction's Impacts on Urban Storm-Water Infiltration. *Journal of Irrigation and Drainage Engineering*, *134*(5), 652–658. https://doi.org/10.1061/(ASCE)0733-9437(2008)134:5(652)

Reisinger, A. J., Groffman, P. M., & Rosi-Marshall, E. J. (2016). Nitrogen-cycling process rates across urban ecosystems. *FEMS Microbiology Ecology*, *92*(12), fiw198. https://doi.org/10.1093/femsec/fiw198

Ribeiro, S., Limoges, A., Massé, G., Johansen, K. L., Colgan, W., Weckström, K., Jackson, R., Georgiadis, E., Mikkelsen, N., Kuijpers, A., Olsen, J., Olsen, S. M., Nissen, M., Andersen, T. J., Strunk, A., Wetterich, S., Syväranta, J., Henderson, A. C. G., Mackay, H., …

Davidson, T. A. (2021). Vulnerability of the North Water ecosystem to climate change. *Nature Communications*, *12*(1). https://doi.org/10.1038/s41467-021-24742-0

Roberts, B. J., Mulholland, P. J., & Hill, W. R. (2007). *Multiple Scales of Temporal Variability in Ecosystem Metabolism Rates: Results from 2 Years of Continuous Monitoring in a Forested Headwater Stream*. https://doi.org/10.1007/s10021-007-9059-2

Sanchez, D. A., Szynkiewicz, A., & Faiia, A. M. (2017). *Determining sources of nitrate in the semi-arid Rio Grande using nitrogen and oxygen isotopes*. https://doi.org/10.1016/j.apgeochem.2017.09.012

Sigman, D. M., Casciotti, K. L., Andreani, M., Barford, C., Galanter, M., & Bo, J. K. (1998). A Bacterial Method for the Nitrogen Isotopic Analysis of Nitrate in Seawater and Freshwater. *Zumft, W. G. Microbiol. Mol. Biol. Rev*, *57*(3), 4145. https://doi.org/10.1021/ac010088e

Silva, S. R., Ging, P. B., Lee, R. W., Ebbert, J. C., Tesoriero, A. J., & Inkpen, E. L. (2002). Forensic Applications of Nitrogen and Oxygen Isotopes in Tracing Nitrate Sources in Urban Environments. *Environmental Forensics*, *3*(2), 125–130. https://doi.org/10.1006/enfo.2002.0086

Smakhtin, V. U. (2004). Estimating continuous monthly baseflow time series and their possible applications in the context of the ecological reserve. *Water SA*, *27*(2), 213–218. https://doi.org/10.4314/wsa.v27i2.4995

Smith, M. B., Rocha, A. M., Smillie, C. S., Olesen, S. W., Paradis, C., Wu, L., Campbell, J. H., Fortney, J. L., Mehlhorn, T. L., Lowe, K. A., Earles, J. E., Phillips, J., Techtmann, S. M., Joyner, D. C., Elias, D. A., Bailey, K. L., Hurt, R. A., Preheim, S. P., Sanders, M. C., … Steven Lindow, E. E. (2015). *Natural Bacterial Communities Serve as Quantitative Geochemical Biosensors*. https://doi.org/10.1128/mBio.00326-15

Steinauer, K., Zytynska, S., Weisser, W. W., & Eisenhauer, N. (2014). Changes in plant community structure and soil biota along soil nitrate gradients in two deciduous forests. *Pedobiologia*, *57*(3), 139–145. https://doi.org/10.1016/J.PEDOBI.2014.01.007

Stelzer, R. S., Effernan, J. H., Ene, G., & Ikens, E. L. (2003). The influence of dissolved nutrients and particulate organic matter quality on microbial respiration and biomass in a forest stream. *Freshwater Biology*, *48*, 1925–1937.

Stoddard, J. L. (1994). *Long-Term Changes in Watershed Retention of Nitrogen Its Causes and Aquatic Consequences* (Vol. 18, pp. 223–284). UTC. https://pubs.acs.org/sharingguidelines

Suberkropp, K., Gulis, V., Rosemond, A. D., & Benstead, J. P. (2010). *Ecosystem and physiological scales of microbial responses to nutrients in a detritus-based stream: Results of a 5-year continuous enrichment*.

Szynkiewicz, A., Borrok, D. M., Ganjegunte, G. K., Skrzypek, G., Ma, L., Rearick, M., & Perkins, G. (n.d.). *Isotopic studies of the Upper and Middle Rio Grande. Part 2-Salt loads and*. Retrieved September 2, 2021, from http://www.elsevier.com/open-access/userlicense/1.0/

Szynkiewicz, A., Olichwer, T., & Tarka, R. (2019). *Delineation of groundwater provenance in Arctic environment using isotopic compositions of water and sulphate*. https://doi.org/10.1016/j.jhydrol.2019.124232

Techtmann, S. M., & Hazen, T. C. (2016). Metagenomic applications in environmental monitoring and bioremediation. In *Journal of Industrial Microbiology and Biotechnology* (Vol. 43, Issue 10, pp. 1345–1354). Springer Verlag. https://doi.org/10.1007/s10295-016-1809-8

Thomas, S., Ledoux, M., Szynkiewicz, A., Faiia, A. M., Mayes, M. A., Mckinney, M. L., & Dean, W. G. (2016). *Chemical and isotope compositions of shallow groundwater in areas*

impacted by hydraulic fracturing and surface mining in the Central Appalachian Basin, Eastern United States. https://doi.org/10.1016/j.apgeochem.2016.05.007

UNESCO, "Ecohydrology". *UNESCO*, 2014, *https://en.unesco.org/themes/water-security/hydrology/ecohydrology*

USEPA, U. S. E. P. A. (Producer). (2016). National Summary of State Information. USEPA. Retrieved from https://ofmpub.epa.gov/waters10/attains_index.control#causes

Kendall, C, "Resources on Isotopes" USGS (2004), https://wwwrcamnl.wr.usgs.gov/isoig/res/funda.html.

United States Department of Agriculture Soil Conservation Service (1981). Agricultural Handbook.

Vierheilig, J., Savio, D., Ley, R. E., Mach, R. L., Farnleitner, A. H., & Reischer, G. H. (2015). Potential applications of next generation DNA sequencing of 16S rRNA gene amplicons in microbial water quality monitoring. *Water Science and Technology*, *72*(11). https://doi.org/10.2166/wst.2015.407

Vystavna, Y., Schmidt, S. I., Diadin, D., Rossi, P. M., Vergeles, Y., Erostate, M., Yermakovych, I., Yakovlev, V., Knöller, K., & Vadillo, I. (2019). Multi-tracing of recharge seasonality and contamination in groundwater: A tool for urban water resource management. *Water Research*, *161*, 413–422. https://doi.org/10.1016/j.watres.2019.06.028

Wavrek, M. T. (2020). *FROM DRONES TO DIRT: COMPREHENSIVE ECOLOGICAL ASSESSMENTS FOR ENHANCING CONSERVATION MANAGEMENT OF URBAN FORESTED NATURAL AREAS*.

Webster, J. R., & Patten, B. C. (1979). Effects of Watershed Perturbation on Stream Potassium and Calcium Dynamics. *Ecological Monographs*, *49*(1), 51–72. https://doi.org/10.2307/1942572

Widder, S., Besemer, K., Singer, G. A., Ceola, S., Bertuzzo, E., Quince, C., Sloan, W. T., Rinaldo, A., & Battin, T. J. (2014). Fluvial network organization imprints on microbial co-occurrence networks. *Proceedings of the National Academy of Sciences of the United States of America*, *111*(35), 12799–12804. https://doi.org/10.1073/pnas.1411723111

World Urbanization Prospects: The 2018 Revision. (n.d.).

Yang, J.-L., & Zhang, G.-L. (2015). Formation, characteristics and eco-environmental implications of urban soils-A review. *Soil Science and Plant Nutrition*, 30–46. https://doi.org/10.1080/00380768.2015.1035622

CHAPTER 3

INVESTIGATING MICROBIAL COMMUNITY ASSEMBLY PROCESSES ACROSS AN URBAN TO FOREST LAND USE GRADIENT

This article was written primarily by Victoria Rexhausen with revisions from Jon Hathaway and input from Clifford Swanson. All analysis was performed by Victoria Rexhausen.

3.0. ABSTRACT

Understanding how urbanization impacts the microbiome is crucial for both human and ecological health during an age of rapid urbanization. Examining the drivers of microbial community assembly is essential to comprehend how microbial communities respond to urbanization. This study delves into variations in microbial community diversity within a heterogeneous urban watershed considering factors such as land use, season, distance to the outlet, and flow type (stormflow or baseflow). The results showed that beta diversity between samples was significantly correlated with land use ($p<0.0001$), flow type ($p=0.0002$) and season ($p<0.0001$). There was not a statistically significant difference in alpha diversity between samples grouped by flow type, percent impervious cover, or distance to the outlet. Differences in alpha diversity were statistically significant between seasons. Phylogenetic diversity metrics offer valuable insights into the mechanisms behind observed diversity changes. Deterministic ecological mechanisms were found to be responsible for 58% of phylogenetic turnover in the spring. Phylogenetic turnover in stormflow was less likely to be affected by drift and more likely to be impacted by selection than in baseflow. These findings have significant implications for the development of biotechnological methods in urban stream management, including bioremediation, source tracking, and the effective implementation of nature-based solutions.

3.1. INTRODUCTION

The interconnected web of dynamic microbial communities found in aquatic ecosystems plays a crucial role in nutrient cycling, water quality, and ecosystem health. The key role that microbes play in biogeochemical cycles make them a particularly potent lens through which we may gain insight into the patterns and drivers of ecosystem response to environmental stimuli (Hosen et al., 2023). Recent advancements in microbial ecology have demonstrated the application of next-generation sequencing of 16S rRNA genes in order to effectively quantify bacterial community composition and microbial community structure. This development is of particular interest to stream ecologists, where the relationship between urbanization and the structure and function of microbial communities and their processes has been identified as one of the 26 most pressing research questions in urban stream ecology (Wenger *et al.*, 2009).

Within microbial ecology, understanding mechanisms diving community assembly is a critical yet poorly understood topic (Zhou & Ning, 2017). Niche-based theory suggests that selective processes driven by environmental filtering strongly influence community composition (Diamond, 1975). Niche-based theory forms the foundational framework for the development and implementation of microbial bioremediation technologies, which aim to harness microbial communities resilient to changes in certain environmental parameters to restore and enhance and ecosystem balance (Lovley et al., 2003). Neutral theory, by contrast, suggests that species are not selected by an ecological hierarchy, but that community diversity is driven primarily by stochastic processes such as birth, death, evolution, extinction, and immigration (Chave, 2004). Studies in the last 20 years have emerged to quantify the relative importance of each of these ecological processes in a variety of microbial communities. In a generally accepted conceptual framework, ecological processes driving assembly have been grouped into four fundamental processes: speciation, selection, dispersal, and ecological drift (Zhou & Ning, 2017).

In recent years, bioinformatic statistical analyses have been applied to microbial community assembly processes to derive quantitative assumptions of the relative importance of deterministic and stochastic processes in microbial communities based on phylogenetic diversity. These

methods use statistics to measure the relatedness between species within and between pairs of communities, attributing larger than expected phylogenetic turnover as driven primarily deterministic selective processes. Studies employing this framework have uncovered significant influence of stochastic processes in the assembly of microbial communities in a variety of ecosystems, including grasslands, wastewater treatment plants, sediment communities.

Implications of urbanizing land use on hydrology and water quality have been well documented (Walsh *et al*., 2005), and these effects provide a myriad of additional environmental stimuli which may affect microbial communities through means of both deterministic and transport mechanisms. Changes in soil moisture content and drying and rewetting patterns impact microbial respiration rates and connected pathways for organism transport/exchange between spatially isolated areas (Evans *et al.*, 2022; Dodds *et al*., 2020; Merbt *et al*., 2016; Junk *et al*., 1989). Turbulent hydraulics of flashy streams impact disrupt benthic bed communities and have implications of the microorganisms resilient to variability in stream pool habitats (O'Driscoll *et al*., 2010; Qu *et al*., 2017; Ouellet *et al*., 2021). There is a shortage of literature exploring microbial community structure in the urban water column, as opposed to sediment and benthic communities. While some studies have begun to investigate microbial community structure in the urban stream water column through measurements of diversity and co-occurrence (Hosen et al., 2017), none of these studies have employed methodologies to quantify the proportion of phylogenetic turnover that can be attributed to selection, dispersal, and drift.

The studies that have included water column communities highlight the need for further research. Studies comparing microbial community response in the water column habitat to benthic/sediment habitats have shown that water column communities are more responsive to changes in land use. Water column and benthic community richness has been shown to suffer in streams with urbanized land use compared to forested land use (Hosen et al., 2017). Bacterial co-occurrence, a measurement of how much overlap there is in occurrence of taxa from sample to sample, also decreases in urban samples indicating a loss of keystone taxa and potentially a decreased ecological resilience (Hosen et al., 2017). Environmental conditions such as nitrate

concentration in the water column, DOC concentration, and electrical conductivity have all been shown to impact microbial community (Lia et al., 2019).

This increased responsiveness to measures of urbanized land use observed in the water column microbial community may be elucidated by quantifying the significance of different ecological assembly processes. This study attempts to investigate the relative importance of drift, dispersal, and selection on the urban water column microbial community in response to urbanization by sampling microbial communities across a small subcatchments with an urban to forest gradient. Based on observations detailed in literature, we hypothesized that microbial communities may be increasingly affected by homogenizing dispersal and homogenizing selection in forested land use. We additionally hypothesized that samples taken during stormflow would have a greater amount of phylogenetic turnover due to dispersal compared to samples taken during baseflow. The results show that flow type, season, percent imperviousness, and distance from the outlet are all relevant to the ecological processes driving community assembly in the water column microbiome.

This paper will investigate both stochastic and deterministic drivers of microbial community assemblage in a heterogeneous, urbanizing watershed. The key objectives of this paper are to determine (1) compare how trends in land use changes versus current land use impact microbial community diversity and composition in a drainage area, and (2) compare OTU indicators of urbanizing watersheds from similar studies in literature. The implications of these result will serve to offer insights into how history of environmental parameters may shape, and thus how microbial community functional diversity offers clues to the trajectory of the watershed's ecological health.

3.2. METHODOLOGY

This investigation took place in the 6.73 km^2 Baker Creek watershed in South Knoxville, TN. The stream has three major inception points feeding to a second order stream with an outlet onto the Tennessee River. Two of the three first order branches of Baker Creek begin in a forested

nature preserve, with 67% deciduous trees, 2% evergreen trees, and 31% a mix of evergreen and deciduous trees. The third of the three first order branches begin in a residentially developed area with an average lot size of approximately 600-1200 m^2 and is directly connected to stormwater drainage infrastructure. As the three branches travel downstream, they encounter increasingly developed terrain, with the longest first order branch meandering under a 4-lane industrial highway. The catchment is located 275m above sea level in the valley and ridge geological region, and is characterized by hilly terrain with deep, well-draining, clayey loamy Telico-Alcoa soils (US Soil Conservation Service, 1981). Knoxville experiences an average annual rainfall of 1270 mm per year.

The study strategically positioned baseflow sampling sites and three hydrologic and stormflow quality monitoring sites across the BC watershed. These hydrologic monitoring stations were strategically placed at key locations: the main discharge point of the forest preserve (FOR), at the outlet of an urban drainage point (URB) with a drainage area comparable to that of FOR, and further downstream where the drainage areas of FOR, URB, and a highly developed four-lane highway converge (COM). Velocity measurements, obtained using a Teledyne ISCO 2150 Area Velocity Doppler flow meter, were employed to establish a stage-discharge relationship for each monitoring site. A 730 bubbler flow module then recorded stage discharge data at one-minute intervals, converted to flow using this relationship. Each monitoring site featured manual and automated tipping bucket rain gauges recording rainfall intensity at five-minute intervals. Average temperature data were sourced from the McGhee Tyson weather monitoring station located 19 km away. The drainage area for each sampling site was determined using the watershed delineation tool in ArcGIS 10.6.1, employing a 1 m resolution digital elevation model (DEM) layer of Knox County. Land use statistics were obtained by clipping the USGS 2016 NLCD land use layer to the delineated subcatchments.

3.2.1. Sample Collection

The study strategically sampled 21 sites during baseflow and 3 sites during stormflow. The baseflow sites were distributed along each of the three first order branches of the creek and on

the downstream second order branch, encompassing the land use changes as the stream flowed towards the outlet. Baseflow sites were sampled throughout the year to assess changes in response to environmental seasons. Samples were taken using an ethanol-sterilized 900 mL polypropylene bottle. Sample bottles and caps were rinsed three times with stream water by gloved hands before being filled with sample water. Samples were transported to the laboratory in a cooler with cool packs immediately after sampling. In the laboratory, samples were prepared for DNA extraction by filtering 500 mL of stream water through 0.22μm Sterivex-GP filters and stored at -20 °C until date of extraction.

The stormflow samples were taken from the inception of the urban first order branch, the point downstream of the largest section of the forest preserve, and just downstream from the 4-lane divided highway where these two branches converge. Samples were obtained using a Teledyne ISCO 6712 Autosampler. Stream water was pumped from the creek into ethanol-sterilized 900 mL polypropylene bottles during each event. Before taking each sample, the autosampler double rinsed the tubing line with stream water. Similarly to the baseflow sampling procedure, samples were transported to the laboratory in a cold cooler immediately following the sampling event and prepared for DNA extraction by filtering 500 mL of sample water through 0.22μm Sterivex-GP filters and stored at -20 °C until date of extraction.

3.2.1.1. Genetic Sampling and Processing

87 samples were selected for 16S rRNA gene extraction and analysis, including baseflow samples from four seasons and stormflow samples from three sites during 2 seasons.

Water column microbial DNA was extracted from Sterevix-GP filters per manufacturer's instructions using a DNeasy PowerSoil Kit by Qiagen. Polymerase chain reaction (PCR) amplification was focused on the V4 region of the 16S rRNA gene using 515F and 806R primers (Cao et al., 2021). Subsequently, the cleaned PCR products underwent paired-end sequencing employing a MiSeq Reagent Kit designed for metagenomics libraries and a MiSeq V2 (300 cycles) Reagent Kit, following the manufacturer's guidelines for 16S amplicon libraries..

3.2.2. Environmental Metadata

Geographical assessments were completed using ArcGIS Pro version 3.0.0 2022. Impervious landcover, tree canopy cover, and developed versus forested land use was quantified using NLCD 2019 Land Cover (CONUS) Products developed by the U.S. Geological Survey (USGS) (Dewitz and USGS, 2021). The raster datasets were imported into ArcGIS Pro. A Knoxville area DEM from KGIS was used to delineate subcatchments drainage areas from the 21 sampling sites throughout the watershed in ArcGIS Pro using the spatial analyst toolkit. The resulting watershed polygons were subsequently used to quantify the distribution of land cover types within each subcatchment area in relation to the NCLD land use map. The tabulate area tool was additionally used to assess the percent imperviousness and the percent tree canopy cover in each subcatchment area. To determine if there is biogeographical bias affecting mechanisms shaping water column community structure as water flowed from upstream to downstream, flow path distance was measured using ArcGIS Pro using the "Locate Features Along Routes" Linear Referencing tool.

3.2.3. Analysis of Sequenced Data

Raw demultiplexed MiSeq files were prepared for further analysis with a cleaning, denoising, clustering workflow using the QIIME2 version 2023.2, a next-generation microbiome bioinformatics platform (Boylon *et al*., 2019). Microbial community fingerprints representing each sample consisted of a list of operational taxonomic units (OTUs) and the number of paired-sequence reads representing each OTU associated with each sample. The resulting table was filtered to exclude OTUs occurring below a relative abundance of 0.005%, which were considered errors (Bokulich et al., 2013).

3.2.3.1. Microbial Diversity and Community Composition

Microbial diversity is quantified by both alpha and beta diversity; alpha diversity measures the variation in species present within a single sample, or species richness. Beta diversity measures the variation between multiple samples, quantifying the evenness of distribution of taxa among

the samples. Alpha diversity was assessed using the Shannon Diversity coefficient, and beta diversity was quantified using the Bray-Curtis dissimilarity statistic. These analyses were performed on rarefied datasets in order to account for differences in sampling depth between samples. To account for loss of statistical relevance from rarefication, each test was assembled 999 times and the average Shannon Diversity Coefficient and Bray-Curtis dissimilarity metric was taken, similarly to other noteworthy studies in microbial ecology (Stegan *et al*., 2013). Microbial diversity computations were completed in RStudio 2022.12.0+53 "Elsbeth Geranium" for Windows using the package *vegan* version 2.6-4 (Oksanen *et al*., 2022).

Response of Diversity to Environmental Parameters

The community diversity response to land cover parameters associated with urbanization was assessed by comparing the diversity metrics to the watershed percent impervious cover and tree canopy cover. Samples were binned into "Urban" or "Forested" land use based on their watershed cover and NLCD land use classification. The diversity metric and log-transformed land use metric were included as a categorical covariate using analysis of covariance (ANCOVA) with the package *mme* (López-Vizcaíno, Lombardía, & Morales, 2013) in RStudio, similar to the methods employed in Hosen *et al.*, 2016. Indicator species were also identified for the land use, flow type, and seasonal groups. Indicator species analysis was conducted using the *indicspecies* package in R to identify taxa that are representative of distinct ecosystem niches. These indicator species, as well as the relative abundance of the most highly represented classes and genera, were compared to the taxa identified as being correlated with urban or forest land use in other studies.

3.2.3.2. Phylogenetic Diversity

Phylogenetic diversity discusses the distance between species in a community of species on a phylogenetic tree. Phylogenetic diversity metrics can be used to quantify community assembly processes, determining how much of the microbial community is influenced by ecological drift, or deterministic niche-based processes, versus neutral, random, or stochastic processes (Stegan *et*

al., 2013). Faith's diversity is an alpha phylogenetic diversity metric telling us how far apart or close together the taxonomy is of the communities making up a sample. Faith's diversity was calculated using similar methods as Bray-Curtis and Shannon diversity metrics (averaging 999 iterations of random sampling computations) within the *vegan* package in RStudio.

In order to understand the phylogenetic similarity between two samples. The abundance weighted beta-mean-nearest taxon distance (beta-MNTD) quantifies the phylogenetic distance between each OTU in one sample's microbial community and its closest relative in the second sample's microbial community. Low beta-MNTD can indicate environmental conditions constraining community composition, while high beta-MNTD indicates divergent environmental conditions (Stegan *et al*., 2013).

Degree in variation of beta-MNTD indicates the overall tendency of the sample group's OTUs to be selected by ecological niches. OTU turnover refers to changes in OTUs within a community over time or across different environments. To quantify the degree in variation of OTU turnover across samples, beta-MNTD is calculated using 999 randomizations, the mean of which is compared to the observed beta-MNTD; the standard deviation of the difference between the observed beta-MNTD and the randomized beta-MNTD is referenced as the beta-nearest taxon index (beta-NTI) (Stegan *et al*., 2013; Wang *et al*., 2013). Beta-NTI values of greater than or less than 2 indicate that phylogenetic turnover was significantly large or small, respectively. Sampled communities with identified high or low phylogenetic turnover were further analyzed using the modified Raup-Crick (RC) index, based on Bray-Curtis Dissimilarity metric. The Bray-Curtis modified RC, or RC_{bray} [RC-bray], accounts for OTU relative abundance/OTU richness and indicates the degree of turnover. Modified RC was calculated using the packed *iCAMP* in R version (Ning *et al*., 2020). Values of $|RC_{bray}| > 0.95$ is interpreted as a degree of turnover significant enough to indicate community selection is determined more by selection than ecological Drift (evolution due to chance) (Chase *et al*., 2011; Stegan *et al*., 2013).

3.3. RESULTS AND DISCUSSION

3.3.1. Richness and Evenness

The Shannon index accounts for both the relative abundance of a species within a community, or species evenness, as well as the richness of biodiversity represented by the sample. Differences in the Shannon index between sample groups was investigated using Kruskal-Wallis rank sum test in r. Differences in sample richness and evenness via the Shannon metric was determined statistically significant across (a) seasons, yet statistically insignificant across all other groups including, (b) flow type, and (c) percent imperviousness (d) distance from the outlet. This means that the number of species accounted for per sample does not change between groups. This is not an uncommon finding across similar studies (Hosen et al., 2017). Figure 3.1 displays box plots of the Shannon metric across each of these sample groups.

3.3.2. Composition of Communities

3.3.2.1. Beta Diversity Metrics and Principal Component Analysis

Beta diversity metrics are used to measure how different the species represented in one sample are from the species represented in another sample. A common measurement of beta diversity is the Bray-Curtis dissimilarity metric. Unlike other metrics which measure diversity, such as Jacquard, Bray Curtis dissimilarity accounts for the nuance of relative abundance of taxa within samples, meaning it resists bias from highly represented taxa. Bray Curtis dissimilarity is a pairwise metric bounded by 0 and 1; a Bray Curtis metric of 0 would indicate the two samples compared have the same composition of taxa, while a metric of 1 would mean the two samples do not share any species.

Due to the pairwise nature of Bray Curtis, principal coordinate analysis is an ordination technique commonly used to visualize the dissimilarity distances between samples. A PCoA plot was prepared to compare the variation of OTUs represented in each sample by land use and season. The PCoA plots based on land use alone did not immediately reveal distinguished clustering. Color-coordinating the same plot based on season reveals distinct grouping between

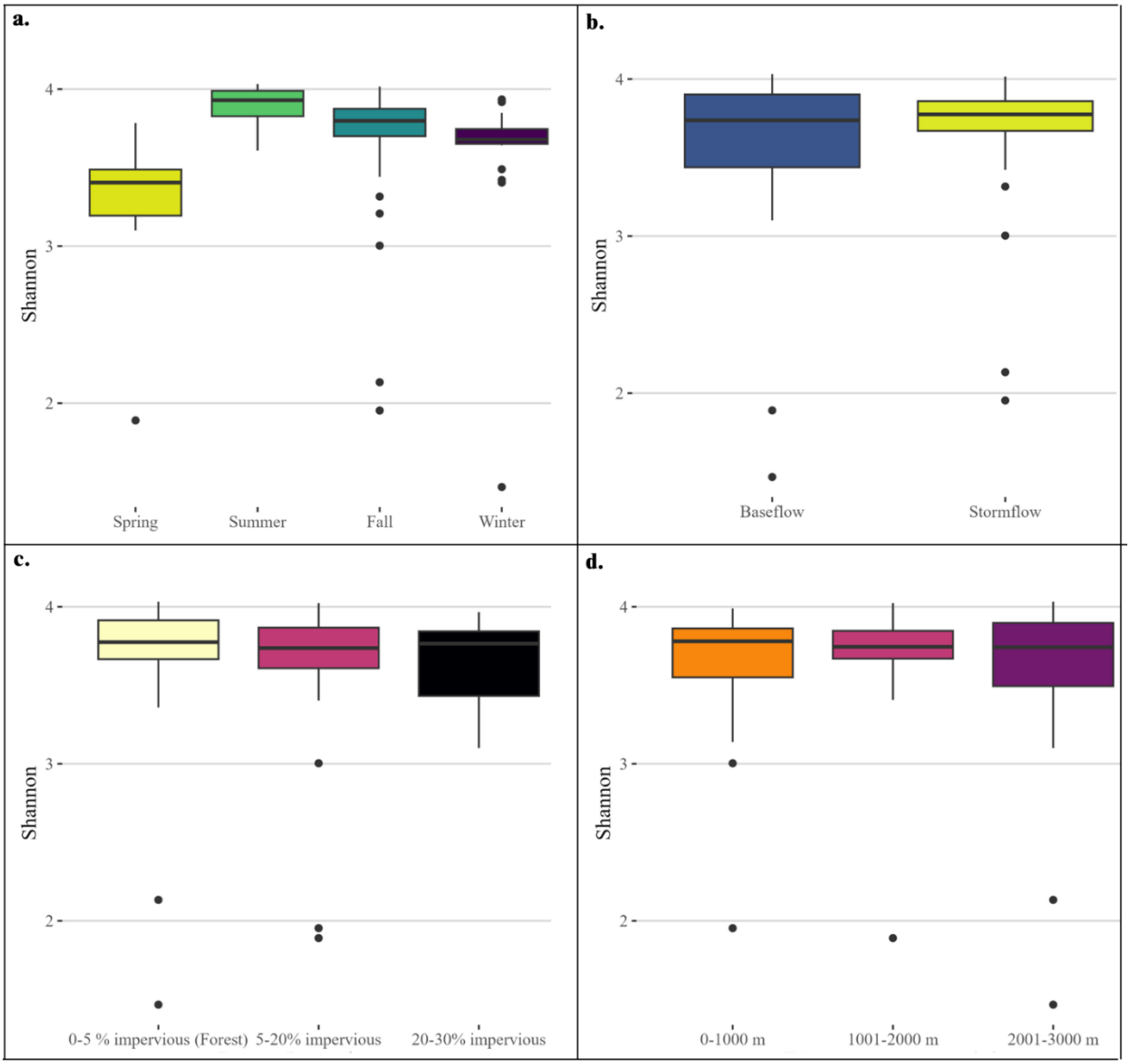

Figure 3.1 Box plots display the distribution of Shannon diversity index for samples grouped by (a) season, (b) flow type, (c) percent imperviousness, and (d) distance from the outlet.

samples (Figure 3.2). It is well known that season impacts microbial diversity (Nemergut et al., 2011; Caporaso et al., 2012; Fortunato et al., 2013), however it is unique to find that samples were distinguishable by land use if first separated into seasons (Figure 3.3a-d), with apparent "outliers" explainable by storm events.

Significance of the clustering observed in the PCoA was determined using a multiple linear regression model. A Spearman's correlation test was used to determine which quantitative environmental data was most correlated with the first dimension of the PCoA performed on the Bray Curtis dissimilarity metrics. The results of the Spearman's correlation test showed that the first PCoA dimension for the Bray Curtis metric, from here forward referred to as Bray_PCoA1, was strongly correlated with the percent impervious cover of the drainage area (rs=-0.81), the percent tree canopy cover of the drainage area (rs=0.80), the percent forested area of the drainage area (rs=0.78). These three metrics, as well as the factors of season and flow type (baseflow or stormflow) were included in several trials to determine the best fit model. Because the percent impervious cover had the highest correlation, this was the land cover parameter included as an effect in the linear regression model.

A multiple linear regression model that accounted for the effect of percent impervious cover of the drainage area, season the sample was taken, and flow type (base flow or storm flow) at the time of sample collection was fitted to the dataset. The type 3 F test revealed that all three factors had a significant effect ($p<0.0001$ for the percent impervious cover of the drainage area, <0.0001 for season, and 0.0002 for flow type, respectively) on the response of Bray_PCoA1. The model had an r-squared of 0.82, and the residuals were normally distributed. The effect of the percent imperviousness on beta diversity is statistically significant but small with an estimated coefficient of -0.004. This means that while it is incredibly likely that the beta diversity has an underlying relationship with percent imperviousness, the effect of imperviousness does not meaningfully impact the result the way that season and flow type do.

A Krushall-Wallis test was also performed on the Bray_PCoA1 values across samples grouped by (a) percent imperviousness, (b) flow type, (c) season, and (d) distance from the outlet.

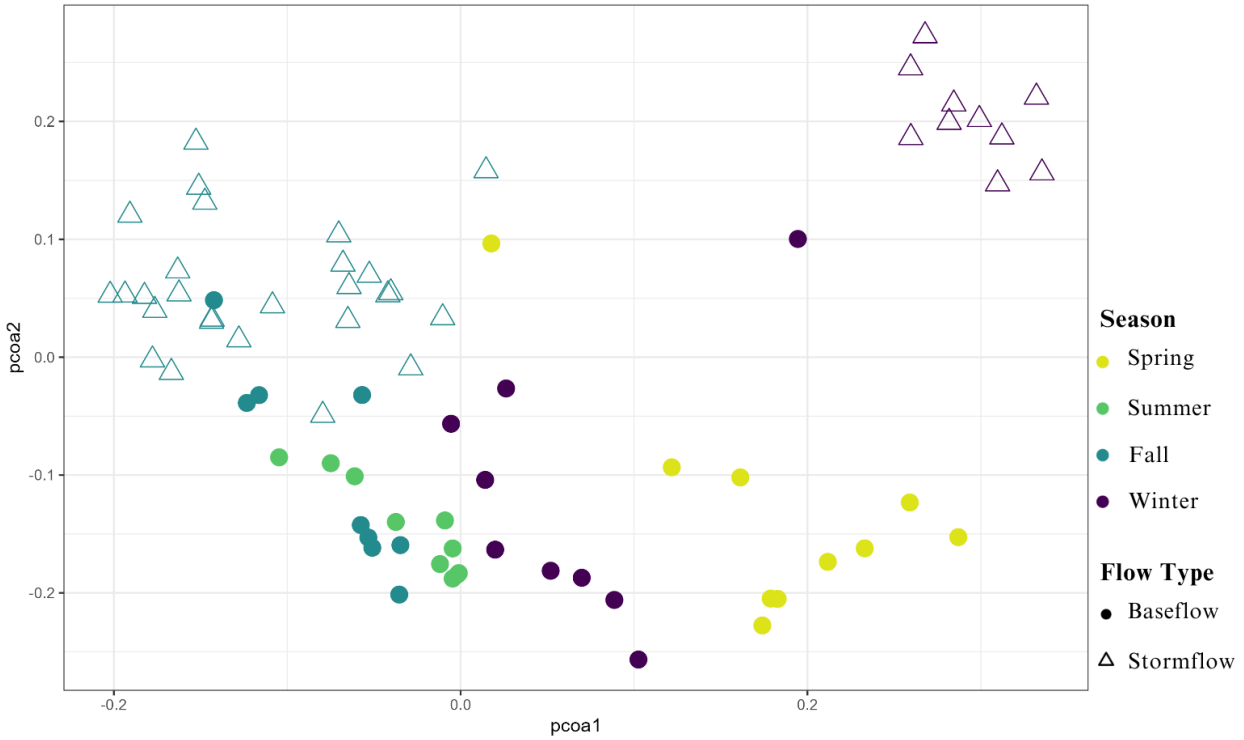

Figure 3.2 The PCoA plots of the Bray Curtis dissimilarity metric, color coordinated by season. Baseflow samples are indicated by a solid circle, while stormflow samples are indicated by a triangle.

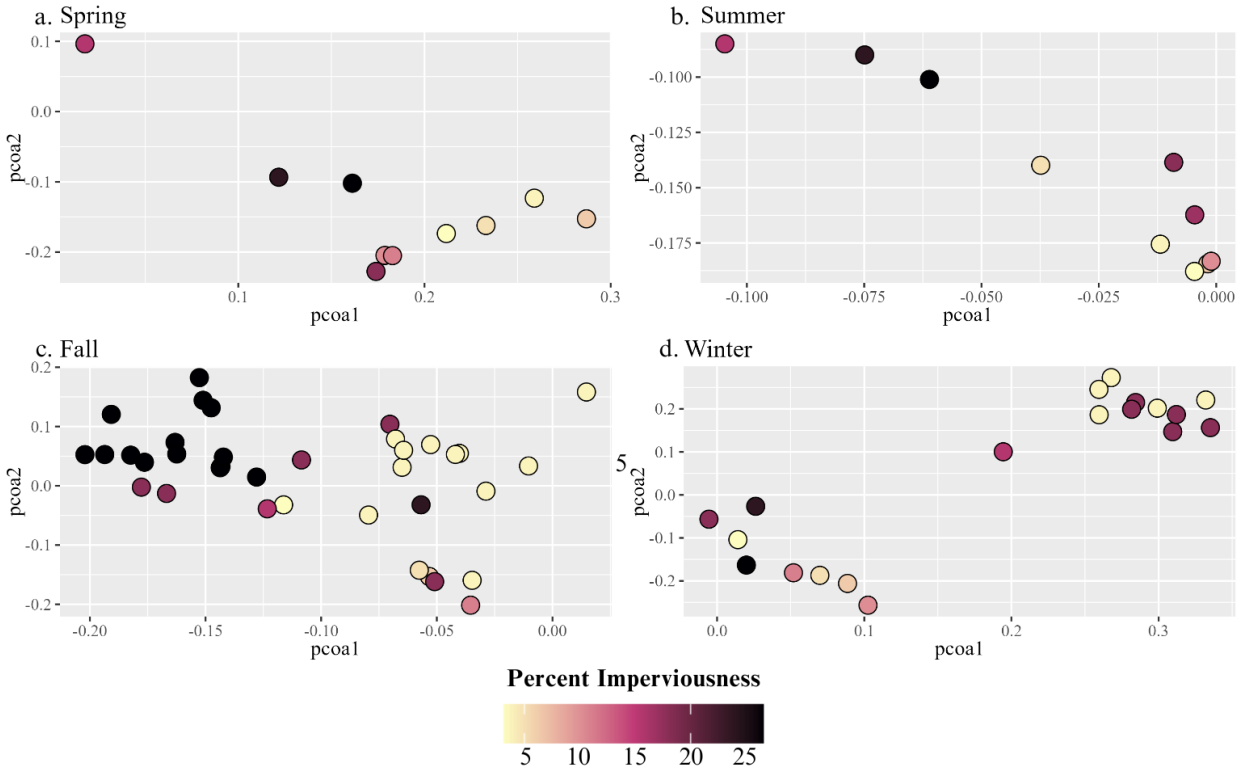

Figure 3.3 The PCoA plots of samples separated by season (a-d). A color scale indicates the percent impervious cover of the drainage area to each site. Yellow dots are >5% impervious cover and are associated with forested sites. Black dots have 25-30% impervious area and are associated with urban sites. Magenta dots represent sites that have a mix of urban and forested land use, ranging from 5-25 % imperviousness.

Differences in Bray_PCoA1 were significant across all groups. Studies have shown statistically significant shift in microbial community correlated with other environmental parameters, such as stream biotic index/macro invertebrate composition (Simonin et al., 2019), environmental concentrations of various pollutants associated with humans like nutrient, manganese, sulfate, and bicarbonate concentrations (Liao et al., 2019; Ren et al., 2019) and temperature (Dodds et al., 2020). Hosen et al., 2017 was also successful in showing statistical significance in changes to Bray_PCoA1 beta diversity with changes in land use as measured by impervious cover.

3.3.2.2. Indicator Species Analysis

In total, there were 2,462 total taxa sequenced with a relative abundance of at least 0.0005% across all samples. 32.8% of taxa were represented by 13 major genera, displayed in Figure 3.4 Because 35.4% of OTUs were not genus specific, and an additional 31.8% of OTUs accounted for less than 1% of the total number of counts across all samples, relative abundance by OTU "class", which was consistent with other studies (Hosen *et al.,* 2017), was considered to compare OTU abundance with literature observations.

Relative abundance of classes based on season are displayed in Figure 3.5. Among seasonal groups, summer samples showed the highest diversity of represented classes, mirroring the alpha diversity represented by the Shannon diversity metric. One class of bacteria specific to summer is Epsilonproteobacteria, a class within the Proteobacteria phylum, has been primarily recognized for harboring pathogenic microorganisms (Nakagawa & Takaki, 2009). Two of the genera present in this sample set from Epsilonproteobacteria, namely *Campylobacteraceae* and *Helicobacteraceae*, are acknowledged for hosting species with pathogenic potential for humans. Notably, none of the OTUs within these genera in our dataset correspond to the specific pathogenic species known as *Wolinella spp., Helicobacter spp.,* and *Campylobacter spp.*

Epsionproteobacteria is also recognized for high metabolic versatility and importance in sulfur rich ecosystems. Epsilonproteobacteria are chemoautotrophic bacteria and have been found to be responsible for CO_2 fixation in ocean communities marine transition zones between oxic and anoxic (Grote et al., 2008) and in low oxygen high sulfide zones in spring outflows (Engel et al.,

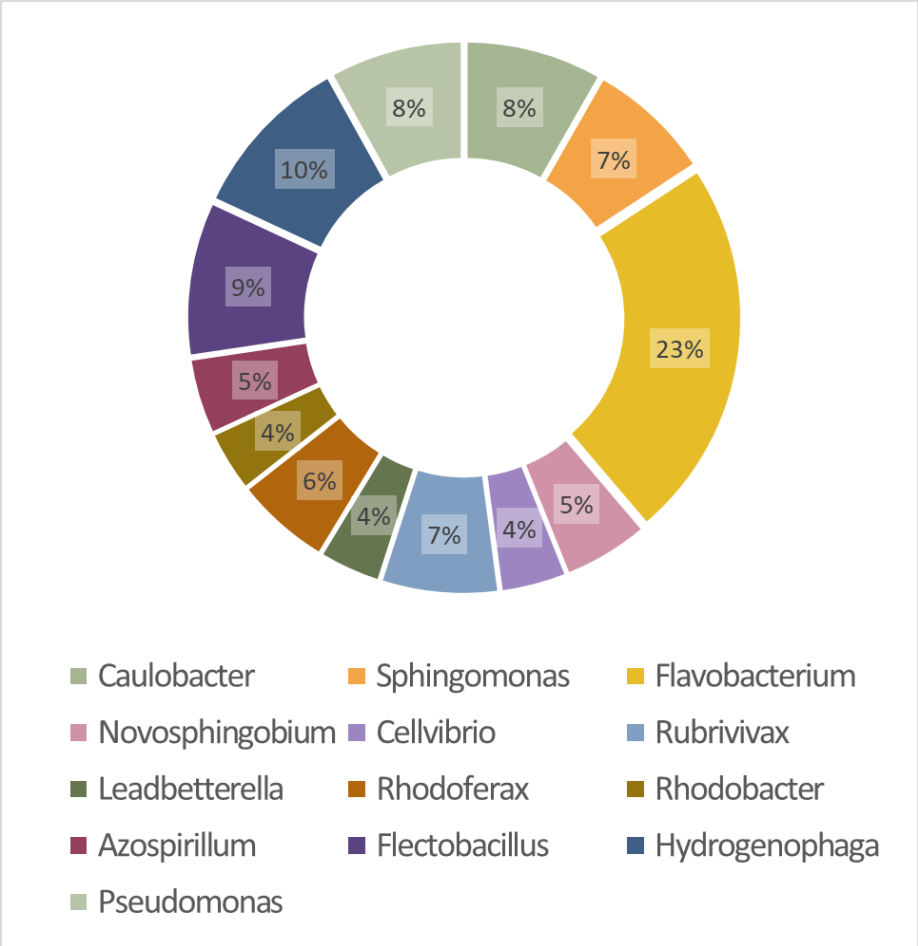

Figure 3.4 Representation of the 13 major genera in all samples. These OTUs represent only 32.8% of total number of sequences from all samples; the remaining 67.2% of taxa were either not distinguished to the genus level (35.4%) or accounted for less than 1% of the total number of counts across all samples.

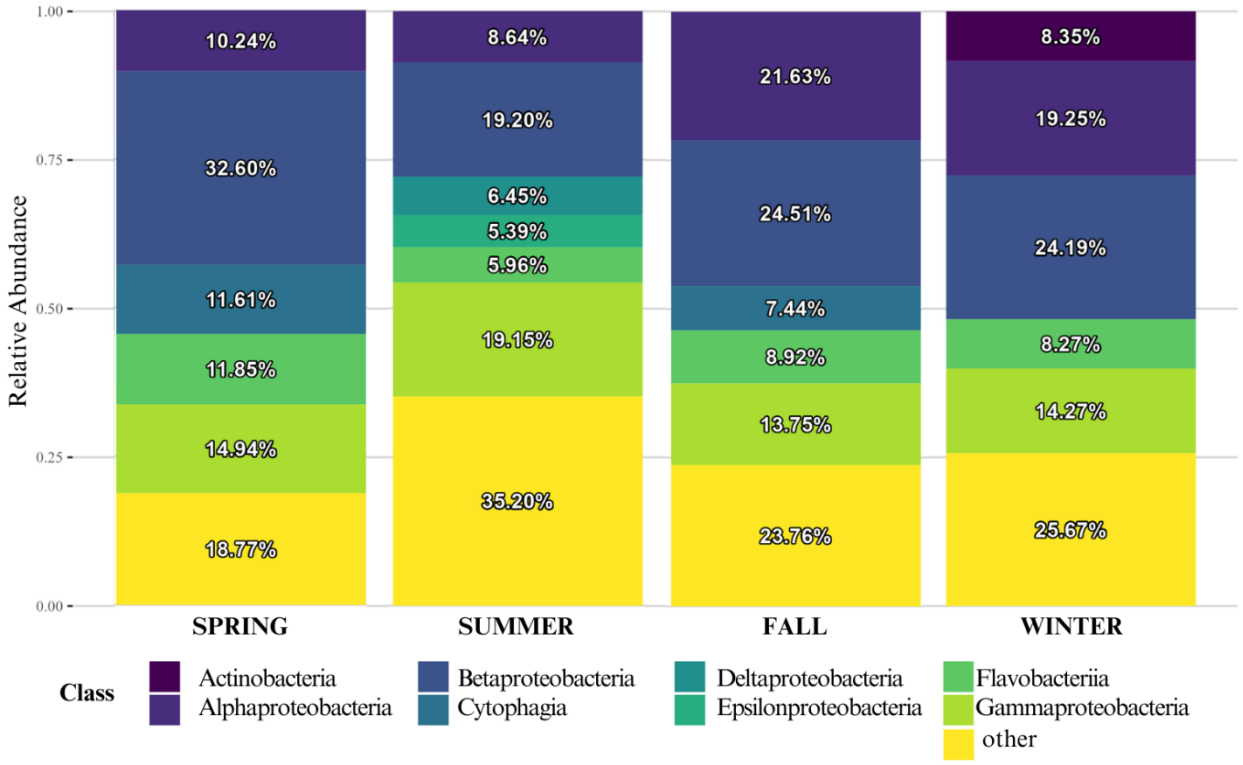

Figure 3.5 Relative abundances of the most abundant classes across samples grouped by season.

2006). Common to subsurface hydrological systems within karst terrains, many groups within Epsilonproteobacteria oxidize reduced sulfur compounds (Engel et al., 2004; Engel et al., 2010) Its high presence in the summer signals changes in the forms and abundances of nutrients influencing functional diversity and may be attributable to low DO caused by seasonal activity from single celled organisms or increased influence from subsurface flow to the stream water column. Winter had a higher abundance of Actinobacteria than other seasons, a diverse species containing pathogens, soil inhabitants, plant commensals, and gastrointestinal commensals (Berka et al., 2015). The most highly represented Family within the Actinobacteria order in winter samples was *Micrococcaceae*, accounting for 2.9% of total reads.

Relative abundance of most abundance OTUs represented by samples with forest vs. urban land use (Figure 3.6) showed an increase in abundance of Saprospirae class in forested samples. Sphingobacteriia and Saprospiraceae are highly related aerobic organotrophs requiring amino acids and are associated with decaying organic matter (Lewin, 2015). As the stream flowed into the second order reach where forested and urban land use combined, the class Gammapreobacteria became more highly abundant while other classes decreased in abundance. Sphingobacteriia and Saprospirae became noise with relative abundancies of less than 3%, grouped into the highly represented "other" category. This signals the loss of nuance in diversity as the samples move downstream, which may be explainable by assembly mechanisms and rates of phylogenetic turnover.

A full list of the indicator species analysis identified using the multiplatt() function in R can be viewed in the attatchments. From this analysis, 10 OTUs were identified as statistically significant indicators of the forested land use sites. OTUs 72 (*Kaistobacter* genus), 64 (*Comamonadaceae* family), 62 (*Ellin517* family), 46 (*Candidatus Rhabdochlamydia* genus), 55 (*Bdellovibrio* genus), 69 (*Prosthecobacter debontii* spp.) and 58 (*Kaistobacter* genus) all exclusively appeared in the forested grouped sites in a relative abundance of less than 1%. Several of the forest land use indicator OTUs were soil builders affiliated with decomposers of plant matter (orders Actinomycetales, Sphingomonada, and Sphingobacteriales). Two OTUs were identified as statistically significant indicators of the urban land use sites, both from the class Alphaproteobacteria: orders Rickettsiales and *BD7-3*. Rickettsiales order contains

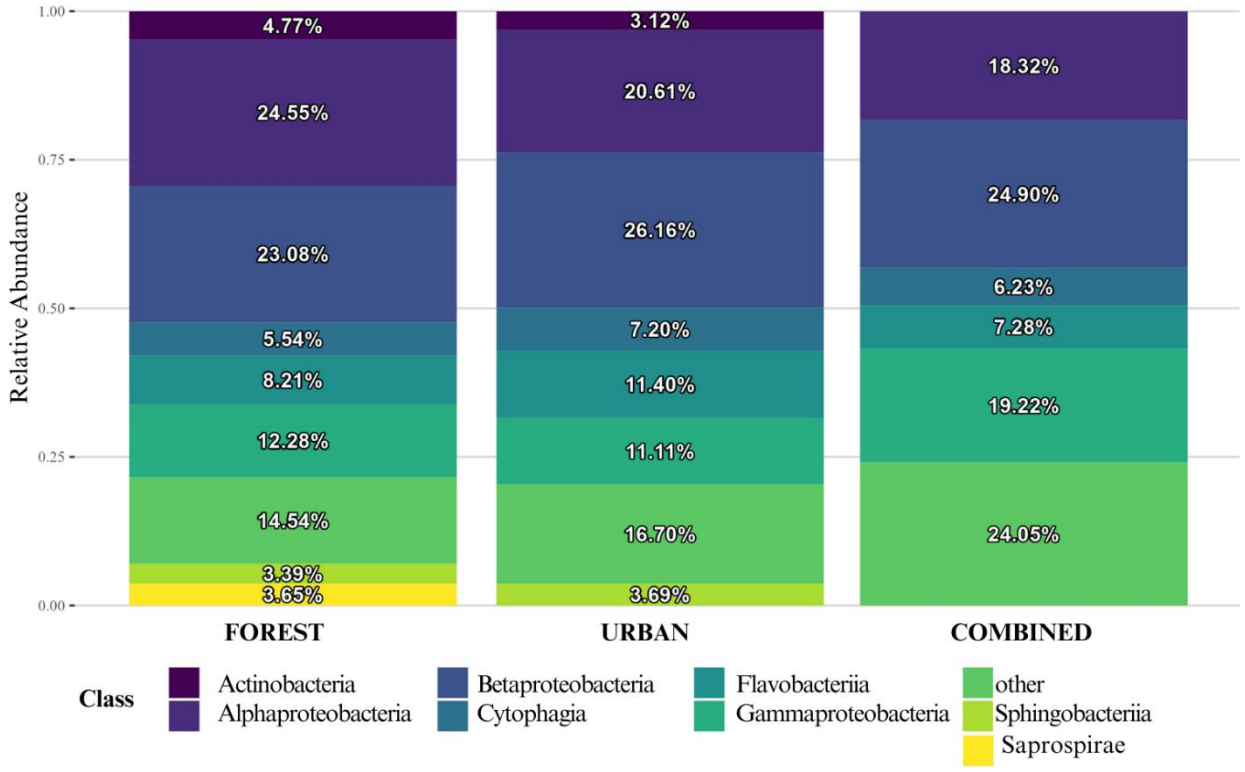

Figure 3.6 Relative abundance of highly represented classes from samples with forested, urban, or combined land use.

endosymbionts and parasites which infect a broadspecturm of eukaryotic hosts including humans, livestock, and insects (Schön et al., 2022).

Comparing most abundant classes represented in baseflow to stormflow (Figure 3.7) revealed a decrease in Saprospirae, the decomposing aerobic organotrophs, from baseflow to stormflow. Several members of the *Sphingomonadaceae* family, including *Sphingobacterium multivorum spp.*—a species affiliated with biodegradation of plant matter—were identified as indicator sof Stormflow (Wang et al., 2021). This is likely explainable by the washout of leaf litter and POM during storm surges. One genera *Sphingobium* from the *Sphingomonadaceae* family was selected through analysis as an indicator species for the fall season group. Only stormflow and fall groups contained indicator species from this family of decomposers. There was an increase in the relative abundance of Actinobacteria and Flavobacteria in baseflow to stormflow. Two OTUs from the genus *Flavobacterium* in order Flavobacteria were identified as indicator species for the summer season. *Flavobacterium* are known to exist in a range of aquatic and soil habitats and generally contribute to mineralization of various organic matter substrates (Bernardet & Bowman, 2006).

Comparing indicator species and relatively abundant OTUs to literature

Upon literature review, a number of OTUs were found as indicators of particular environmental characteristics. For example, *Polynucleobacter, Albidiferax, gallionella spp., Candidatus Plankophila*, and *Methylococcales* were genera found as keystone taxa within urbanized stream communities (Hosen et al., 2017). Similarly, *Hyphomicrobium, rhizobiales spp.*, *Crenothrix*, and *Nitrospira* were found as indicators of forested stream communities (Hosen et al., 2017). None of these species were identified as an indicator species in our analysis. However, OTU3 in the family *Hyphomicrobiaceae*, closely related to *Hyphomicrobium*, was identified as an indicator species for the summer season.

Simonin et al. (2019) categorized OTUs as “tolerant” vs. “intolerant” to land use development in watersheds based on correlations with environmental and relative abundance across samples with land uses ranging from 0-83% developed. Simonin et al. (2019) found a threshold of 12.1%

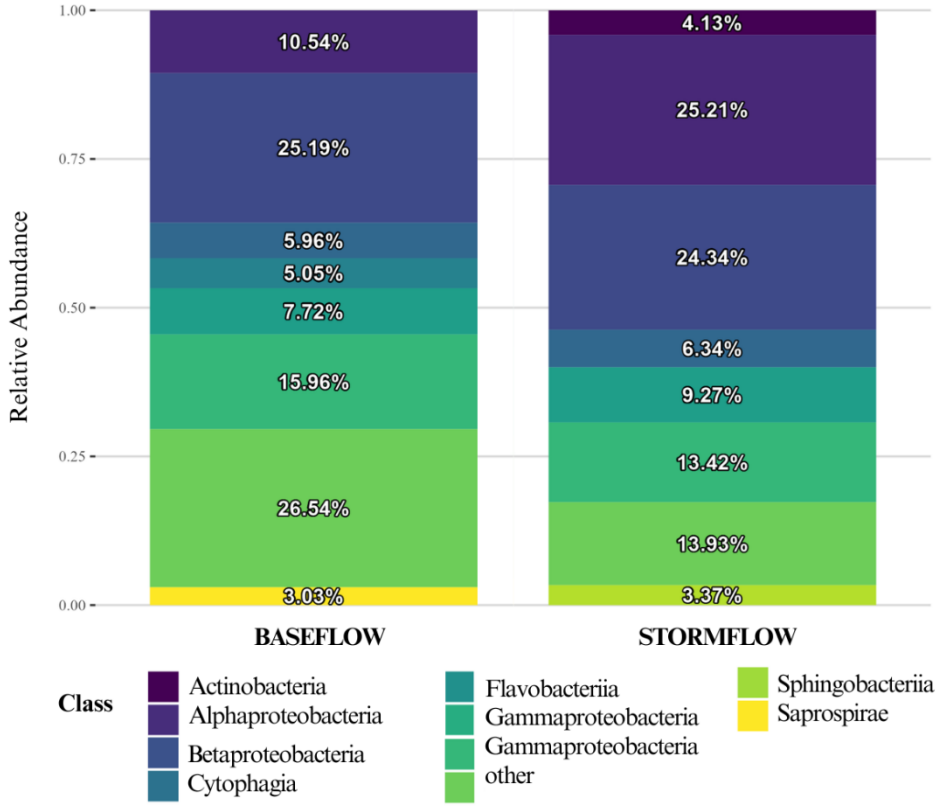

Figure 3.7 Relative abundance of highly represented classes within samples taken during baseflow and stormflow.

developed watershed area where intolerant taxa were lost from the sediment communities. A few OTUs were found to be not only tolerant of developed land use, but actually showed a positive response to increased % development: Bacteroidetes (class) Bacteodietes Vadinha17, Bacteroidetes Proxilbacteraceae BSV13, Deltaproteobacteria (class) Desulfatirhabdium, and 4 OTUs from the Betaproteobacteria class: 1 from the *Thodocyclaceae* family, 2 from the *Rhodocyclaceae* family, and 1 from the *Comamdaceae* family. Within our own dataset, the *Comamdaceae* family occurred as OTU indicator species for 4 separate groups: OTU 64 was identified as an indicator of forested land use and of stormflow. OTU 1 was identified as an indicator of baseflow and of the summer season. *Comamdaceae* was not identified as an indicator of developed land use for this dataset.

Numberger et al. (2022) investigated the impacts of urbanization in freshwater lake microbiomes. The study compared amplicon sequence variants (ASV, a cluster of microbes similar to OTUs but derived from a different 16S data processing pipeline) specific to urban and rural lakes as well as wastewater with a focus on genera that include known potential pathogens. In this study, Gammaproteobacteria Burkholderiales order members *Burkholderiaceae*, *Comamonadaceae*, and *Methylophilaceae* were all considered in higher abundance in the urban lake than is typical for freshwater lakes in literature. Again, in our study, members from the *Commonadaceae* family were identified as indicators for the forested water column, as previously mentioned. Genera with known potential pathogens were not identified as indicator species in our analysis.

Overall, there limited overlap between these studies of indicator OTUs and ASVs outside of some the most common orders of bacteria found in freshwaters, such as Betaproteobacteria. Because Betaproteobacteria is so ubiquitous to freshwater ecosystems, there were some discrepancies between studies. One study cited this class of bacteria as decreasing significantly in urban streams, while it remained significantly “tolerant” to urbanization in others (Simonin et al., 2019; Hosen et al., 2017). This is why it is important to utilize proper methodologies to identify indicator species using verified methods with statistical power informed by

bioinformatics. Other studies that have investigated OTUs associated with urban land use have relied primarily on relative abundance or on association with geochemical conditions correlated with urbanization (Hosen et al., 2017; Ouyang et al., 2020; Liao et al., 2019; Simonin et al., 2019).

Choosing OTUs representative of environmental groups based on relative abundance data may lack statistical power, as relying entirely on relative abundance fails to adequately measure the degree of association between target species and groups of sites, including the predictive value of a species as an indicator for the group in question as well potential preference of the species for the environmental conditions which distinguish the groups (De Cáceres et al. 2010; De Cáceres, Legendre & Moretti, 2010). This can make it challenging to detect subtle but biologically meaningful changes in specific taxa. For example, differential abundance does not account for rare taxa that do not have a high impact on relative abundance, but that are truly selected for in the environments of interest. Additionally, as exemplified with this dataset, an indicator species may be only one OTU represented within a class with a high relative abundance. Multiple OTUs within the same class, or even genus, that are distinguishably separate DNA sequences yet cannot be identified to the species level, may act as indicator species for several different groups including opposing groups such as stormflow vs. baseflow. Therefore, relying on relative abundance as an OTU indicator will not provide results that are specific about which OTUs are truly representative of the group of interest.

Considering these challenges, the Burkholderiales order consistently increases in relative abundance in urban environments across studies. However, in our study, this order was identified as an indicator bacterium for the forested landscape. This may be because the forest in our study is surrounded by more urban area, and thus it could have different indicators than pristine or rural areas.

3.3.3. Phylogenetic Diversity and Mechanisms Driving Assembly

Because the water column communities showed a stronger connection to watershed urbanization than sediment communities, Hosen et al. (2017) hypothesized that microbial communities in the

water column were more strongly influenced by dispersal mechanisms driven microbes being imported from upstream regions and the surrounding watershed. The study did not, however, investigate or quantify microbial community assembly processes by state of the science bioinformatic statistical analysis. In this section, we investigate the relative importance of selection, drift alone, dispersal and drift, and homogenizing dispersal using the methodology outlined in Stegen et al. (2013) to our dataset.

The assembly and sustenance of microbial community structures reflect the cumulative outcome of numerous ecological processes. Deterministic ecological processes, such as succession, competition, disturbance, dispersal, or climate change, often act on groups of species based on the similarity of function, shape, or relatedness (Chai et al., 2016). Taxonomic classification attempts to account for these similarities of function. For this reason, phylogenetic diversity, or the measure of relatedness by taxonomic distance between species within a community, is a way to measure if the community is being shaped selectively.

Beta nearest taxon index (Beta-NTI) refers to the standard deviation of the difference between the beta-mean nearest taxon distance (Beta-MNTD) and the Beta-MNTD across 999 randomized calculations to account for a null distribution (Stegen et al., 2013). A Beta-NTI that is > 2 or < -2 indicates a higher than expected phylogenetic turnover, indicating that environmental conditions are contributing to distinct set of OTUs and selection plays a significant role in assembly processes. Contrarily, a Beta-NTI with a n absolute value >2 would indicate stochastic processes such as dispersal (the movement of microorganisms from one location to another) or drift (random changes in population sizes due to death and reproduction). The second step uses the Raup-Crick (RC) index RC-Bray to quantify the breakdown of stochastic assembly processes into the relative importance of dispersal limitation acting in tandem with drift (RC-Bray > 0.95), homogenizing dispersal (RC-Bray < -0.95), or drift alone ($|\text{RC-Bray}| < 0.95$). The results of the quantified relative importance of the assembly mechanisms selection, drift, dispersal coupled with drift, and homogenizing dispersal by baseflow vs. stormflow as well as by urban vs. forested land use can be seen in Figure 3.8.

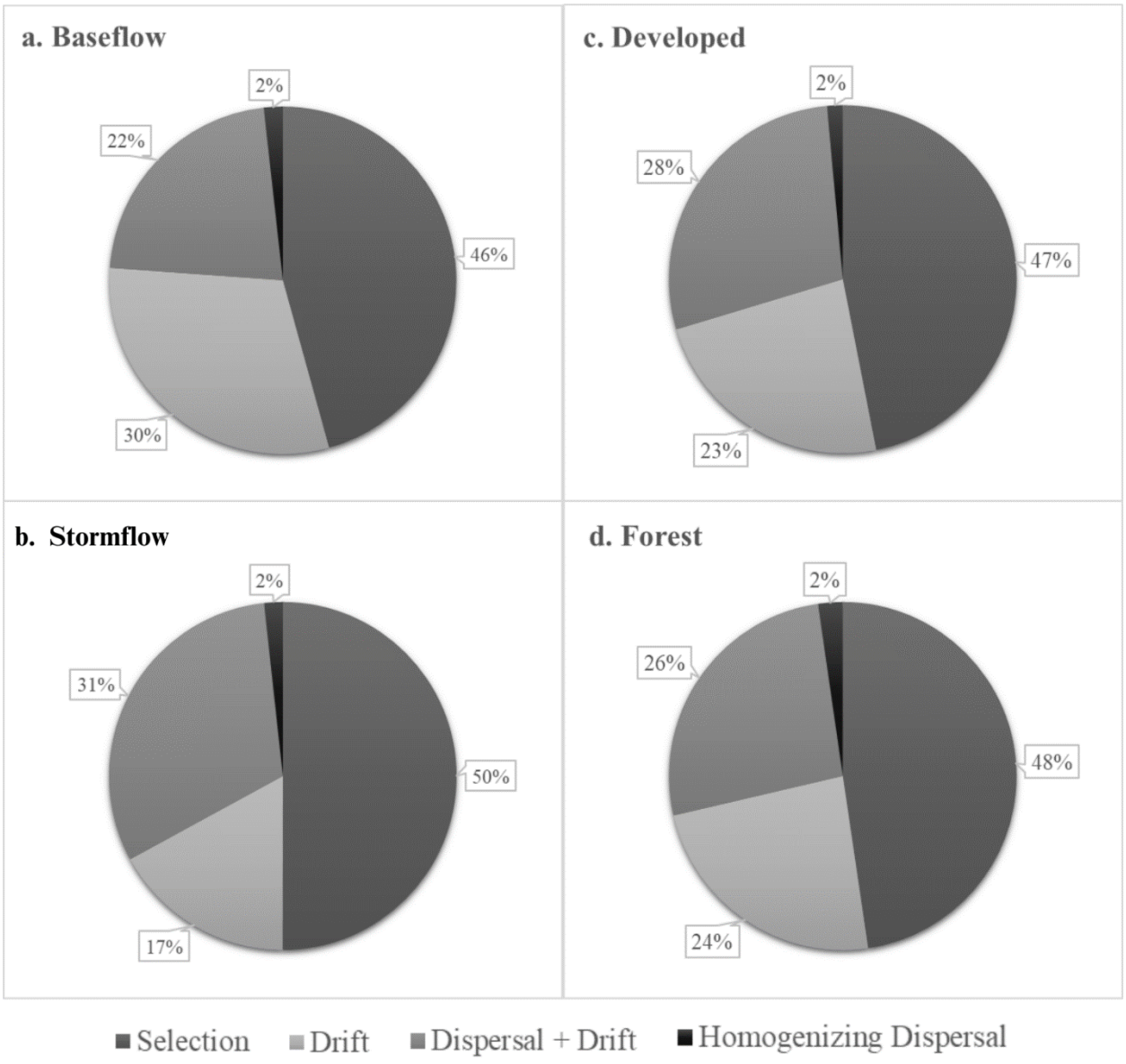

Figure 3.8 The proportion of phylogenetic turnover that can be attributed to selection, drift alone, dispersal acting in concert with drift, and homogenizing dispersal based on the method proposed by Stegen et al., 2013 for (a) samples taken during baseflow, (b) samples taken during stormflow, (c) samples taken from sites with urbanized land use, and (d) samples taken from sites with forested land use.

In forested land use catchments, 48% ± 0.75 of turnover was primarily due to selection, 24% ± 0.81 of turnover could primarily be attributed to drift alone, 28% ± 0.63 of turnover was primarily due to dispersal limitation acting in concert with drift, and 2.28 % ± 0.13 of turnover could primarily be attributed to homogenizing dispersal. Phylogenetic turnover at urbanized grouped sites is virtually indistinguishable from forested sites, with 47% ± 0.83 of turnover primarily attributed to selection, 23% ± 0.69 to drift alone, 26% ± 0.93 due to dispersal limitation acting in concert with drift, and 1.45 % ± 0.09 primarily attributed to homogenizing dispersal. The higher amount of turnover attributed to homogenizing dispersal compared to dispersal acting in concert with drift in forested sites could suggest a homogenization of community structure across forested sites. This was further investigated by checking the % of selection that leaned towards homogenization based on the Beta-NTI. The Beta-NTI for forested sites with an absolute value greater than 2, indicating selection, had a higher proportion of smaller than expected turnover where Beta-NTI < -2 (compared to greater than expected, where Beta-NTI > 2) than at urbanized sites. Beta-NTI values indicated that 22% of selection driven phylogenetic turnover were diversifying rather than homogenizing, compared to 15.5% at forested sites. This supports the observations in Hosen et al., 2017 that forested microbial community networks are more interconnected compared to networks in more developed land use.

In comparing samples taken during stormflow to samples taken during baseflow, we see a more pronounced difference in the mechanisms driving assembly. In samples taken during baseflow, we see a stronger influence of drift on the rates of turnover: 46% ± 0.43 of turnover in baseflow was primarily due to selection, 30% ± 0.41 of turnover could primarily be attributed to drift alone, 22% ± 0.42 of turnover was primarily due to dispersal limitation acting in concert with drift, and 1.76 % ± 0.05 of turnover could primarily be attributed to homogenizing dispersal. In contrast, stormflow samples showed 50% ± 0.55 of turnover due to selection, 17% ± 0.40 to drift alone, 31% ± 0.42 primarily due to dispersal limitation acting in concert with drift, and 1.73 % ± 0.08 of turnover primarily due to homogenizing dispersal. Based on the hypothesis made by Hosen et al., 2017 that microbial communities in the water column are more likely to be assembled by dispersal mechanisms due to contribution from overland flow, it makes sense that stormwater would have a much higher rate of stochastic mechanisms driven by dispersal in concert with drift rather than by drift alone.

From a hydrologic perspective, the water column in the stream during stormflow is going to have a surge of water that has drained over the contributing drainage area, transporting bacteria from a variety of surface types to the stream. The water samples taken during stormflow also show a greater than normal amount of phylogenetic turnover attributed primarily to selection assembly processes. The rapid change in hydrologic state may create specific water chemistry conditions that add significant environmental stress, creating competition and selecting for a specific group of microbes. The storm event may also be introducing non-native bacteria from human sources, such as wastewater, or bacteria from sediment communities due to runoff, through flow, or resuspension of benthic sediment from turbulent flow regimes. The temporally limited sampling conditions may also contribute to a smaller amount of turnover attributed to drift, as there is less time for random (not selective) population fluctuations to balance community composition.

Phylogenetic turnover for baseflow samples parsed by distance upstream from the outlet revealed a linear relationship for each of the for ecological selection mechanisms (Table 3.1). Selection and homogenous dispersal decreased with increasing distance upstream, while drift and dispersal acting in concert with drift both increased with increasing distance upstream. This trend may be indicative of a biogeographical distance-decay pattern wherein community similarity decreases due to dispersal limitations as distance increases. As discussed in the previous section, distance from the outlet was strongly correlated with the microbial community composition and beta diversity, however its correlation was not statistically significant.

Phylogenetic turnover was then considered by season (Figure 3.9). Turnover primarily due to selection was very close to the baseflow average in the fall and winter (45% ± 1.74 and 42% ± 1.76, respectively), but especially high in the spring (58% ± 1.31) and low in the summer (37% ±1.67). Turnover primarily due to drift was close to the baseflow average during the spring and summer (30% ± 1.15 and 28% ± 1.52, respectively), but especially low in the fall (22% ±1.28) and high in the winter (41% ± 2.11). Dispersal in concert with drift was primarily responsible for an especially high proportion of turnover in the summer and fall (33% ± 0.98 and 32% ± 2.29, respectively) and an especially low proportion of turnover in the spring and winter (9% ± 1.06 and 16% ± 1.26, respectively). Homogenizing dispersal, as is typical, saw the least variation between group; however, homogenizing dispersal was responsible for a higher than average

Table 3.1 Average Shannon index and percentage ± uncertainty of phylogenetic turnover attributed primarily to each of the four section mechanisms for sites binned by increased distance from the stream outlet.

Distance (m)	Shannon	Selection	Drift	Dispersal + Drift	Homogeneous Dispersal
0-1000	3.66	50% ± 1.3	29 ± 0.99	19% ± 1.35	2.42% ± 0.20
1001-2000	3.60	47% ± 1.14	31% 1.10	21% ± 1.28	1.59% ± 0.13
2001-3000	3.522	42% ± 1.29	32% 1.34	25% 1.21	1.38% ± 0.10

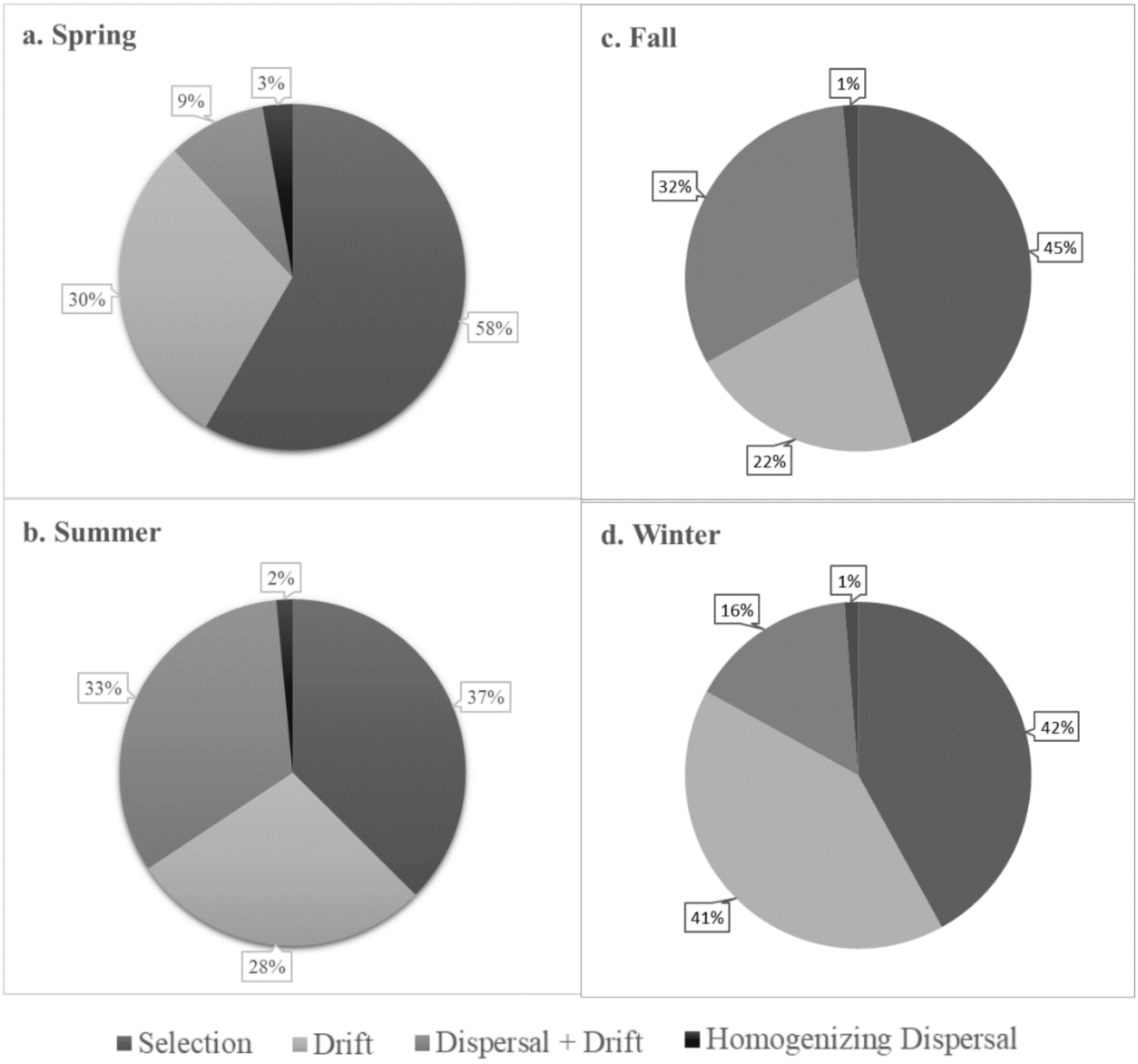

Figure 3.9 The proportion of phylogenetic turnover that can be attributed to selection, drift alone, dispersal acting in concert with drift, and homogenizing dispersal based on the method proposed by Stegen et al., 2013 for baseflow samples taken during the (a) spring, (b) summer, (c) fall, and (d) winter.

proportion of turnover in the spring (2.79% ± 1.06). These results suggest that the environmental conditions that come with the spring, including increased sunlight hours, temperature changes, increased precipitation, and activity of aquatic organisms, may play a stronger role in the seasonal variation seen in the aquatic microbial community. The increased role of drift alone in phylogenetic turnover of the microbial community in the baseflow water column during the winter months indicates reduced microbial activity (due to decreased temperatures) and increased stability in the water column due to freezing conditions and decreased precipitation. This would explain why there is a more distinct difference between stormflow and baseflow samples during the winter evident in the principal component analysis of Bray Curtis beta diversity metric. Storm events in the winter would provide a lot of stimulation to an otherwise more stagnant system. The elevated turnover attributed to dispersal in conjunction with drift during the fall and summer seasons could result from intermittent dry spells observed in the upstream reaches amid hot weather and limited precipitation, causing a disconnection between rain events. Wet weather would restore the connection, facilitating the transfer of distinct microbial communities and introducing new nutrient sources to downstream reaches. The warm weather and heightened solar radiation may boost dispersal processes, diminishing the relative significance of selection processes in the summer.

3.4. CONCLUSION

This study supported previous research findings that impervious area is significantly correlated with microbial community composition. In comparing indicator OTUs for urbanized landscapes with literature, this study found inconsistent results, highlighting the need for utilizing proper statistical analysis in identifying indicator taxa. This also reiterated the need for increased comparative studies across different regions and cities to compare commonalities and differences in microbial diversity considering factors such as climate, geography, and infrastructural design.

This study found conclusive evidence that assembly processes of the water column microbial community are increasingly driven by dispersal acting in concert with drift and ecological selection over drift alone during stormflow conditions compared to baseflow. We hypothesize this is due to the influx of bacteria communities transported to the stream from the surrounding

watershed through runoff, the turnover of benthic sediment during increased flow rates, and *in situ* conditions created by the storm event drastically contrasting from baseflow. This study found limited evidence for differences in microbial community assembly between urban and forested land use, however we did find that the average phylogenetic distance among the forested microbial community skewed to the left, contributing evidence that water column microbial communities in forested streams are more driven by homogenous selection than heterogeneous selection compared to those in urban streams. Through the same methods, we were able to obtain insights into seasonal assembly processes. The turnover of water column communities were much more likely to be driven by selection rather than stochastic processes in the spring compared to all other seasons. Of the stochastic processes considered for this analysis, drift alone played a much larger role in the assembly of the winter communities compared to other seasons.

This study contributed to evidence that there could be overlapping biogeographical patterns in microbial community assembly from lotic ecosystem continuity and urbanizing land use gradients. This study shows that distance-decay trends can be observable in the water column, even in small tributary watersheds, though a larger sample size from repeated efforts over a variety of land use trends will be necessary. More research with increased sample size is needed to untangle the assembly mechanisms driven by land use gradient versus connectivity in streamflow.

While this study provided insights to water column microbial community diversity and assembly processes in a heterogeneous urban watershed, there is still a huge need for investigating the response of microbial communities to urbanization. As our philosophy on urban development trends in the trajectory of sustainable and equitable cities, is imperative that we prioritize the microbiome (Diaz et al., 2012). Doing so is necessary for protection of human health by preventing the establishment of potential pathogens and antibiotic resistant genes into the environment as well as ecological health by creating robust, resilient, and cooperative microbial communities equipped for the nutrient and chemical loads in the stream (Lambirth et al., 2018; Files et al., 2018; Mills et al, 2017; Numberger et al., 2022).

Increasing our understanding of assembly and diversity in urban stream microbial communities could be used to develop biotechnological applications for solving water quality problems in urban streams. For example, microbial communities in the water column could serve as indicators of the effectiveness of green infrastructure and nature-based solutions in facilitating the successful reintegration of water waste, such as wastewater and graywater, or excessive stormwater runoff, back into the environment (Matsui & Miki, 2023; Liguori et al., 2021; Codello et al., 2023). Highly sophisticated tracking techniques using microbial community fingerprints could be developed to answer remaining questions about water quality, quantity, and connectivity (McCarthy et al., 2017). The more we understand about community selection, the more we can apply to developing bioremediation methods for managing and restoring water quality to urban surface waters.

REFERENCES

Barka, E. A., Vatsa, P., Sanchez, L., Gaveau-Vaillant, N., Jacquard, C., Klenk, H. P., ... & van Wezel, G. P. (2016). Taxonomy, physiology, and natural products of Actinobacteria. Microbiology and molecular biology reviews, 80(1), 1-43.

Bernardet, J. F., & Bowman, J. P. (2006). The genus flavobacterium. The prokaryotes, 7, 481-531.

Bolyen E, Rideout JR, Dillon MR, Bokulich NA, Abnet CC, Al-Ghalith GA, Alexander H, Alm EJ, Arumugam M, Asnicar F, Bai Y, Bisanz JE, Bittinger K, Brejnrod A, Brislawn CJ, Brown CT, Callahan BJ, Caraballo-Rodríguez AM, Chase J, Cope EK, Da Silva R, Diener C, Dorrestein PC, Douglas GM, Durall DM, Duvallet C, Edwardson CF, Ernst M, Estaki M, Fouquier J, Gauglitz JM, Gibbons SM, Gibson DL, Gonzalez A, Gorlick K, Guo J, Hillmann B, Holmes S, Holste H, Huttenhower C, Huttley GA, Janssen S, Jarmusch AK, Jiang L, Kaehler BD, Kang KB, Keefe CR, Keim P, Kelley ST, Knights D, Koester I, Kosciolek T, Kreps J, Langille MGI, Lee J, Ley R, Liu YX, Loftfield E, Lozupone C, Maher M, Marotz C, Martin BD, McDonald D, McIver LJ, Melnik AV, Metcalf JL, Morgan SC, Morton JT, Naimey AT, Navas-Molina JA, Nothias LF, Orchanian SB, Pearson T, Peoples SL, Petras D, Preuss ML, Pruesse E, Rasmussen LB, Rivers A, Robeson MS, Rosenthal P, Segata N, Shaffer M, Shiffer A, Sinha R, Song SJ, Spear JR, Swafford AD, Thompson LR, Torres PJ, Trinh P, Tripathi A, Turnbaugh PJ, Ul-Hasan S, van der Hooft JJJ, Vargas F, Vázquez-Baeza Y, Vogtmann E, von Hippel M, Walters W, Wan Y, Wang M, Warren J, Weber KC, Williamson CHD, Willis AD, Xu ZZ, Zaneveld JR, Zhang Y, Zhu Q, Knight R, and Caporaso JG. 2019. Reproducible, interactive, scalable and extensible microbiome data science using QIIME 2. Nature Biotechnology 37: 852–857. https://doi.org/10.1038/s41587-019-0209-9

Chase JM, Myers JA. (2011). Disentangling the importance of ecological niches from stochastic processes across scales. *Philos Transact Royal Soc B Biol Sci* 366: 2351-2363. https://doi.org/10.1098/rstb.2011.0063

Chave, J. Neutral theory and community ecology. Ecol. Lett. 7,241–253 (2004).

Codello, A. (2023). Microbial approaches for monitoring the ecological condition of aquatic environments (Doctoral dissertation, Macquarie University).

De Cáceres, M., Legendre, P., & Moretti, M. (2010). Improving indicator species analysis by combining groups of sites. Oikos, 119(10), 1674–1684.

De Cáceres, M., Sol, D., Lapiedra, O., & Legendre, P. (2011). A framework for estimating niche metrics using the resemblance between qualitative resources. Oikos, 120(February), 1341–1350.

Dewitz, J., and U.S. Geological Survey, 2021, National Land Cover Database (NLCD) 2019 Products (ver. 2.0, June 2021): U.S. Geological Survey data release, https://doi.org/10.5066/P9KZCM54

Diamond, J. M. In Ecology and Evolution of Communities (eds Diamond, J. M. & Cody, M. L.) 14 (Harvard Univ. Press, 1975).

Dodds, W K, Lydia H Zeglin, Robert J Ramos, Thomas G Platt, Aakash Pandey, Theo Michaels, Mohammadali Masigol, Anna M L Klompen, Michelle C Kelly, Ari Jumpponen, Emma Hauser, Paige M Hansen, Mitchell J Greer, Niloufar Fattahi, Camille S Delavaux, R Kent Connell, Sharon Billings, James D Bever, Niloy Barua, Folashade B Agusto. (2020). Connections and Feedback: Aquatic, Plant, and Soil Microbiomes in Heterogeneous and Changing Environments, *BioScience*, 70:7, 548-562, https://doi.org/10.1093/biosci/biaa046

Engel, A. S., Lee, N., Porter, M. L., Stern, L. A., Bennett, P. C., & Wagner, M. (2003). Filamentous “Epsilonproteobacteria” dominate microbial mats from sulfidic cave springs. Applied and Environmental Microbiology, 69(9), 5503-5511.

Engel, A. S., Stern, L. A., & Bennett, P. C. (2004). Microbial contributions to cave formation: new insights into sulfuric acid speleogenesis. Geology, 32(5), 369-372.

Engel, A., Meisinger, D., Porter, M. et al. Linking phylogenetic and functional diversity to nutrient spiraling in microbial mats from Lower Kane Cave (USA). ISME J 4, 98–110 (2010). https://doi.org/10.1038/ismej.2009.91

Evans, S. E., Allison, S. D., & Hawkes, C. V. (2022). Microbes, memory and moisture: Predicting microbial moisture responses and their impact on carbon cycling. *Functional Ecology*, 36, 1430–1441. https://doi.org/10.1111/1365-2435.14034

Flies, E. J., Skelly, C., Lovell, R., Breed, M. F., Phillips, D., & Weinstein, P. (2018). Cities, biodiversity and health: We need healthy urban microbiome initiatives. *Cities & Health*, *2*(2), 143-150.

Grote, J., Jost, G., Labrenz, M., Herndl, G. J., & Jürgens, K. (2008). Epsilonproteobacteria represent the major portion of chemoautotrophic bacteria in sulfidic waters of pelagic redoxclines of the Baltic and Black Seas. Applied and environmental microbiology, 74(24), 7546-7551. DOI: https://doi.org/10.1128/AEM.01186-08

Hosen JD, Febria CM, Crump BC and Palmer MA (2017) Watershed Urbanization Linked to Differences in Stream Bacterial Community Composition. *Front. Microbiol*. 8:1452. doi: 10.3389/fmicb.2017.01452

Lambirth, K., Tsilimigras, M., Lulla, A., Johnson, J., Al-Shaer, A., Wynblatt, O., ... & Gibas, C. (2018). Microbial community composition and antibiotic resistance genes within a North Carolina urban water system. *Water*, *10*(11), 1539.

Lewin, R. A. (2015). Saprospira. Bergey's Manual of Systematics of Archaea and Bacteria, 1-6.

Liguori, R., Rommel, S. H., Bengtsson-Palme, J., Helmreich, B., & Wurzbacher, C. (2021). Microbial retention and resistances in stormwater quality improvement devices treating road runoff. *FEMS microbes*, *2*, xtab008.

López-Vizcaíno, M., Lombardía M, Morales D (2013a). "Multinomial-based small area estimation of labour force indicators." Statistical Modelling, 13, 153–178.

Martiny, J., Bohannan, B., Brown, J. *et al.* Microbial biogeography: putting microorganisms on the map. *Nat Rev Microbiol* **4**, 102–112 (2006). https://doi.org/10.1038/nrmicro1341

McCarthy, D. T., Jovanovic, D., Lintern, A., Teakle, I., Barnes, M., Deletic, A., ... & Henry, R. (2017). Source tracking using microbial community fingerprints: method comparison with hydrodynamic modelling. Water research, 109, 253-265.

McLellan, S. L., Fisher, J. C., & Newton, R. J. (2015). The microbiome of urban waters. *International microbiology: The official journal of the Spanish Society for Microbiology*, *18*(3), 141.

Merbt, S. N., Proia, L., Prosser, J. I., Marti, E., Casamayor, E. O., & von Schiller, D. (2016). Stream drying drives microbial ammonia oxidation and first-flush nitrate export. Ecology, 97(9), 2192–2198. https://doi.org/10.1002/ECY.1486

Mills, J. G., Weinstein, P., Gellie, N. J., Weyrich, L. S., Lowe, A. J., & Breed, M. F. (2017). Urban habitat restoration provides a human health benefit through microbiome rewilding: the Microbiome Rewilding Hypothesis. Restoration ecology, 25(6), 866-872.

Nakagawa, S., & Takaki, Y. (2009). Nonpathogenic epsilonproteobacteria. eLS. https://doi.org/10.1002/9780470015902.a0021895

Ning D, Yuan M, Wu L, Zhang Y, Guo X, Zhou X, Yang Y, Arkin A, Firestone M, Zhou J (2020). "A quantitative framework reveals ecological drivers of grassland microbial community assembly in response to warming." Nature Communications. doi:10.1038/s41467-020-18560-z.

Numberger, D., Zoccarato, L., Woodhouse, J., Ganzert, L., Sauer, S., Márquez, J. R. G., ... & Greenwood, A. D. (2022). Urbanization promotes specific bacteria in freshwater microbiomes including potential pathogens. Science of the Total Environment, 845, 157321.

O'Driscoll, M., Clinton, S., Jefferson, A., Manda, A., & McMillan, S. (2010). Urbanization effects on watershed hydrology and in-stream processes in the southern United States. *Water (Switzerland)*, *2*(3), 605–648. https://doi.org/10.3390/W2030605

Oksanen, J., Blanchet, F. G., Friendly, M., Kindt, R., Legendre, P., McGlinn, D., et al. (2022). *Vegan: Community ecology Package.* Available online at: hyyps://CRAN.R-project.org/package=vegan

Ouellet, V., Daniels, M. D., Peipoch, M., Zgleszewski, L., Watson, N., Gibson, E., Krause, S., & Kan, J. J. (2022). Beyond the light effect: How hydrologic and geomorphologic stream features control microbial distribution across pool sequences in a temperate headwater stream. Ecohydrology, 15(2), e2380. https://doi.org/10.1002/eco.2380

Qu, X., Ren, Z., Zhang, H. *et al.* Influences of anthropogenic land use on microbial community structure and functional potentials of stream benthic biofilms. *Sci Rep* **7**, 15117 (2017). https://doi.org/10.1038/s41598-017-15624-x

Schön, M.E., Martijn, J., Vosseberg, J. et al. The evolutionary origin of host association in the Rickettsiales. Nat Microbiol 7, 1189–1199 (2022). https://doi.org/10.1038/s41564-022-01169-x

Stegen JC, Lin X, Fredrickson JK, Chen X, Kennedy DW, Murray CJ, Rockhold ML, Konopka A. Quantifying community assembly processes and identifying features that impose them. ISME J. 2013 Nov;7(11):2069-79. doi: 10.1038/ismej.2013.93. Epub 2013 Jun 6. PMID: 23739053; PMCID: PMC3806266.

Walsh, Christopher J., Allison H. Roy, Jack W. Feminella, Peter D. Cottingham, Peter M. Groffman, and Raymond P. Morgan II. “The Urban Stream Syndrome: current knowledge and the search for a cute.” Journal of the North American Benthological Society 2005 24:3, 706-723. https://doi.org/10.1899/04-028.1

Wang Y, Brons JK, van Elsas JD. Considerations on the Identity and Diversity of Organisms Affiliated with Sphingobacterium multivorum—Proposal for a New Species, Sphingobacterium paramultivorum. Microorganisms. 2021; 9(10):2057. https://doi.org/10.3390/microorganisms9102057

Wenger, S. J., Allison H. Roy, C. Rhett Jackson, Emily S. Bernhardt, Timothy L. Carter, Solange Filoso, Catherine A. Gibson, W. Cully Hession, Sujay S. Kaushal, Eugenia Martí, Judy L. Meyer, Margaret A. Palmer, Michael J. Paul, Alison H. Purcell, Alonso Ramírez, Amy D. Rosemond, Kate A. Schofield, Elizabeth B. Sudduth, Christopher J. Walsh "Twenty-six key research questions in urban stream ecology: an assessment of the state of the science," Journal of the North American Benthological Society, 28(4), 1080-1098, (27 October 2009)

Zhou, J. & Ning, D. Stochastic community assembly: does it matter in microbial ecology? Microbiol. Mol. Biol. Rev. 81, e00002–17 (2017).

CHAPTER 4

ROADWAYS, GRASSES, AND FORESTS, OH MY! MICROBIAL COMMUNITY FINGERPRINTS EFFECTIVELY PREDICT RUNOFF PARTITIONING BY LANDSCAPE TYPE

This article was written primarily by Victoria Rexhausen with revisions from Jon Hathaway.

4.0. ABSTRACT

Urban stormwater runoff drives transport of pollutants to receiving streams (Muller *et al.*, 2019). Re-defined drainage conveyances and patchy land covers due to impervious surfaces obfuscates direct pathways of pollutants. To mitigate risk to urban ecology and downstream bodies, it is critical to accurately assess the timing and volumetric proportion of runoff from different surfaces within the urban watershed. This will allow for improved water quality modeling sensitive to site-specific nuance. Advancements in the field of microbiology have illuminated microbial source tracking using ribosomal DNA as a promising way to approximate source contributions by the mixing of their microbial communities (Knight *et al*., 2009; McCarthy *et al*., 2016). These techniques have been used in multiple contexts, but never to partition hydrographs by surface runoff source in urban watersheds. It is known that surface water microbial communities are shaped by the environment they encounter, but little is known as to the unique fingerprints of urban land cover microbial communities (McLellan et al., 2015). This study uses a Bayesian mixing model analysis to approximate microbial community contributions of grass runoff, road runoff, urban baseflow, and forest baseflow to a receiving urban stream with forested headwaters. Microbial communities are quantified using 16S rRNA metagenomic sequencing. Thes study provides evidence that MST may be an effective way to approximate the influence of runoff from different landscapes to the receiving stream's microbial community. The MST results were consistent with hydrologic theory, showing 118% increase in estimated contribution of runoff from grassy landcover between storm events of 0.52 and 1.9 in of rainfall. MST results predicted 9.34% of the water column microbial community during storm events was contributed to by the forested land cover microbial signature, while curve number method predicts ~5% of total runoff comes from forested landcover. More research is needed to develop sampling methodology that results in distinct microbial communities between land covers, because road runoff and grass runoff community diversity largely overlaps. Still, the results show there is promise in the technique to be sensitive to hydrologic timing of runoff arrival especially if a more sophisticated hydrologic model is applied.

4.1. INTRODUCTION

Urbanization has profoundly altered the hydrological dynamics of urban watersheds, resulting in a cascade of ecological ramifications (Walsh et al., 2005). Increased runoff from impervious surfaces and impacted soils in developed land uses results in a combination of diffuse and point sources contributing a variety of pollutants to receiving surface waters (Booth & Jackson, 1997; Paul & Meyer, 2001). Originally designed for flood mitigation, conventional urban drainage infrastructure directly connects runoff from impervious surfaces to receiving streams, rapidly increasing water quantity and exacerbating impacts on stream health (Epps & Hathaway, 2018; Shuster et al., 2005). This portion of impervious area, referred to as effective impervious area (EIA), has been identified as a more important measurement responsible for the implications of urban hydrology on stream water quality and quantity compared to total impervious area (TIA) (Walsh et al., 2005; Epps & Hathaway, 2018; Fletcher et al., 2014). The EIA of a watershed shows a quick response to small, low-intensity storm events, acting as a watershed within a watershed and driving much of the impact of runoff volume and timing.

Urban stormwater, and subsequently EIA, is a driver for pollutant transport to streams in many watersheds (Muller *et al.*, 2019). Surface runoff picks up anthropogenic pollutants such as heavy metals, biological contaminants, nitrogen (N) and phosphorus (P) from fertilizers applied to lawns and gardens, building materials and TSS loads resulting from construction disturbances, and much more (Muller *et al*., 2019). Mitigation of these pollutants are particularly challenging due to limitations in effective modeling strategies, especially for hydrologic conditions during extreme storm events (Borah & Bera, 2004; Borah et al., 2019). Because of the impact of EIA on pollutant transport, accurately quantifying and spatially identifying EIA in urban watersheds is critical to enhancing pollutant mitigation by enhancing model representations and effectively distributing green infrastructure practices (Epps & Hathaway, 2019). While techniques to spatially-identify EIA using rainfall-runoff data have been developed in recent years, the accuracy of these methods has yet to be verified (Epps & Hathaway, 2019).

Improvement of runoff source approximation from watersheds with patchy land covers is paramount to the verification of spatially identified EIA methods and the advancement of water quality in urban watersheds. Source-control policies are the most cost-effective management tool for mitigating diffuse pollutants (Marsalek and Viklander, 2011). However, implementing these strategies requires adequate knowledge of sources and their pollution mechanisms (Loganathan *et al.*, 2013). Being able to account for the source of diffuse pollutants, identify the timing of their arrival, and estimate their proportionate volumetric contribution to the stream would improve calculations of total maximum daily loads (TMDLs) and enlighten pollutant transport patterns unique to specific watersheds of interest.

Source tracking methodologies traditionally use tracer elements, dyes, or biological contaminants as markers to time the arrival of water sources to a receiving node. In hydrology, tracers such as dyes or chemical substances may be introduced to a stream or groundwater to quantify seepage rates and specific 1:1 source-fate pathways (Flury & Wait, 2003). These methods may be useful for testing the time required to drain individual runoff pathways, but they are not practical for partitioning total surface contribution to a storm hydrograph. Using stable isotope tracers has gained momentum in the field of hydrology for their ability to provide insight into runoff sources, flow paths, and water age (Birkel & Soulsby, 2015). Applications of stable isotope tracers are limited to distinguishing between chemical processes and physical changes that result in unique kinetic and equilibrium isotope fractionations, and their application to runoff sources is limited to the transformations performed on pollutants and other constituents carried by runoff and processes causing fractionations in the water molecules themselves such as evaporation and condensation. Microbial source tracking (MST) utilizes microbial contaminants, such as bacteria or viruses, to discriminate among sources. Most commonly, these techniques are applied to detect human-sourced pollution such as fecal contaminants. This method is unable to provide information about the origin host of the fecal pollution, sometimes produces conflicting results, and remains inconclusive as to which indicators are best suited for environmental applications (Hagedorn et al., 2011).

Microbial communities are assemblies of bacterial populations characterized by the measurement of their relative abundance in relation to one another and are distinctly shaped by prevailing environmental conditions (Cao *et al.,* 2011). Analyzing the relative abundance of distinct microbial populations in a water sample can provide insights to sources contributing to the sampled body of water (Hagedorn et al., 2011). Advances in microbiology have allowed scientists to effectively quantify microbial communities through analysis of paired-end sequences of ribosomal DNA. This development of microbial community characterization has allowed for an updated MST methodology, where relative contributions of different microbial community sources can be estimated in a sink using a Bayesian mixing model analysis (Knight et al., 2011). This advancement lends promise for using MST to distinguish between communities of different surface types, and thus partition contribution to stream water from EIA or TIA driven runoff.

Microbial communities in runoff are shaped by the soils, plants, and the built environment the water comes into contact with on its journey from source to stream (McLellan et al., 2015). These communities can then be found imprinted on the natural community of the receiving surface water. Other studies have successfully partitioned the major sources of water responsible for bacterial loadings in an estuary, validated by a hydrodynamic model (McCarthy *et al*., 2016). This work was largely successful because salt and freshwater are known to have a very distinct microbial community composition due to the polarity of the environmental conditions. The differences between microbial communities existing in stormwater runoff and stream water remains poorly understood. Previous attempts to quantify microbial contributions to stormwater runoff in streams have focused on the presence of fecal microbial pollutants as total coliform counts, or by directly comparing abundances of operational taxonomic units (OTU) in stream water to runoff during storm events (Wyckoff *et al*., 2017). By only looking for specific indicators or at most highly abundant taxa, this method neglects to incorporate nuances of community composition that distinguish one community fingerprint from another.

Other applications using SourceTracker analysis have partitioned between the contributions of streambed sediment, storm drain outfall, and upstream conditions to stream microbial

composition during dry and wet weather (Baral et al., 2018). This study successfully showed the temporal variation in source contributions through a storm event, but it did not attempt to distinguish between microbial communities from gray infrastructure derived runoff characteristic of EIA and the microbial community contributed by runoff from grass covered landscapes. It is unknown if microbial communities contributed to runoff from different landscape types are distinguishable enough to use for effective source tracking. In this study, we employ a Bayesian mixing model analysis to estimate the relative contributions of the microbial communities from different runoff originating from various land covers to a receiving urban creek with forested headwaters. Microbial communities of urban and forested baseflow and runoff types are quantified by 16S rRNA sequencing. Sources were classified as forest baseflow, urban baseflow, road runoff, and grass runoff. The aims of this analysis are to assess if source approximations using the SourceTracker model can be validated by a basic hydrologic model.

4.1. METHODS

4.2.1. Watershed Overview and Hydrology

The study takes place within the Baker Creek watershed in Knoxville, TN (Figure 4.1). The 0.84 km^2 subcatchment of interest, referred to from here on as URB, is primarily residential land use, with 90% developed land cover, 8% forested land cover, and 2% other including hay/pasture, wetland or open water according to the 2019 U.S. Geological Survey (USGS) National Land Cover Database (NLCD). The residential area consists of homes primarily built in the 1940s with an average lot size of approximately 600-1200 m^2. Rooftops primarily drain to grass lawns via gutter systems. The city has separate stormwater and wastewater sewers. The catchment is 275 m above sea level with well-draining, clayey loamy Telico-Alcoa soils (US Soil Conservation Service, 1981). According to KnoxGIS LiDAR data, the subcatchment is 26.6% impervious surface. Average rainfall in the area is 1270 mm per year.

A stream gauge station was installed on Baker Creek where it flows through a 0.91 m. diameter conveyance structure into Mary James Park. This location was directly connected to the stormwater drainage infrastructure, resulting in flashy hydrologic response to wet weather events

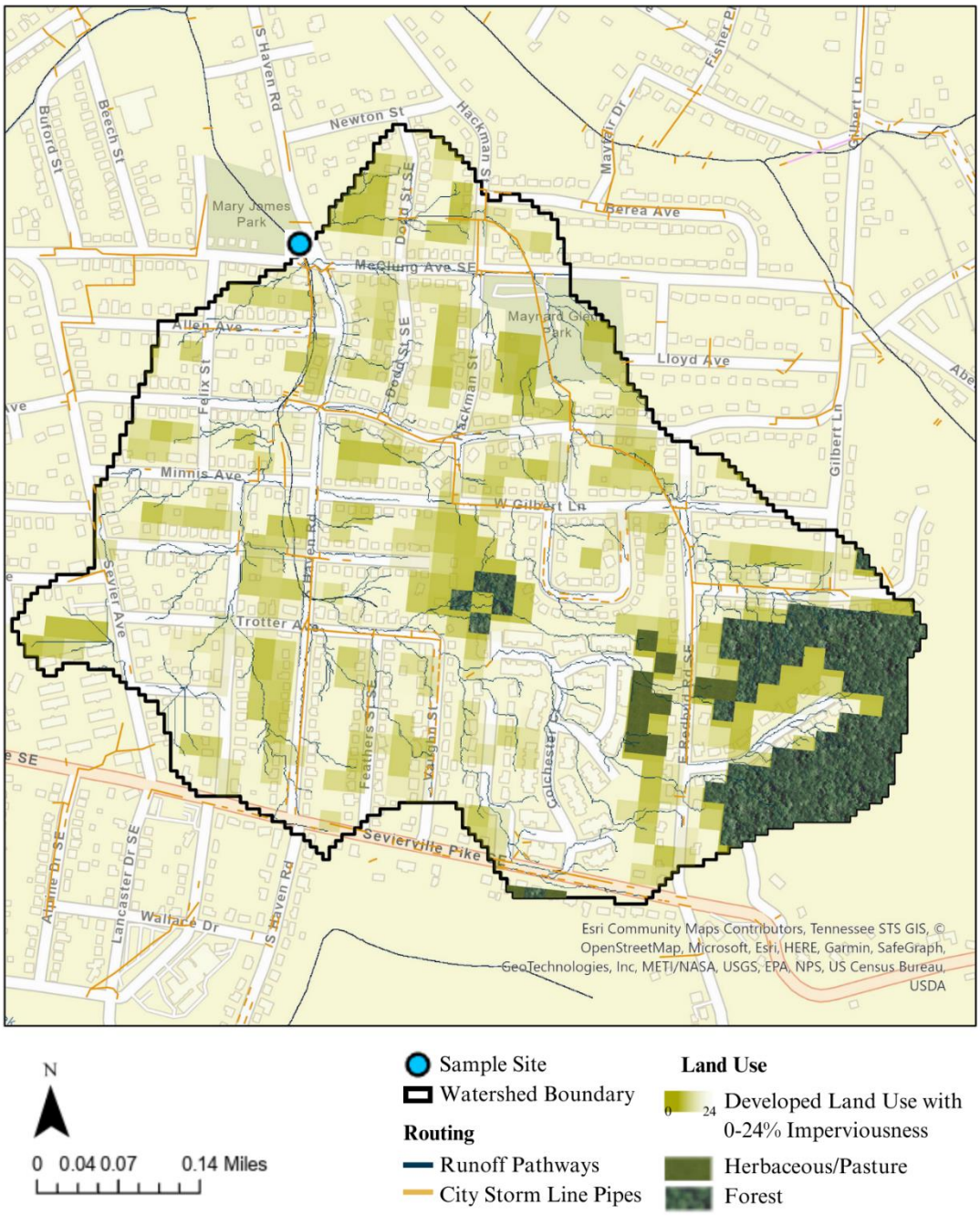

Figure 4.1 A street map of the URB subcatchment can be seen below. Developed areas of the catchment with less than 24% impervious surface cover, assumed to be grass, are represented by a light green gradient overlay. Less impervious surface will show as a darker shade of green. Approximate runoff flow paths delimited by the ArcGIS Flow Accumulation geospatial analysis tool are marked in dark blue lines, and municipal stormwater lines are indicated in orange.

and seasonal variability of baseflow levels. The drainage area at the point of this conveyance structure delimited using a 1m resolution digital elevation model (DEM) layer of Knox County in ArcGIS Pro. The gauge station was outfitted with a Teledyne ISCO 2150 Area Velocity Doppler flow meter, a Teledyne ISCO 6712 autosampler, a manual rain gauge, and an automated tipping bucket rain gauge. Stream flow and level were collected at 1-minute intervals. Rainfall intensity was measured at a 5-minute time step using the tipping-bucket rain gauge. The 5-minute time step gave resolution to the watershed's hydrologic response to rainfall intensity. The manual gauge allowed for verification of storm volume and proper functioning of the automatic rain gauge. In the event of malfunction of the 5-minute gauge, data from the nearby NOAA meteorological station using a 20-minute time step was consulted.

4.2.2. EIA estimation using Runoff/Rainfall Pairs

Runoff-rainfall pairs from 300 days of stream flow and rain gauge data were used to estimate the EIA using methods adopted from Boyd (1993) and Ebrihimian (2016). Stream flow data was processed in R, where linear interpolation was used to smooth sensor artifacts in the time series resulting from debris or sediment before baseflow separation. Baseflow was separated from streamflow using an adapted USGS HYSEP Local Minimum Method. Local-minimum baseflow separation was determined to be the best method for this site due to flashy stormflow and seasonal variability of baseflow. The method assesses each discharge rate individually to determine if it was the minimum

within the range of +/- 720 minutes (or ½ a day). This interval was chosen based on the expected time of concentration for the drainage area of the watershed being less than the minimum of 0.67 days according to the HYSEP method. The minimum points on the hydrograph were then connected via linear interpolation. Because this watershed showed significant seasonal, diurnal fluctuations in baseflow during warm weather, the local minimum method was discarded and instead the baseflow was determined as equal to the total stream flow during periods where the antecedent dry period was greater than or equal to 2 days and the average daily temperature was greater than 68 degrees Fahrenheit. Runoff contribution to streamflow, referred

to in this paper as stormflow, was then determined by subtracting baseflow from the stormflow. Stormflow was then used to determine total runoff volume for each storm event.

Event runoff-rainfall pairs were used to determine the fraction of EIA for subcatchment EIA using the successive ordinary least squares (OLS) method described by Ebrahimian & et al. (2016). This method removes the subjectivity in determining EIA versus non-EIA events (Ebrahimian et al., 2016). An OLS regression was iteratively fitted to the runoff-rainfall pairs which fit withing the threshold of an EIA criterion, or δ_c, described as:

$$\delta_c = max\left[2 * \sqrt{MSE}, 0.39\ in\right] \quad (1)$$

In Eq. 1, δ_c is defined as the maximum of either two times the root mean square of the residuals or 10 mm (Ebrahimian et al., 2016). The mean square of the residuals, or MSE, is based on the OLS regression predicted values ($\hat{y}$) of runoff compared to observed values (y) for n unique events and is represented by Eq. 2. In this work, it can be assumed that events above the EIA criterion are contributed to by runoff sources other than EIA due to antecedent soil moisture conditions (Ebrahimian & et al., 2016; Boyd & et al., 1993).

$$MSE = \frac{\sum_{i=1}^{n}(y_i - \hat{y}_i)^2}{n} \quad (2)$$

4.2.3. Curve Number Method

Runoff depths (Q) from the various land covers of the watershed were determined using the United States Department of Agriculture (USDA) Curve Number (CN) Method. The CN method is one of the most widely accepted techniques for estimating surface runoff. Land cover within the watershed generally consisted of three categories: pervious areas (forests, lawns, etc.), impervious areas that drain to green space, and EIA. Impervious area that drains to green space functionally acts as the pervious area of the land class (forest or residential/developed) it is a part of. For the pervious areas, the area of each land cover class within the drainage area URB was

calculated using 2019 NLCD raster data and ArcGIS. The proportion of each land cover that belonged to each hydrologic soil group (HSG) occurring within the watershed was then tabulated using the Union Analysis tool within ArcGIS (Jabri and Hessane, 2020; Ross 2018). This procedure was repeated to determine the percentage of impervious area for each land cover class.

Discrete CNs were then calculated for forested area and residential/developed area within the catchment based on estimations for CN from the TR-55 manual (Anderson et al., 1976; USDA, 1986). Effectively impervious surfaces were given a curve number of 98 as is the standard assumption outlined in the TR-55. The parameters and geospatial analysis results used to estimate the CNs are summarized in Table 3.1 in the results/discussion section.

4.2.4. Microbial Fingerprints

Source microbial fingerprints were derived from runoff and baseflow water samples. Between September and October 2020, water samples from road (n=4) and grass (n=5) runoff were collected within the drainage area of the stream gauge station for 16S rRNA. Roadway samples were taken from stormwater drainage infrastructure on residential streets, and grass samples were taken from ponded areas in Mary James Park, grassy lawns, and grassy swales. In-stream water column samples were taken by hand from the middle of stream flow during baseflow during 4 distinct seasons to account for variability (n=4). Samples from the forested headwaters (n=4) of the greater subcatchment were also used to assess the resilience of the forested microbial fingerprint in more urbanized land use downstream and in stream segments that appear disconnected based on surface water flow accumulation. Three storm events with sizes ranging from 132 cm – 6.93 cm were targeted for sampling efforts at site URB. Multiple samples were collected from the water column to capture the entire storm profile using the Teledyne ISCO 6712 Autosampler with sampler tubing affixed to the base of the drainage infrastructure. 5 were selected to represent the hydrograph's rising limb, peak, and falling limb segments. Streamflow and runoff samples were all taken with ethanol-sterilized 900 mL polypropylene bottles. Sample bottles and caps were rinsed three times with stream water before filling and being transported to Science and Engineering Research Facility on University of Tennessee Knoxville campus in a

cold cooler. Runoff samples were typically taken during the peak intensity of a rain event. 500 mL of sample water was filtered through 0.22μm Sterivex-GP filters as soon as possible. Filters were immediately stored at -20 °C inside sterile 100 mL falcon tubes until date of DNA extraction.

Microbial DNA was extracted from the water samples using Qiagen's Sterevix-GP filters and a DNeasy PowerSoil Kit. Polymerase chain reaction (PCR) amplification targeted the V4 region of the 16S rRNA gene sing 515F and 806R primers (Cao et al., 2021). Paired-end sequencing of the cleaned PCR products was completed using a MiSeq Reagent Kit for metagenomics libraries and a MiSeq V2 (300 cycles) Reagent Kit according to the manufacturer's instructions for 16S amplicon libraries. Microbial community fingerprints representing each sample were obtained via processing paired-end sequences with QIIME2 Version 2020.6 (Boylen et al., 2019). Relative contributions of source communities to storm samples were approximated using SourceTracker, a microbiome-based source identification tool. SourceTracker uses Bayesian statistics to quantitatively assign proportions of source microbiome profiles in each sink sample. A proportion of the sink's microbiome profile that is not assigned to any identified sources is classified as unknown (Knight et al., 2011). Diversity among samples chosen for each source metric was analyzed with the Shannon alpha diversity metric and by principal coordinates analysis of the weighted Bray Curtis beta diversity metric using the ecodist package in R (Goslee & Urban, 2007).

4.3. RESULTS AND DISCUSSION

4.3.1. Effective Impervious Area

The hydrological analysis of runoff-rooftop pairs revealed an estimated 5.9% EIA for the watershed out of a TIA of 27% (Figure 4.2). This is within a comparable to similarly sized urban watersheds, with respect to their relative total impervious area (TIA). Similar studies in Knoxville, TN found an EIA of 10.3% for a watershed with 35% TIA in a 13.8 km^2 drainage area, and 13.8% EIA in a 6.71 km^2 watershed with 26.9% TIA (Epps & Hathaway, 2018).

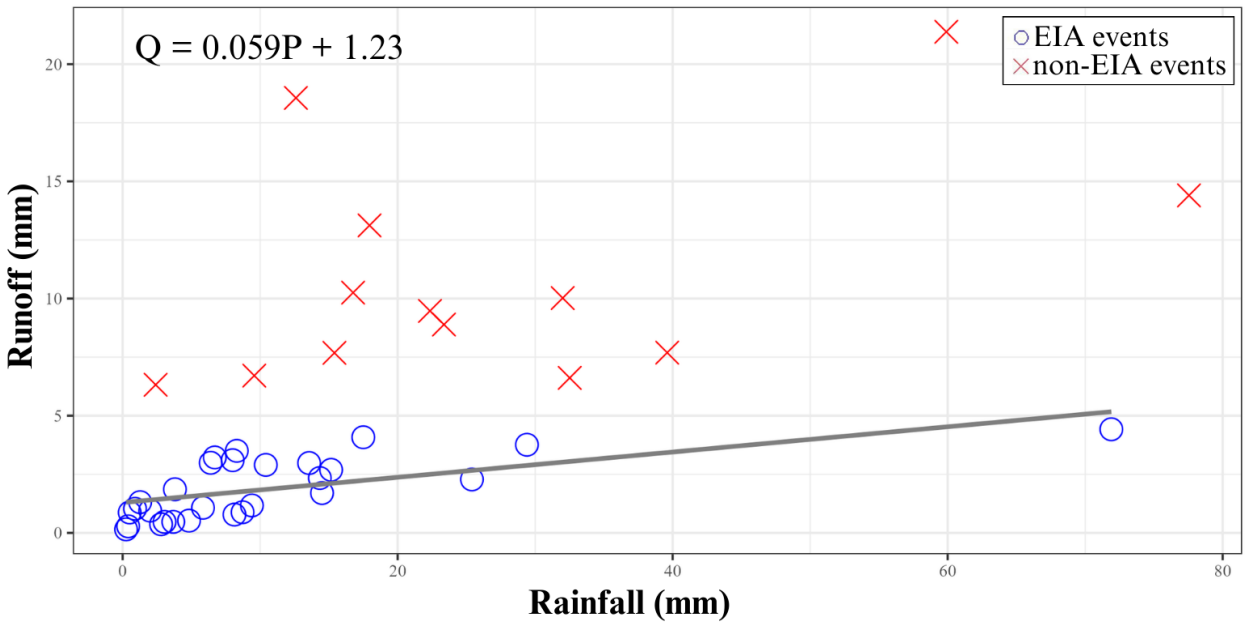

Figure 4.2 Graphical EIA regression results for observed rainfall-runoff data in subcatchment. EIA events are represented by a blue circle, while non-EIA events are represented with a red X.

4.3.2 Curve Number Runoff Approximation

The weighted CN for residential/developed pervious surfaces (grass/lawns) and impervious surfaces that drain to grass was initially calculated as 73.7, and the CN for forested pervious spaces and impervious surfaces that drain to forest was initially calculated as 70.3. These values were calibrated to 74.3 and 71, respectively, according to observed hydrologic conditions. Calibration was performed by adjusting the CN until the percent error between estimated and observed runoff depth was minimized for all three events. This is justified based on inherent uncertainty with the CN and the soil conditions in the watershed (Ajmal et al., 2020). The CN for EIA, which is assumed to be representative of stormwater runoff contributed by roadways, was fixed at 98 as there is no uncertainty of soil characteristics for paved surfaces (USDA, 1986). Geospatial statistics used to calculated CNs are found in Table 4.1.

Estimations of runoff from grass, forested, and EIA land covers based on the weighted CN analyses for the sampled storm sizes (1.27, 4.66, and 6.69 cm, referred to as events 1, 2, and 3, respectively) are summarized in Table 4.2 below. The distributed CN method resulted in

Table 4.1 A summarization of geospatial analysis results and non-EIA CN estimations from the TR-55.

				CN by Hydrologic Soil Group (TR—55)		% Area of Grass Landscape and Non-EIA Draining to Grass		% Area of Forest Landscape and Non-EIA Draining to Forest	
	Land Cover Class	**Area (m^2)**	**% TIA**	**C**	**C/D**	**C**	**C/D**	**C**	**C/D**
22	Developed: Open Space	260,896	22.2	75	77	31.7	0	N/A	N/A
23	Developed: Low Intensity	380,865	29.9	80	82	45.5	0	N/A	N/A
24	Developed: Medium Intensity	118,107	38.5	83	85	14.0	0	N/A	N/A
25	Developed: High Intensity	2,700	46.4	88	90	0.31	0	N/A	N/A
71	Herbaceous	7,200	2.8	71	73	0.9	1	N/A	N/A
81	Hay/Pasture	2,480	17.2	76	78	0.3	0	N/A	N/A
41	Deciduous Forest	45,992	9.7	72	74	N/A	N/A	49.9	0
42	Evergreen Forest	900	0.1	72	74	N/A	N/A	1.4	0
43	Mixed Forest	1,800	13.2	72	74	N/A	N/A	26.9	0
	SUBCATCHMENT TOTAL	**837,140**	**27**			**Grass CN**	**74.3**	**Forest CN**	**71**

Table 4.2 Estimations of total runoff, runoff from impervious surfaces, runoff from grass/non-EIA area that drains to grass, and forest/non-EIA area that drains to forest based on the composite curve number and the weighted curve number analyses for storm size of 1.32, 4.83, and 6.93 cm.

		CN Estimated Runoff Depth by Landscape Type					CN Estimated Runoff Relative Contribution by Landscape Type		
Storm Size (cm)	**Observed Runoff (cm)**	**Grass/Non-EIA Runoff (cm)**	**Forest/Non-EIA Runoff (cm)**	**EIA Runoff (cm)**	**Sum of Runoff (cm)**	**Percent Error**	**Grass/Non-EIA**	**Forest/Non-EIA**	**Road/EIA**
1.32	0.13	0.00	0.00	0.05	005	60.3%	0%	0%	100%
4.83	0.99	0.69	0.04	0.25	0.98	0.85%	70.0%	4.45%	5.45%
6.93	2.13	1.66	0.12	0.37	2.15	-0.90%	77.2%	5.45%	17.4%

accurate estimations of total runoff for events 2 and 3, however there is a high percent error for event 1—the smallest storm event. This is likely explained by an incorrect assumption of the initial abstraction storage, as the CN method is not recommended for smaller storm events due to its presumed fixed initial abstraction coefficient (USDA, 1986; Ajmal et al., 2020). Additionally, the CN model is not sensitive to the timing components of the antecedent dry period or storm duration. It cannot account for site-specific variability and flow routing via drainage infrastructure.

The CN approximated relative contributions from road, grassy, and forest surfaces to total runoff are outlined in Table 4.1. These calculations show that runoff from road and other EIA surfaces dominated the total runoff for the smaller storm event, as would be expected based on hydrologic theory (Boyd et al., 1993). For the larger event sizes, the majority of runoff came from grass surfaces. Approximately 65% of the watershed comprises developed grassy spaces, such as residential lawns and parks. An additional 20% of the watershed area is impervious surface which drains to grass, such as rooftops with gutters that drain to lawns. For this reason, it makes sense that grassy spaces would contribute 70-77% of runoff to the stream as the CN method suggests.

4.3.3. MST Results

4.3.3.1. Evaluation of Source Communities

Discrepancies between the MST and CN results may be explained by analyzing the community composition of the source samples. Table 4.3 displays the alpha diversity metrics for the runoff source samples and the stream flow sink samples. Alpha diversity is a measurement of how many taxa are represented within a sample. The average Shannon index ranged from 3.12 - 3.78 for source samples. This is relatively low compared to similar studies, where environmental samples for dry weather water, peak flow water, and street sweepings were 6.0, 6.9, and 7.3, respectively (Baral et al., 2019). The average number of species represented by our samples ranged from 33- 50, a fraction of those from similar studies (Baral et al., 2019). The alpha

Table 4.3 Average alpha diversity metrics for the three sources used in the analysis. The alpha diversity metrics speak to the number of species represented in the community.

Source Type	Average Shannon	Average Number of Species
Forest Baseflow	3.76	43.6
Grass Runoff	3.78	49.7
Road Runoff	3.16	33.5
Urban Baseflow	3.46	40.0

diversity of our source samples was more comparable to the microbial communities from fecal samples.

The principal component analysis of the Bray Curtis diversity metric, which describes many species in one sample that are unique from the species represented in another, is shown in Figure 4.3. The forest baseflow source is the most distinguishable source from other sources based on Bray Curtis beta diversity metric. The forest samples may show the most distinguishable microbial diversity because it is the source that has the most samples contributing to its microbial profile, or because forest samples have a greater average Shannon index alpha diversity metric compared to other source samples indicating there are more species representing the community fingerprint. Both of these explanations could also be at play, indicating some feedback between the two. The forest samples may also show more consistency due to increased environmental continuity such as buffers from high fluctuations in temperature and moisture and increased surface area for an integrated microbial community structure (Hosen et al., 2017).

The Bray Curtis of the "Urban" and "Grass" runoff microbial profiles largely overlap, meaning these two sources may not be highly distinguished as inputs to the Bayesian mixing model. This increases the model's uncertainty, making it easier to identify general trends than find concrete estimations. The "Road" runoff source may also contribute a smaller bacterial load than "Grass" runoff, which could distort its representation in terms of microbial community diversity. While 16S rRNA analysis does not indicate the abundance of microbial cells in a sample, the diversity analysis does reveal that road runoff has the smallest total number of species comprising the microbial community, while grass runoff has the highest total number of species. Microbial community measured from street sweepings has shown higher alpha diversity metrics than embankment soil in similar studies (Baral et al., 2019)

The "Urban" baseflow source samples show the most variation and overlap with each of the other sources. Previous literature exploring the response of water column microbial communities to land use gradients in urban catchments showed that water column communities are highly responsive to the dispersal of organisms from the urban landscape (Hosen et al., 2017). This

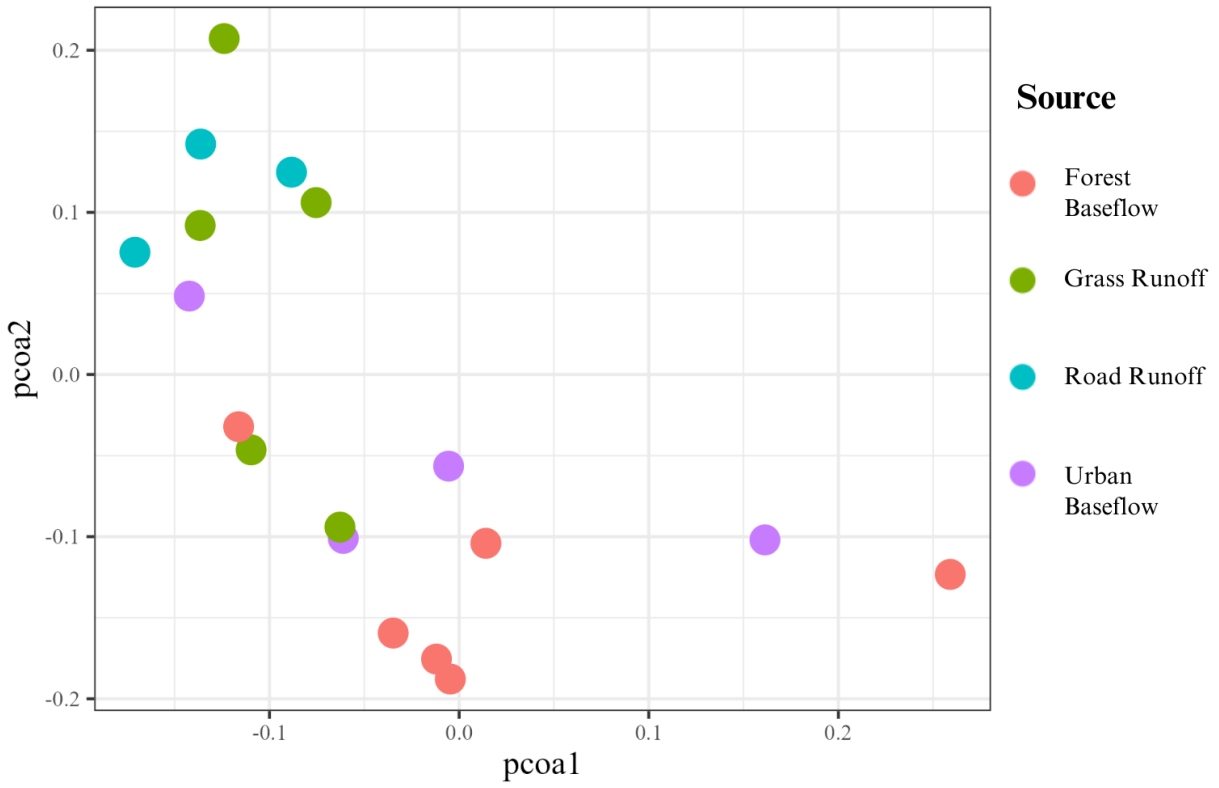

Figure 4.3 A plotted Principal Coordinate Analysis of weighted Bray Curtis dissimilarities distance for the source samples visualize the overlap in OTUs comprised in the samples representing each source.

supports the explanation that “Urban” baseflow samples may be highly influenced by interactions with other landscape-oriented sources analyzed in this study. Because the forested samples have the greatest alpha diversity and the most distinguished beta diversity, indicating that are not present in other source types, this source might be the easiest to distinguish using the SourceTracker mixing model.

4.3.3.2. Relative contribution from various landscapes

The MST analysis approximates that 25% of the microbial community in the water column during the smallest storm event can be attributed to the grass runoff source microbial community (Figure 4.4). According to the CN estimated contributions, grass surfaces do not contribute to total runoff for the 1.35 cm storm event. Based on the weighted CN for pervious spaces, the initial extraction storage space is assumed to be 1.78 cm, and storm events smaller than 1.78 cm will not contribute runoff from grass.

As the limitations of the CN method have been previously discussed, this estimation cannot properly account for scenarios where stormwater drainage is transported to the stream over tightly packed pervious surfaces or grassy swales (which is present in this watershed) where the initial abstraction may be lower than estimated by the weighted CN. Pervious runoff could depend on storm intensity and duration, antecedent conditions, or proximity of source areas to the drainage area or streams (Boyd *et al.*, 2009). Runoff from impervious areas may route to greenspaces that become saturated and generate runoff during high intensity events, for example. Therefore, under the appropriate conditions, it is likely that some grassed area will contribute runoff even during small events. This is exemplified by the EIA regression in Figure 4.2, where events of less than 1.78 cm have been deemed “non-EIA” events where runoff from non-EIA area contributed to streamflow. In these scenarios, is possible for microbial communities in road runoff to have picked up a grass microbiome signature on its way to the stream. Additionally, some of the runoff sampled during stormflow at the gauging station may consist of return flow from water that has already percolated into the soil and interacted with that microbial community. Because the sink analyzed using MST is the total flow in the stream, it would be

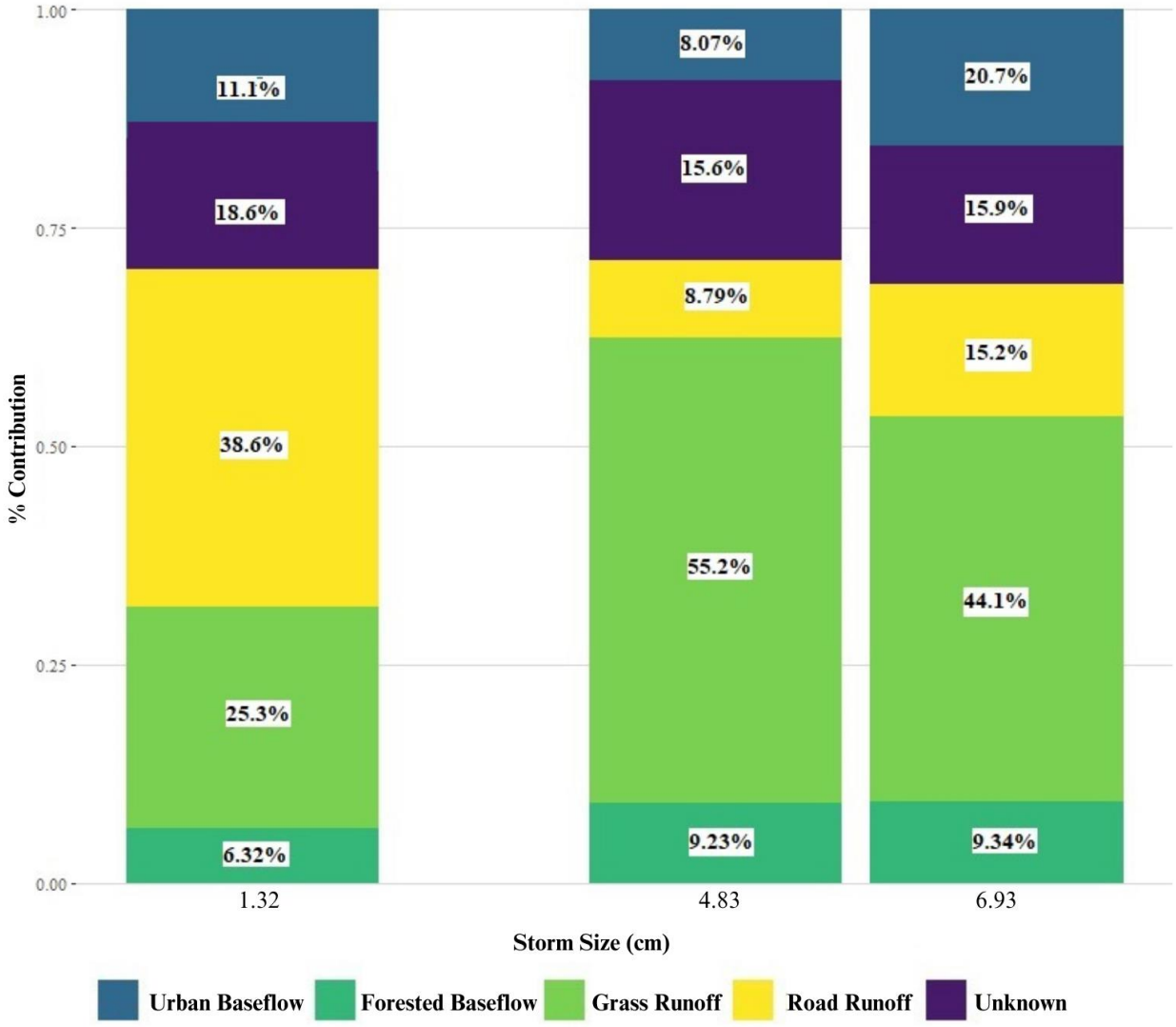

Figure 4.4 Estimations of percent contributions of sources to stream flow for three storm sizes using microbial source tracking, averaged over all samples specific to that event. Forest baseflow, grass runoff, road runoff, urban baseflow, and unknown sources are represented by separate colors indicated by the legend. The percentage contribution of each source is labeled in a white box for each bar plot segment.

difficult to distinguish between water contributed to the stream by overland flow versus return flow from this analysis alone. A more integrated hydrodynamic and infiltration coupled model may clarify how much of the MST approximation is expected to represent surface runoff versus return flow.

For the larger events where CN approximations of runoff volume had a very low percent error, the MST approximation of grass runoff contribution to stormflow shows improved accuracy. The MST results suggest that the contribution of grass runoff to the stormflow microbial community does increase significantly for storm events larger than 1.78 cm, which mirrors what is expected based on the hydrologic model. MST estimates that the proportion of the microbial community in stormflow influenced by the grass runoff microbial community increases from 25.3% in event 1 to 55.2% in event 2 and 44% in storm 3. Excluding microbial community which can be attributed to baseflow, this equates to 36%, 78.6%, and 62.7% of runoff compared to road and forest. This presents a percent error of 12.3% and 18.8% for MST approximated contribution of grassy landscapes to runoff for events 2 and 3, respectively. This uncertainty can be attributed to the "unknown" proportion of the MST results and the site-specific limitations of the CN method discussed in the context of the smaller storm event.

With forested land use comprising 6.9% of the pervious area, the small yet persistent presence of the microbial fingerprint representing forest source (ranging from 6-9%) is plausible. Runoff from the forested areas was expected to contribute 4.45% and 5.45% of runoff from two larger storm events. The overprediction of the MST method may be explained by the uncertainty of the model or by overlaps in the forest and grass microbiome (Figure 4.4). The overprediction may also be explained by baseflow and by subsurface flow. As the storm surge fills catchment storage and increases underground connectivity, more distant reaches of the watershed may be connected and flushed from the water table. This is significant because while the drainage area contains forested land use, the stream branch in this study area does not flow through the forested area. The site may be distantly connected through estimated runoff flow paths during large storm event, where runoff from the forested landscape would travel over a great distance of various paved and/or unpaved surfaces before making it through the conveyance structure at Mary James

Park. This means that either runoff from the forested reach retains the species-specific to the forested ecosystem over its travel time, or, more likely due to the timing of the samples taken, distant reaches of the watershed are hydrologically connected via the vadose zone allowing for the ecological exchange of water column species.

The contribution of EIA to the microbial community in the water column are high for event 1 (38.6%), and decrease during events 2 and 3 (7.8% and 15.2%), respectively. The decrease between storms 1 and 2 matches hydrologic theory as grass spaces begin to become saturated and produce runoff. The decrease between events 2 and 3, however, suggests that there may be a non-linear pattern of how roadways contribute to stormflow that is related to storm intensity and timing.

4.3.3.3. Timing of Sources

In urban watersheds, there is a timing component as to when runoff reaches the stream from a given land cover. Perhaps most significantly, the earliest parts of an event are dominated by runoff from directly connected impervious areas drained via efficient stormwater conveyance (Boyd et al., 2009). Similarly, delivery of runoff from pervious area is delayed (1) until after the initial abstraction of storage capacity is filled, and (2) due to higher friction land cover and less efficient conveyances. Responses of soil moisture, and the subsequent relationship with runoff generation and flowpaths, are well documented (Singh et al., 2021).

Further evidence of the potential for MST in urban hydrologic applications was observed by interpreting the results with reference to the stream discharge at the time the samples were taken. Figures 4.5 and 4.6 display the hydrograph for events 2 and 3, respectively, with symbols indicating the time during the event in which the samples were taken. The MST derived source approximations to the microbial community in the water column are displayed in the corresponding figure. For event 2, which had a total precipitation of 7.83 cm and an observed runoff depth of 0.99 cm, rising limb, peak, and falling limb of the second peak in the storm's hydrograph are well represented by the samples. It is important to note that the initial flush of runoff was not represented in the samples. For this reason, it makes sense that the contribution

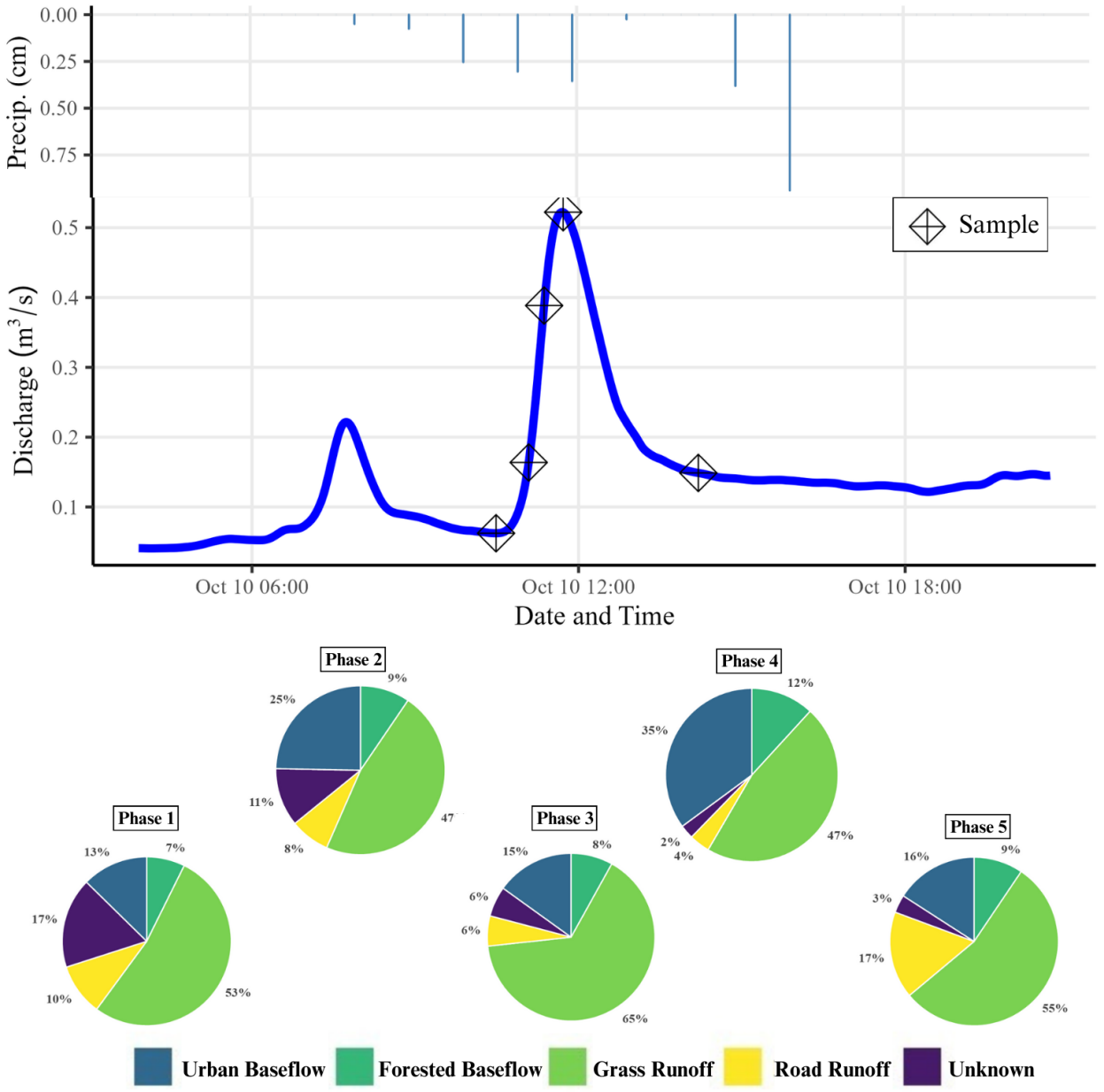

Figure 4.5 A storm hydrograph for Event 2 displays 60-min interval precipitation, total stream discharge, and timing of water column samples taken by the autosampler. The MST results for each of the 5 samples are displayed below the hydrograph.

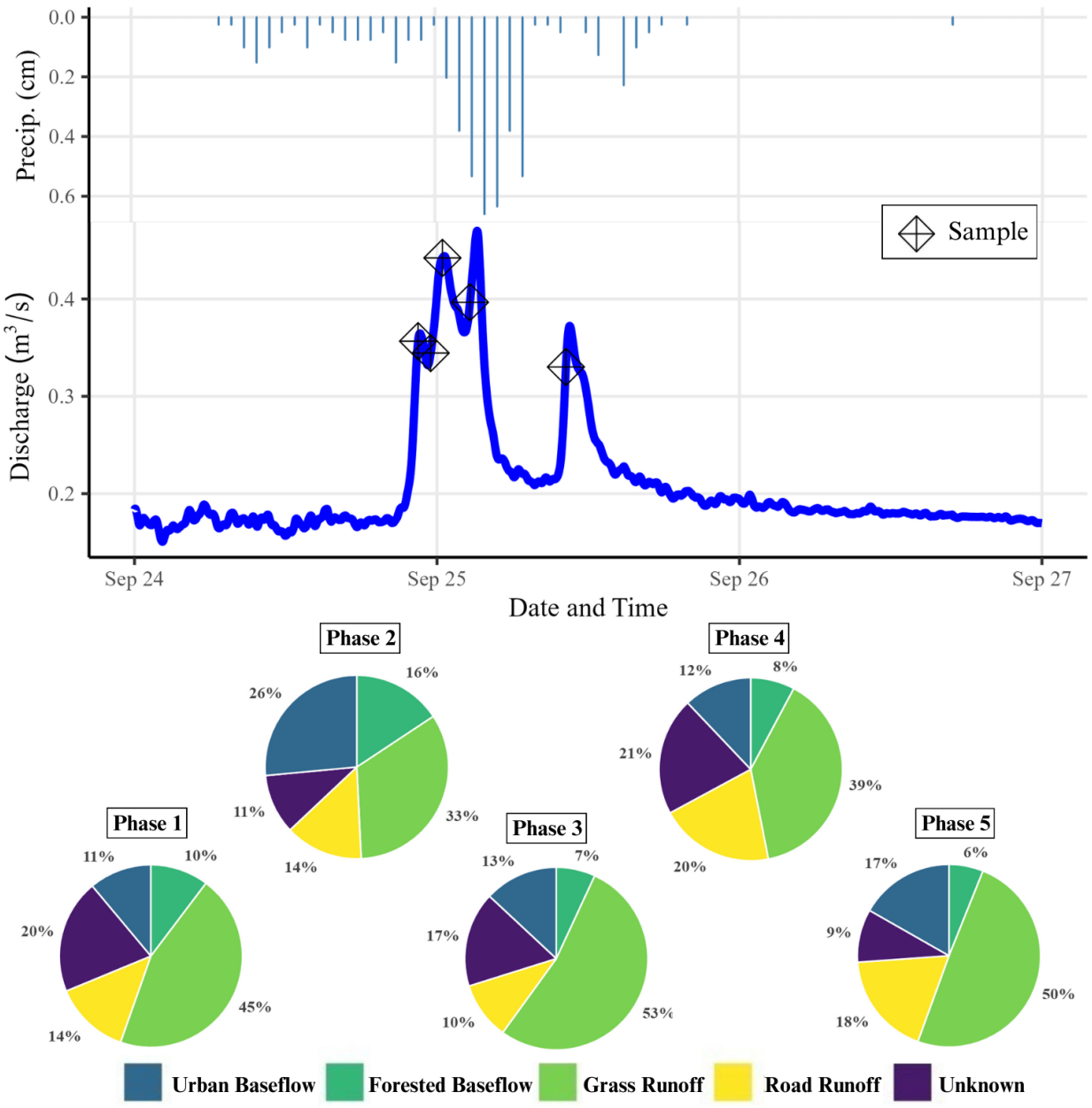

Figure 4.6 A storm hydrograph for Event 3 displays 20-min interval precipitation, total stream discharge, and timing of water column samples taken by the autosampler. The MST results for each of the 5 samples are displayed below the hydrograph.

from roadway samples is smaller than might be expected during the rising limb, ranging from 6-10% of the composite microbial community fingerprint. In contrast, runoff from grass landscapes and impervious surfaces that drain to grass landscapes dominate the microbial signature throughout the event, ranging from 47-65%. This is likely because sampling began after initial storage in the soil was filled, and grassed landscapes were already contributing runoff. The peak flow rate, represented by the "Phase 4" MST sample, represents the smallest contribution of microbial communities from runoff derived from EIA surfaces (4%) and the highest contribution from urban baseflow (35%). The high proportion of baseflow at the peak of the event indicates that the observed stormflow reflects a transient saturation of hill-slope creating subsurface flow connectivity with upland (Blume et al., 2015; Han et al., 2020). This occurrence is further evidenced by the lag in baseflow drawdown observed on the tail end of the hydrograph, after rainfall has commenced. The forested flow contributed a steady 7-9% to the microbial community throughout most of the storm event, with a slight increase to 12% at peak flow. This coincides with the maximum contribution from urban baseflow. This may be further evidence of a saturated catchment area increasing subsurface connectivity to upland areas. This may also be indicative of the overlapping diversity between the urban and forest baseflow microbial community signatures. The amount of unknown sources decreases over the course of the storm event, with the smallest unknown occurring during the peak of the event. This would indicate that the MST sources are well suited for partitioning the peak stormflow microbial community.

Event 3 saw a total precipitation of 6.93 cm and 2.13 cm of runoff. Sample pacing was less adept at capturing the rising and falling limbs of the hydrograph, and the rainfall intensity resulted in a less clear moment of "peak" flow. Instead, we see 4 observable peaks for this storm event, with 2 separate hydrograph "curves". Therefore, we must note that discharge in the stream is increasing at during storm phase samples 1, 2, 4, and 5, but discharge in the stream is at a "peak" or transitioning from increasing to decreasing during storm phase sample 3. The lowest observed road runoff contribution is during a peak in the hydrograph, where there is a higher contribution from urban and forest baseflows and lower unknown. Baseflow contribution to microbial community is relatively steady throughout this storm event, compared to event 2 in figure 4.5. Contribution from grass is more significant towards the end of the event.

Overall, the results suggest that EIA contributes runoff to this watershed throughout a storm event, with a less blatant bias at the start of the event. Because this is a small watershed and the sampling equipment was installed in a stormwater conveyance structure directly fed by EIA, this makes sense. For both storm events, influence on the microbial community from road runoff appeared to be more correlated with rainfall intensity, either at peak intensity or during a lull in intensity, than with hydrograph timing.

4.4. CONCLUSION

The results of this study showed that a Bayesian mixing model analysis of microbial communities extracted from runoff samples and quantified using 16S rRNA synthesis shows promise for portraying proportions of runoff from different types of landscapes estimated by CN analysis for larger storm events. Although source samples could be more distinct form each other, some grouping was present in the Principal Component Analysis, in particular for road runoff and forest flow. Both a simple hydrologic model using the USDA Curve Number method and the SourceTracker results were used to estimate the proportion of stormflow originating from various land covers in an urban watershed. The results between the two methodologies were comparable and consistent with urban hydrologic theory whereby effective impervious areas contribute more runoff during small events, and during the beginning of larger events. The two methodologies were complementary, with the hydrologic model ensuring MST results were reasonable, and the MST model identifying limitations to the CN method. Specifically, the smallest event would produce no runoff in pervious areas according to the CN method, yet the MST identified non-EIA sources in the runoff. In a practical sense, this is more likely as runoff from event impervious areas is likely to contact surfaces such as grassy swales. The results also suggest MST may be a valuable tool for tracking the timing of delivery of various land covers over the course of a hydrograph, and that hydrologic response in small urban catchments appears to much more complex than we give it credit for. It is popular for hydrologists to study the ideal bell-curved hydrograph, when oftentimes the response is much more sensitive and case-dependent (Han et al., 2020).

The limitations of this study, including a shortage of samples to maximize the definition of source microbial communities, the assumptions required by the CN method, and the uncertainty of the SourceTracker mixing model, will require additional research before this method can be reliably employed to larger hydrologic modeling pollutant tracing efforts. Neither the MST method nor the CN method was suitable for distinguishing between runoff and through flow from grassy landscapes, leading to increased uncertainty in the approximated proportion of "Grass" runoff to the total flow's microbial community. An increased number of samples to represent each landscape's runoff microbial community, including soil or sediments samples and/or street sweepings, may improve the resolution of the SourceTracker results. The presence of overlapping microbial community members in road and grass runoff microbial profile may skew the Bayesian mixing model analysis results. More research is needed to understand what parameters define the microbial communities on different surfaces and to identify the best sampling practices for runoff sources. It is important to understand what specific conditions the microbial community is most sensitive to for improvement of sampling techniques for effectively representing runoff from each landscape. This will help us determine how we can most accurately distinguish a "Road" runoff microbiome source from a "Grass" runoff microbiome source, as well as identify a "road mixed with grass" source. Additionally, having enough replications for a holdout set of "Urban" baseflow samples would allow for a more thorough analysis of the representation of "Forest" baseflow OTUs in the "Urban" baseflow microbial community samples.

It is recommended that an increased number of storm sizes and conditions are sampled in order to properly assess if this MST method is sensitive enough to account for the hydrologic timing of the delivery of sources. A more sophisticated model than the CN method is better suited to demonstrate timing of runoff delivery. If the study scope was able to implement such a model and verify the timing of the delivery of runoff sources to the gage station with respect to storm duration, MST could be become a valuable tool for verifying subsurface and surface connectivity between watershed reaches. This would advance our understanding of connectivity in stream science. Future studies may wish to explore this hypothesis by increasing the number of sites sampled during the storm events to organize a hierarchical arrangement of connectivity and

nested sources would increase resolution of source contribution and account for uncertainty associated with overlapping landscape interactions.

The study results suggest that MST has high potential of accurately determining contributions of microbial communities to stream water columns from different surface runoff. MST approximations of source follow a pattern of increasing contribution form grassy, pervious area for larger storm events that fill permeable storage capacity. More research is needed to determine what environmental parameters result in the most distinguished road and grass runoff communities, and to account for site-specific hydrologic characteristics such as return flow, effective impervious area (EIA) overflow, duration of event, and antecedent conditions. Still, the results show there is promise in the technique to be sensitive to hydrologic timing of runoff arrival if a more sophisticated hydrologic model is applied.

REFERENCES

Anderson, J. R., Hardy, E. E., Roach, J. T., & Witmer, R. E. (1976). A Land Use and Land Cover Classification System for Use with Remote Sensor Data. United States Geological Survey Professional Paper 964.

Ajmal, M., Waseem, M., Kim, D., & Kim, T. W. (2020). A pragmatic slope-adjusted curve number model to reduce uncertainty in predicting flood runoff from steep watersheds. *Water*, *12*(5), 1469.

Baral, D., Speicher, A., Dvorak, B., Admiraal, D., & Li, X. (2018). Quantifying the relative contributions of environmental sources to the microbial community in an urban stream under dry and wet weather conditions. *Applied and environmental microbiology*, *84*(15), e00896-18.

Beven, Keith J. (2011). Rainfall-runoff modelling: the primer. John Wiley & Sons.

Bhaduri, B., Harbor, J., Engel, B., & et al. (2000). Assessing watershed-scale, long-term hydrologic impacts of land-use change using a GIS-NPS model. Environmental Management, 26(5), 643–658. https://doi.org/10.1007/s002670010122

Birkel, C., & Soulsby, C. (2015). Advancing tracer-aided rainfall–runoff modelling: A review of progress, problems and unrealised potential. *Hydrological Processes*, *29*(25), 5227-5240.

Blume, T., & Van Meerveld, H. J. (2015). From hillslope to stream: methods to investigate subsurface connectivity. *Wiley Interdisciplinary Reviews: Water*, *2*(3), 177-198

Bolyen E, Rideout JR, Dillon MR, Bokulich NA, Abnet CC, Al-Ghalith GA, Alexander H, Alm EJ, Arumugam M, Asnicar F, Bai Y, Bisanz JE, Bittinger K, Brejnrod A, Brislawn CJ, Brown CT, Callahan BJ, Caraballo-Rodríguez AM, Chase J, Cope EK, Da Silva R, Diener C, Dorrestein PC, Douglas GM, Durall DM, Duvallet C, Edwardson CF, Ernst M, Estaki M,

Fouquier J, Gauglitz JM, Gibbons SM, Gibson DL, Gonzalez A, Gorlick K, Guo J, Hillmann B, Holmes S, Holste H, Huttenhower C, Huttley GA, Janssen S, Jarmusch AK, Jiang L, Kaehler BD, Kang KB, Keefe CR, Keim P, Kelley ST, Knights D, Koester I, Kosciolek T, Kreps J, Langille MGI, Lee J, Ley R, Liu YX, Loftfield E, Lozupone C, Maher M, Marotz C, Martin BD, McDonald D, McIver LJ, Melnik AV, Metcalf JL, Morgan SC, Morton JT, Naimey AT, Navas-Molina JA, Nothias LF, Orchanian SB, Pearson T, Peoples SL, Petras D, Preuss ML, Pruesse E, Rasmussen LB, Rivers A, Robeson MS, Rosenthal P, Segata N, Shaffer M, Shiffer A, Sinha R, Song SJ, Spear JR, Swafford AD, Thompson LR, Torres PJ, Trinh P, Tripathi A, Turnbaugh PJ, Ul-Hasan S, van der Hooft JJJ, Vargas F, Vázquez-Baeza Y, Vogtmann E, von Hippel M, Walters W, Wan Y, Wang M, Warren J, Weber KC, Williamson CHD, Willis AD, Xu ZZ, Zaneveld JR, Zhang Y, Zhu Q, Knight R, and Caporaso JG. (2019). Reproducible, interactive, scalable and extensible microbiome data science using QIIME 2. Nature Biotechnology 37: 852–857. https://doi.org/10.1038/s41587-019-0209-9

Borah, D. K., & Bera, M. (2004). Watershed-scale hydrologic and nonpoint-source pollution models: Review of applications. *Transactions of the ASAE*, *47*(3), 789-803.

Borah, Deva K., Ebrahim Ahmadisharaf, G. Padmanabhan, Sanaz Imen, and Yusuf M. Mohamoud. "Watershed models for development and implementation of total maximum daily loads." *Journal of Hydrologic Engineering* 24, no. 1 (2019): 03118001.

Booth, D. B., & Jackson, C. R. (1997). Urbanization of aquatic systems: degradation thresholds, stormwater detection, and the limits of mitigation 1. *JAWRA Journal of the American Water Resources Association*, *33*(5), 1077-1090.

Cao L, Yang L, Swanson CS, Li S, & He Q. (2021). Comparative analysis of impact of human occupancy on indoor microbiomes. Front Environ Sci Eng; 15:89.

Epps, T. H., & Hathaway, J. M. (2018). Establishing a framework for the spatial identification of effective impervious areas in gauged basins: review and case study. *Journal of Sustainable Water in the Built Environment*, *4*(2), 05018001.

Epps, T. H., & Hathaway, J. M. (2019). Using spatially-identified effective impervious area to target green infrastructure retrofits: A modeling study in Knoxville, TN. *Journal of hydrology*, *575*, 442-453.

Flury, M., & Wai, N. N. (2003). Dyes as tracers for vadose zone hydrology. *Reviews of Geophysics*, *41*(1).

Goslee, S. C., & Urban, D. L. (2007). The ecodist Package for Dissimilarity-based Analysis of Ecological Data. Journal of Statistical Software, 22(7), 1–19. https://doi.org/10.18637/jss.v022.i07

Han, X., Liu, J., Srivastava, P., Mitra, S., & He, R. (2020). Effects of critical zone structure on patterns of flow connectivity induced by rainstorms in a steep forested catchment. *Journal of Hydrology*, *587*, 125032.

Hagedorn, C., Blanch, A. R., & Harwood, V. J. (Eds.). (2011). *Microbial source tracking: methods, applications, and case studies*. Springer Science & Business Media.

Hosen J., Ferbia C., Crump B., Palmer M. (2017). Watershed Urbanization Linked to Differences in Stream Bacterial Community Composition. *Frontiers in Microbiology* 9, 1452. doi:10.3389/fmicb.2017.01452

Jabri B, & Hessane M. (2020) Production of a Curve Number map using GIS Techniques in the watershed of the high Sebou (Morocco). E3S Web of Conferences 150, 03003. https://doi.org/10.1051/e3sconf/202015003003

Knights D, Kuczynski J, Charlson E, Zaneveld J, Mozer M, Collman R, & et al. (2011). Bayesian community-wide culture-independent microbial source tracking. Nat Methods 2011; 8:761e3.

Loganathan, P., Vigneswaran, S., Kandasamy, J., 2013. Road-deposited sediment pollutants: a critical review of their characteristics, source apportionment, and management. Crit. Rev. Environ. Sci. Technol. 43 (13), 1315–1348.

McCarthy, D.T., Jovanovic, D., Lintern, A., Teakle, I., Barnes, M., Deletic, A., Coleman, R., Rooney, G., Prosser, T., Coutts, S., Hipsey, M.R., Bruce, L.C., & Henry, R. (2016). Source tracking using microbial community fingerprints: Method comparison with hydrodynamic modelling. Water Research 109, 253-256. 10.1016/j.watres.2016.11.043

McLellan, S.L., Fisher, J.C., Newton, R.J. (2015). The microbiome of urban waters. *International Microbiology* 18:141-149. doi:10.2436/20.1501.01.244.

Paul, M. J., & Meyer, J. L. (2001). Streams in the urban landscape. *Annual review of Ecology and Systematics*, *32*(1), 333-365.

Ross, C.W., L. Prihodko, J. Anchang, S. Kumar, W. Ji, and N.P. Hanan. (2018). HYSOGs250m, global gridded hydrologic soil groups for curve-number-based runoff modeling. *Scientific Data* 5, 180091. https://doi.org/10.1038/sdata.2018.91

Shuster, W. D., Bonta, J., Thurston, H., Warnemuende, E., & Smith, D. R. (2005). Impacts of impervious surface on watershed hydrology: A review. *Urban Water Journal*, *2*(4), 263-275.

Singh, N. K., Emanuel, R. E., McGlynn, B. L., & Miniat, C. F. (2021). Soil moisture responses to rainfall: Implications for runoff generation. *Water Resources Research*, *57*(9), e2020WR028827.

United States Department of Agriculture. (1986). Urban Hydrology for Small Watersheds - TR-55. Natural Resources Conservation Service, National Engineering Handbook, Section 4. USDA.

Walsh, C. J., Roy, A. H., Feminella, J. W., Cottingham, P. D., Groffman, P. M., & Morgan, R. P. (2005). The urban stream syndrome: current knowledge and the search for a cure. *Journal of the North American Benthological Society, 24*(3), 706-723.

Wycoff, K., Chen, S., Steinman, A., & He, Q. (2017). Impact of Roadway Stormwater Runoff on Microbial Contamination in the Receiving Stream. Journal of Environmental Quality, (2017), 1065-1071, 46(5). 10.2134/JEQ2017.03.0116

CHAPTER 5
CONCLUSION

This dissertation investigated the implications of two juxtaposing measurements of connectivity – impervious connectivity and floodplain/hill slope connectivity – on nitrate sources and microbial community. The study involved installation and maintenance of stream gauge stations, obtaining of hydrologic and meteorological data from APIs and online databases, water quality sampling and laboratory testing, and methodical handling of large geospatial-geochemical datasets. Data manipulation, analyses, and graphical representation of results were executed in the R programming language. The study employed two different forms of source tracking techniques (stable isotope and microbial source tracking), a basic hydrologic model, bioinformatic statistical analysis, geospatial analysis in ArcGIS, mixed linear regression modeling, and more techniques to analyze novel hypotheses. We were able to deduce novel findings as well as verify emerging ideas in the field of hydrologic science. From the independent findings of each chapter, a few overarching themes stood out.

Seasonal trends in ecological processes make significant impacts on small urban streams. Evidence in shifting indicator species, microbial community diversity, and microbial assembly ecological processes were observed in stream water. Seasonal variations in nitration concentration hot spots were also observed in the stream using stable isotope analysis.

While seasonal variations were observed especially in geospatial relationship to the urban forest preserve, trends in microbial community and nitrate sources along the forest-urban gradient were less pronounced. This may be because the forest is rather small, heavily trafficked, and while on higher elevation, surrounded by urbanized area and airborne anthropogenic pollution. Variations between stormwater flows and baseflows, on the contrary, were quite pronounced. This speaks to the need for more work to understand the implications for hydrologic on microbial functional potential.

The results of this study piqued the interest in the hydrogeology of the system and the possible implications of karst geology on subterranean connectivity in the watershed. The presence of sulfur-oxidizing bacteria common to cave systems in the creek and the sulfate enriched with heavier sulfur and oxygen isotope compositions may lend evidence to the impacts of geomorphological karst phenomenon on Baker Creek. More research is needed to understand the potential impact of karst topography on ecological function on this stream and those like it.

These findings all lend valuable insight to the trajectory of urban water resource management becoming increasingly ecologically mindful. The results show that there is promise in more research to develop biotechnology methods, such as source tracking and bioremediation, to assess and mitigate implications of urbanization on urban stream health. The results also highlight the need to be mindful of ecological patterns in nutrients and microbial communities when developing water quality regulations. It is no longer conceivable that a 1-size fits all solution will be effective for holistic and integrated water resource management decisions.

VITA

Victoria Rexhausen came to Knoxville, TN from her home state of Georgia in 2018 as a new Graduate Research Assistant and a Tennessee Fellow of Graduate Excellence. Over the following five years, Victoria worked with major advisor Jon Hathaway on developing a doctoral dissertation which combined her interests of microbial ecology and hydrology. During this time, she also found many ways to serve her local and scientific community including: serving as the Outdoor Coordinator for the Dogwood Service Unit of the Girl Scouts of the Southern Appalachians, serving as co-chair of the "Accessibility, Justice, Equality, Diversity, and Inclusion" (AJEDI) and member of the Outreach committees on the American Geophysical Union (AGU) Hydrology Student Subcommittee (H3S), serving as a mentor in the Clean Water Science Network, and contributing to multiple scientific outreach events for children at the elementary, middle, and high school levels. To date, her work has contributed to 1 conference publication and 15 conference presentations (5 oral, 10 poster), and 1 award of the EPA P3 grant.